Cloning and Expression Studies of the Human Type I Inositol 1,4,5-Trisphosphate Receptor

Ting-Kuang Niu

A thesis submitted for the degree of Doctor of Philosophy at the University of Edinburgh
2000

Declaration

The work reported in this thesis was carried out under the supervision of Dr. Richard H. Ashley at the Department of Biomedical Sciences, University of Edinburgh. All results presented, unless otherwise stated, are the sole work of the author, as is the composition of this thesis.

Acknowledgements

I would like to thank Dr. Richard Ashley and all members in the membrane biology group for their support and guidance through my study.

I am also grateful to Dr. Christopher Ross for the human *IP_3RI* cDNA, Dr. Joe Lewis for the Sf9 and Sf21 cell, Prof. Malcolm Walkinshaw for the human *FKBP12* cDNA, Prof. Katsuhiko Mikoshiba for the mouse *IP_3RI* cDNA and Linda Sharp for assistance of confocal microscope.

Finally, I would like to thank my family and friends for their invaluable support during this long time.

Contents

Figures

Tables

Chapter 1

Chapter 2

Abbreviation

A	Ampere
AEBSF	4-(2-aminoethyl)benzenesulfonyl fluoride
AIF	Apoptosis-inducing factor
AM	Amplitude modulation
AMPAR	α-amino-3-hydroxy-5-methyl-4-isoxazole propionic acid receptor
AMP-PCP	β, γ-methyleneadenosine 5'-triphosphate
ATP	Adenosine 5'-triphosphate
5-HT	5-hydroxytryptamine
cADPR	Cyclic ADP-ribose
CaMKII	Ca^{2+}-calmodulin dependent protein kinase II
cAMP	Adenosine 3', 5'-cyclic monophosphate
cGMP	Guanosine 3', 5'-cyclic monophosphate
CIAP	Calf intestinal alkaline phosphatase
CICR	Ca^{2+}-induced Ca^{2+} release
CNS	Central nervous system
CRAC	Ca^{2+}-release-activated Ca^{2+} channel
CREB	cAMP response element binding protein
Da	Dalton
ddNTP	dideoxynucleotide
DEPC	Diethyl pyrocarbonate
DHP	Dihydropyridine
DHPR	Dihydropyridine receptor
DMEM	Dulbecco's modified Eagle medium
DMSO	Dimethyl sulphoxide
dNTP	deoxynucleotide
DNA	Deoxyribonucleic acid
EDTA	Ethylenediaminetetraacetic acid
EGTA	Ethylene glycol-bis-(β-aminoethyl ether) N,N,N',N'-tetraacetic acid
EPSC	Excitatory postsynaptic current
EC	Excitation-contraction
f	Fico
FKBP	FK506-binding protein
FKBP12	12 kDa FK506-binding protein
FM	Frequency modulation
FRB	Formaldehyde running buffer
g	Gravity, gram
Glu	Glutamate
h	Hour
HEPES	N-(2-hydroxyethyl)piperazine-N'-(2-ethanesulfonic acid)
Hz	Hertz
IP_3	Inositol 1,4,5-trisphosphate
IP_3R	Inositol 1,4,5-trisphosphate receptor
IP_3RI	Type I inositol 1,4,5-trisphosphate receptor
IP_4	Inositol 1,3,4,5-tetrakisphosphate

k	Kilo
KAR	Kainate receptor
LB	Luria-Bertani
LGCC	Ligand-gated non-selective cation channel
LTD	Long-term depression
LTP	Long-term potentiation
m	Milli
M	Molar concentration
min	minute
MOPS	3-(N-morpholino)propanesulfonic acid
n	Nano
nAChR	Nicotinic acetylcholine receptor
NF-ATs	Nuclear factor of activated T cells
NMDAR	N-methyl-D-aspartate receptor
p	Pico
PBS	Phosphate buffered saline
PEG	Polyethylene glycol
PKA	cAMP-dependent protein kinase
PKC	Protein kinase C
PKG	cGMP-dependent protein kinase
PMCA	Plasma membrane Ca^{2+}-ATPase
QED	Quantum emission domain
RACC	Receptor-activated Ca^{2+} channel
RNA	Ribonucleic acid
rpm	Revolutions per minute
RyR	Ryanodine receptor
RyR1	Type 1 ryanodine receptor
s	Second
S	Siemen
SDS	Sodium dodecyl sulphate
SDS-PAGE	Sodium dodecyl sulphate-polyacrylamide gel electrophoresis
SERCA	Sarco/endoplasmic reticulum Ca^{2+}-ATPase
SMOC	Spontaneous miniature outward current
SOC	Store-operated Ca^{2+} channel
SR/ER	Sarco/endoplasmic reticulum
STOC	Spontaneous transient outward current
TBE	Tris-borate containing EDTA
TE	Tris containing EDTA
TM	Transmembrane segment
Tris	Trishydroxymethyl aminomethane
TRP	Transient receptor potential
TRPL	Transient receptor potential like
μ	Micro
UV	Ultraviolet
V	Volt
VOCC	Voltage-operated Ca^{2+} channel

v/v	Volume/volume
W	Watt
w/v	Weight/volume
X-gal	5-bromo-4-chloro-3-indoyl-β-D-thiogalactopyranoside

Abstract

Ca^{2+}, including Ca^{2+} released from intracellular stores, plays a versatile role in controlling many different cellular functions, including fertilisation, muscle contraction and neuronal signalling. The inositol 1,4,5-trisphosphate receptor (IP_3R) is an important intracellular Ca^{2+}-release channel located primarily in sarco/endoplasmic reticulum (SR/ER). Three different *IP_3R* genes (type I, II and III) have been molecularly cloned and functionally studied. IP_3R type I protein (IP_3RI) has been identified in many tissues, and is the predominant receptor in human brain.

In this study, a full-length human *IP_3RI* was assembled from three overlapping fragments obtained from a human brain cDNA library. In initial work using *in vitro* coupled transcription/translation and *in vivo* expression in HEK293 cells, a C-terminally truncated IP_3RI was obtained. Further sequence analysis identified a nucleotide deletion at position 6429, which caused the reading frame to be shifted and a stop codon to be generated at position 6455 resulting in a 200 kDa protein rather than 260 kDa. After correcting this by subcloning, full-length recombinant human IP_3RI was expressed from an *in vitro* system and in HEK293 cells. Indirect immunofluorescence confirmed that overexpressed IP_3RI was located in the ER. In contrast, the FK506-binding protein FKBP12, expressed from another cloned cDNA in the same cells, was mainly cytoplasmic. However, the overexpressed IP_3RI did not have measurable IP_3 binding activity, or channel activity when reconstituted in planar lipid bilayers, probably because of the low expression level following transient expression. Attempts to establish a stable cell line were unsuccessful, and a baculovirus expression vector system was therefore used to obtain high level

expression. Full-length expressed IP_3RI had an IP_3 binding activity of about 0.6 pmol/mg of microsomes, which is much lower than that reported elsewhere. This suggests that further optimisation of expression is required. However, the truncated protein, which contained the N-terminal part of IP_3RI responsible for binding IP_3, bound about 3 pmol/mg of microsomes. This is similar to results published for other IP_3Rs. Moreover, despite the absence of the C-terminus containing all the putative membrane-spanning domains, the truncated protein still appeared to be an intrinsic membrane protein. This suggests that there may be other membrane-spanning domains in the human IP_3RI not previously described in other IP_3Rs.

FKBP12 has previously been shown to associate with IP_3RI. In future studies, coexpression of FKBP12 and IP_3RI will be useful to study how FKBP12 modifies the function of recombinant human channels.

Chapter 1

Introduction

1.1 Ca^{2+} Ions in Biology

Ca^{2+} plays a very important role in controlling many physiological functions, including fertilisation, cell growth, secretion, muscle contraction and neuronal signalling (Berridge, 1993, 1997, 1998; Clapham, 1995). Why has nature chosen this ion to mediate so many signalling processes? Unlike many other second-messengers, Ca^{2+} cannot be metabolised, and cells tightly regulate intracellular levels through numerous procedures. The intracellular level of Ca^{2+} must be kept low because it precipitates phosphate, the "energy currency" of cells. The normal free intracellular Ca^{2+} concentration is ~100 nM in unexcited cells, but the extracellular Ca^{2+} concentration is ~1 mM, ~10,000 fold higher. Yet if Ca^{2+} were distributed passively, at electrochemical equilibrium, its concentration would be some 100 fold higher inside the cell than outside. In fact, cells use either Ca^{2+}-ATPases or Na^{+}/Ca^{2+} exchangers to transport Ca^{2+} out in order to maintain this low Ca^{2+} level. This steep gradient presents cells with an excellent opportunity, because the cytosolic Ca^{2+} concentration can be raised abruptly for signalling purpose by transiently opening calcium channels in the plasma membrane, or by releasing Ca^{2+} stored within intracellular membrane-bound compartments.

Ca^{2+} can bind tightly to proteins, particularly to negatively charged oxygens (from the side chains of glutamate and aspartate) and uncharged oxygens (main chain carbonyls, and side-chain oxygens from glutamine and asparagine). This allows Ca^{2+} to cross-link different regions of a protein, and induces large conformational changes. Ca^{2+} is able to accommodate 4-12 oxygen atoms in its primary coordination sphere, but coordination numbers of 6-8 are most common (McPhalen *et al.*, 1991).

Furthermore, the binding of Ca^{2+} can be highly selective. Mg^{2+} is a potential competitor in cells because its concentration is ~1,000 fold higher than Ca^{2+}. However, Mg^{2+} does not have appreciable affinity for uncharged oxygen atoms, so it cannot compete with Ca^{2+}. Another difference between Ca^{2+} and Mg^{2+} ions is that Mg^{2+} prefers to form small and symmetric coordination shells, whereas Ca^{2+} can form asymmetric complexes with a larger radius. Thus, Ca^{2+} is suited for binding to irregularly shaped crevices in proteins, and can be selected for over Mg^{2+}.

1.2 Ca^{2+} Efflux from the Cytoplasm

1.2.1 Plasma Membrane Ca^{2+}-ATPases (PMCAs)

PMCAs extrude Ca^{2+} from the cytoplasm to extracellular regions in order to maintain low intracellular Ca^{2+} levels. Four types of PMCAs with a molecular weight of ~130 kDa have been molecularly cloned from human and rat, and at least two alternatively spliced variants are present for each type (Keeton *et al.*, 1993; Strehler, 1991). The topological distribution of the PMCA includes ten transmembrane domains, with minimal protein mass on the extracellular side of the membrane and a large portion protruding from the cytosolic side of the membrane. Both the N- and C-termini are in the cytoplasm. The C-terminus is the most diverse region of different types of PMCA, and contains a calmodulin binding site that regulates the activity of the transporter (Penniston and Enyedi, 1998). In the absence of calmodulin, the pump is relatively inactive, while binding of calmodulin stimulates its activity. Phosphorylation of the PMCA with protein kinase A or C may also modify this regulation.

1.2.2 Intracellular Ca^{2+} Pumps

Sarco/endoplasmic reticulum (SR/ER) Ca^{2+}-ATPases (SERCAs) are found, as the names suggested, in the SR/ER membrane. SERCAs can sequester Ca^{2+} from the cytoplasm into the SR/ER lumen. At least three genes encoding SERCAs have been molecularly cloned and isoforms arising from alternatively spliced variants have also been identified (MacLennan *et al.*, 1997). The molecular weight of SERCA proteins is ~110 kDa. Like PMCAs, SERCAs contain ten transmembrane segments and a large portion of the protein on the cytosolic side of the membrane. The vectorial movement of Ca^{2+} from the cytoplasm to the SR/ER lumen has been proposed to occur as follows: (1) binding of two Ca^{2+} ions to the cytoplasmic domain of the SERCA, (2) phosphorylation of an aspartate residue by one molecule ATP, (3) change in conformation of the SERCA to cause the release of Ca^{2+} into the SR/ER lumen, (4) cleavage of the phosphate bond and return to the original state. In addition, proton countertransport has also been shown during the reaction cycle (Yu *et al.*, 1993). Under optimal conditions, the utilisation of one mole of ATP is accompanied by the transport of two moles of Ca^{2+} into the SR/ER lumen and ejection of two moles of luminal H^+ into the cytoplasm. PMCAs may use the same mechanism to transport Ca^{2+}.

Mitochondria contain Ca^{2+} uniporters, Na^+/Ca^{2+} exchangers and "permeability transition pores", and sequester and release large amounts of Ca^{2+} (Babcock and Hille, 1998). The outer mitochondrial membrane is very permeable to small molecules, so the specific machinery for Ca^{2+} transports lies in the inner membrane.

These transporters have still not been molecularly cloned or purified. It has also been shown that mitochondria and mitochondrial Ca^{2+} play an important role in apoptosis. This function will be discussed in section 1.7.

1.3 Ca^{2+} Influx Across the Plasma Membrane of Cells

1.3.1 Voltage-Operated Ca^{2+} Channels (VOCCs)

1.3.1.1 Molecular Components of VOCCs

Ca^{2+} channels were first purified from the transverse tubule membranes of skeletal muscle (Curtis and Catterall, 1983, 1984), and three subunits, including α_1, β, and γ, were identified. Further analysis have been showed that the α_1 and β subunits are substrates for cAMP-dependent protein kinases (Curtis and Catterall, 1984, 1985). An additional $\alpha_2\delta$ subunit was found co-migrating with the α_1 subunit (Hosey *et al.*, 1987; Leung *et al.*, 1987; Takahashi and Catterall, 1987). After thorough biochemical studies, a structural model has been proposed, which includes a major transmembrane α_1 subunit of 190 kDa associated with a disulfide-linked $\alpha_2\delta$ subunit of 170 kDa, an intracellular β subunit of 55 kDa, and a transmembrane γ subunit of 33 kDa (Takahashi and Catterall, 1987). This model is summarised in Figure 1-1A.

The α_1 subunit contains four repeated domains (I-IV) which each has six transmembrane segments (S1 to S6) and a channel-lining loop between S5 and S6 (Figure 1-1B). This topology has also been found in the Na^+ channel (Tanabe *et al.*, 1987). The β subunit is an intracellular protein, whereas the γ subunit contains four transmembrane segments and can be glycosylated (Jay *et al.*, 1990; Ruth *et al.*, 1989)

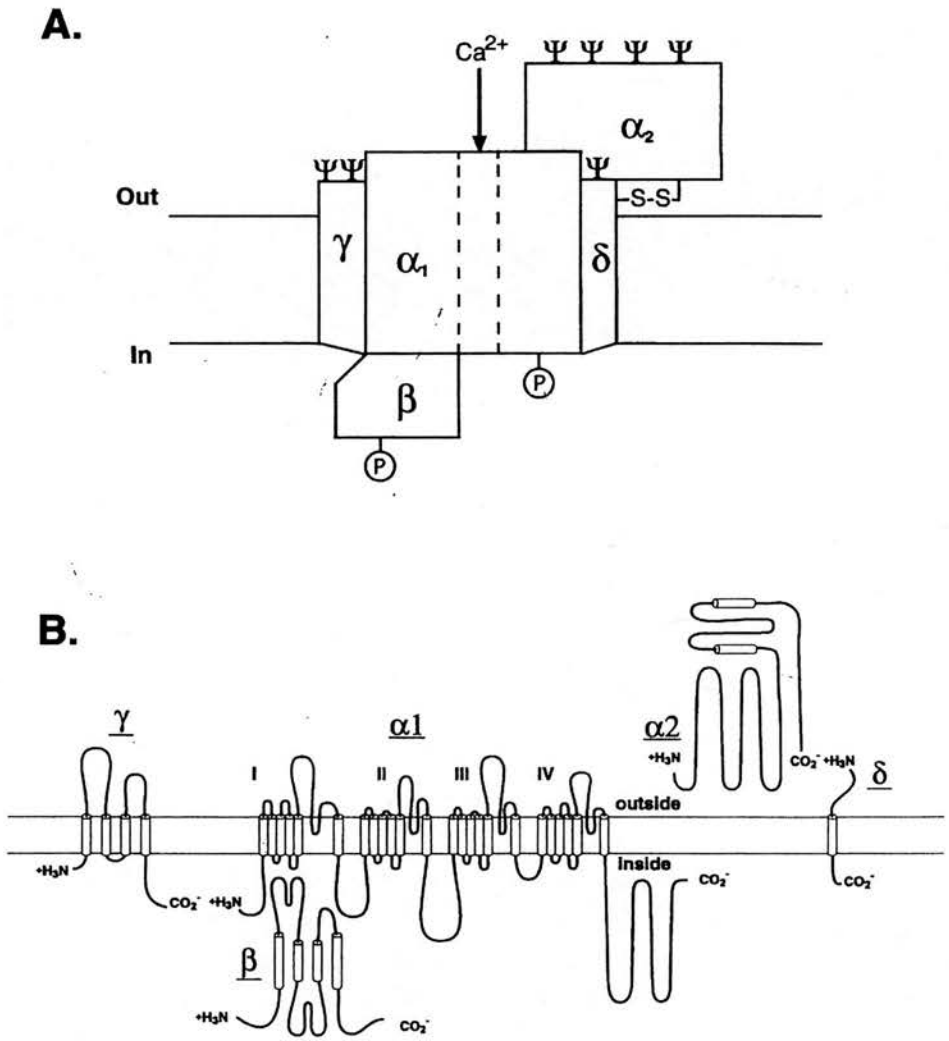

Figure 1-1. Subunit structure of voltage-gated Ca^{2+} channels.

A, The subunit composition and structure of a typical Ca^{2+} channels. P, sites for phosphorylation by cAMP-dependent protein kinase. Ψ, sites for N-linked glycosylation. B, transmembrane folding models for the Ca^{2+} channel subunits. Predicted alpha helices are depicted as cylinders. Adapted from Catterall (1998).

(Figure 1-1B). The α_2 subunit is an extracellular protein and contains many glycosylation sites. It binds to the δ subunit through a disulfide linkage (Gurnett *et al.*, 1996). Interesting, the δ subunit is encoded by the 3'end of the coding sequence of the same gene as the α_2 subunit. The $\alpha_2\delta$ subunit is formed by post-translational proteolytic processing and disulfide linkage (De Jongh *et al.*, 1990; Jay *et al.*, 1991).

1.3.1.2 Subtypes of VOCCs

In cardiac, smooth and skeletal muscle, the major Ca^{2+} currents are distinguished by requiring highly depolarising voltages for activation, and by having large single channel conductances and slow voltage-dependent inactivation. They are regulated by cAMP-dependent protein kinases, and inhibited by specific Ca^{2+} antagonist drugs (Reuter *et al.*, 1983). These drugs include the dihydropyridines (DHPs), and the channels are also described as DHP receptors (DHPRs). These Ca^{2+} currents have been designated L-type, as they are long-lasting (Nowycky *et al.*, 1985). L-type Ca^{2+} currents are also recorded in endocrine cells (Milani *et al.*, 1990) and neurons (Bean, 1989).

A different type of VOCC has been identified in starfish eggs, cerebellar Purkinje neurons and dorsal root ganglion neurons (Hagiwara *et al.*, 1975; Llinas *et al.*, 1981; Nowycky *et al.*, 1985; Swandulla and Armstrong, 1988). The Ca^{2+} currents activate at more negative membrane potentials, inactivate rapidly, have a relatively small single channel conductance and are insensitive to Ca^{2+} antagonist drugs. They were designated low-voltage-activated Ca^{2+} currents or T-type channels from their transient kinetics (Nowycky *et al.*, 1985).

In dorsal root ganglion neurons, additional N-type Ca^{2+} currents have also been found (Nowycky *et al.*, 1985). These Ca^{2+} currents have intermediate voltage dependence, and a rate of inactivation between L- and T-type Ca^{2+} channels. The activity of N-type channels can be blocked by the cone snail peptide ω-conotoxin GVIA (McCleskey *et al.*, 1987). This pharmacological property has become an important method to identify N-type Ca^{2+} channels in different neurons, because they are difficult to specify just by their voltage dependence and kinetics.

Furthermore, since more peptide toxins have been discovered, three additional VOCCs have been found. P-type Ca^{2+} channels with high sensitivity to the spider toxin ω-agatoxin IVA have been found in Purkinje neurons (Llinas *et al.*, 1989). On the contrary, Q-type Ca^{2+} channels have a low sensitivity to ω-agatoxin IVA (Randall and Tsien, 1995). R-type Ca^{2+} channels are defined as resistant to all Ca^{2+} channel blockers, and may contain different subtypes (Randall and Tsien, 1995; Tottene *et al.*, 1996). Taken as a whole, L- and T-type Ca^{2+} channels have been identified in a wide variety of cells, while N-, P-, Q-, and R-type Ca^{2+} channels are predominant in neurons, and play a crucial role in controlling neuron-specific functions.

1.3.1.3 Functional Roles of VOCCs in Neurons

L-type Ca^{2+} channels have primarily been localised to cell bodies and proximal dendrites (Westenbroek *et al.*, 1990) instead of nerve terminals, so it has been assumed that they are not essential in modulating neurotransmitter release. It has been shown that L-type Ca^{2+} channels play a crucial role in the regulation of gene transcription. For example, activation of the transcription of immediate early genes

requires Ca^{2+} influx through L-type Ca^{2+} channels (Murphy *et al.*, 1991). Moreover, activation of the transcription factor CREB (cAMP response element binding protein) also relies on Ca^{2+} influx through L-type Ca^{2+} channels, rather than the influx through N-methyl-D-aspartate (NMDA) receptors (Bading *et al.*, 1993; Rosen *et al.*, 1995). These results show L-type Ca^{2+} channels are important in "excitation-transcription" coupling in neurons.

In contrast to L-type Ca^{2+} channels, N- and P/Q-type Ca^{2+} channels are found in nerve terminals, and thus they are important in the regulation of synaptic transmission (Robitaille *et al.*, 1990; Sugiura *et al.*, 1995; Westenbroek *et al.*, 1992; 1995). First, Kerr and Yoshikami (1984) found that ω-conotoxin GVIA inhibits neurotransmission at the frog neuromuscular junction. From many studies, it has been identified that N-type Ca^{2+} channels are predominant at many peripheral synapses (Olivera *et al.*, 1994). In contrast, P/Q-type Ca^{2+} channels have been found primarily at many central synapses and control synaptic transmission. Although the difference between P- and Q-type Ca^{2+} channels in controlling neurotransmission is not clear (Dunlap *et al.*, 1995), N-, P- and Q-type Ca^{2+} channels play a crucial role in "excitation-transmission" coupling in neurons.

1.3.2 Ligand-Gated Non-Selective Cation Channels (LGCCs)

1.3.2.1 Ionotropic Glutamate Receptor Channels

1.3.2.1.1 N-Methyl-D-Aspartate Receptors (NMDARs)

NMDAR proteins can be divided into two subfamilies: NR1 and NR2. NR1 has a large extracellular N-terminus, three putative transmembrane segments

(TM1,TM3 and TM4) , a hydrophobic channel-lining loop (M2) and an intracellular C-terminus. This topology is identical in all ionotropic glutamate receptor families (Bennett and Dingledine, 1995) (Figure 1-2). They can assemble as either homo- or hetero-pentamers. NR1 itself can form functional homomeric channels. NR1 shares only 25-29% homology with non-NMDA glutamate receptors, but still contains the typical structure of ligand-gated ion channels as mentioned above. NR2 contains four subunits: NR2A, NR2B, NR2C and NR2D, which share 42-56% identity with each other and 21-27% homology with other GluRs. Although these four subunits have the same basic structure as NR1, they have a larger C-terminal domain. None of the four NR2 subunits assembles into functional homomeric channels when expressed in oocytes or cell lines (Hollmann and Heinemann, 1994). However, coexpression of NR1 with each of the four NR2 subunits can form functional heteromeric channels. NR1 has been found in all central neurons, and NR2 is expressed differentially in different brain regions, which enable NMDARs to possess specific functions.

NMDARs mediate the slow excitatory postsynaptic current (EPSC). They are highly permeable to Ca^{2+} with a relative Ca^{2+} to monovalent cation permeability of ~10. Their activity can be blocked by extracellular Mg^{2+} (McBain and Mayer, 1994). It has been shown that an asparagine residue (N) in the M2 region (the Q/R/N site) of the NR1 subunit is an important factor for the modulation of Ca^{2+} permeability, single-channel conductance and voltage-dependent block by extracellular Mg^{2+} (Figure 1-2).

NMDAR-mediated Ca^{2+} influx is essential for the induction of long-term potentiation (LTP) and long-term depression (LTD) (Bliss and Collingridge, 1993).

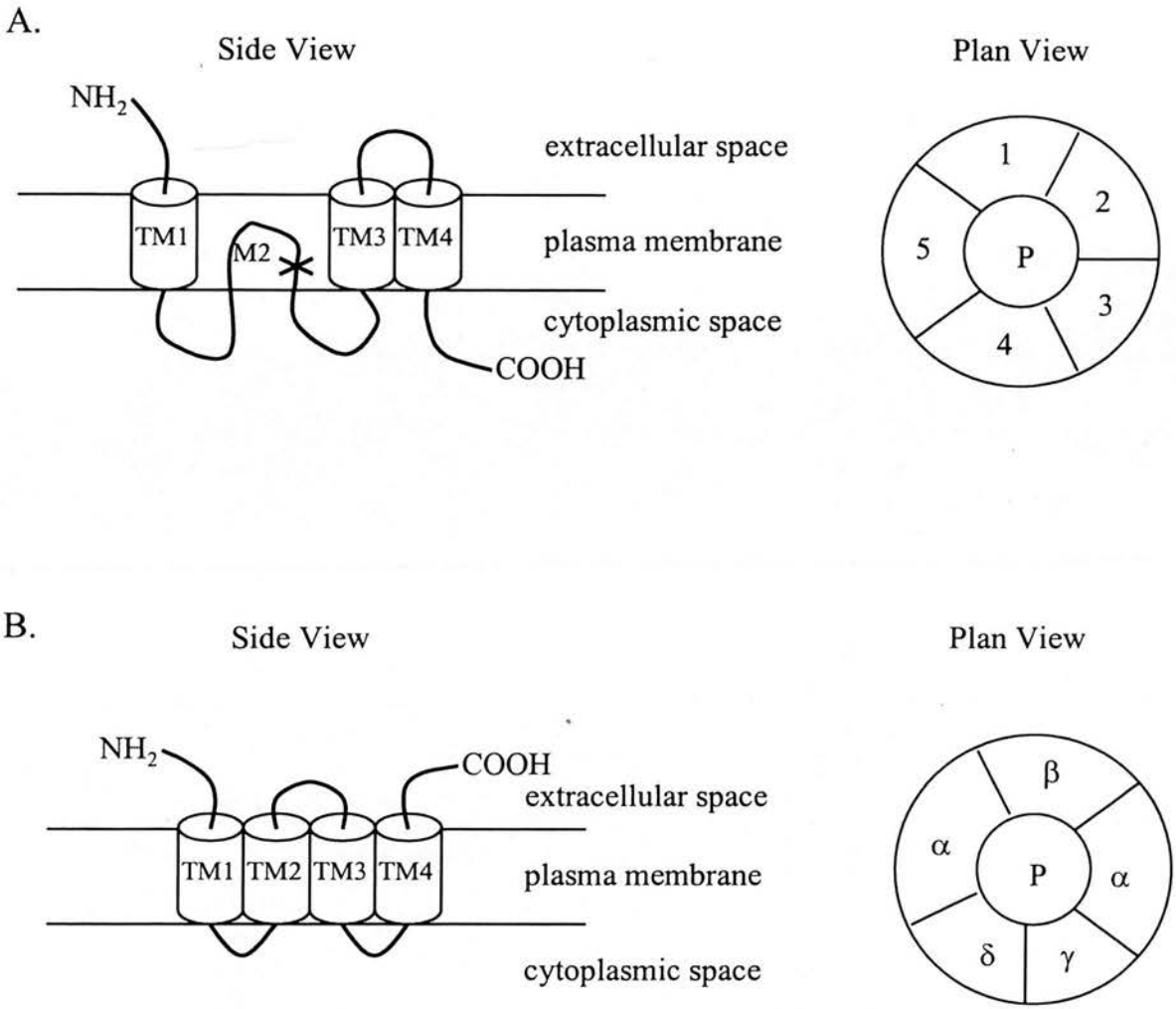

Figure 1-2. The topology of LGCCs.

A. The topology of ionotropic GluRs. From side view, TM1, TM3 and TM4 are transmembrane segments. The cross in M2 (channel-lining loop) shows the Q/R/N site. From plan view, pentameric structure is formed by five subunits (from 1 to 5). P is the channel pore.
B. The topology of nAChRs. From side view, TM1 to 4 are transmembrane segments. From plan view, pentameric skeletal muscle nAChRs are formed by two α, one β, one δ, and one γ subunit. P is the channel pore.

Because LTP is induced only when many synapses on a single postsynaptic neuron are activated simultaneously, a cooperative mechanism is required. The mechanism proposed is that during early stimulation, AMPARs (see the following section for a description), which control the fast EPSC, are activated and depolarise the postsynaptic membrane. The depolarisation of the membrane causes the dissociation of Mg^{2+} blocker from NMDARs, making NMDARs become active with subsequent Ca^{2+} influx. Ca^{2+} then induces the synthesis of NO, which can diffuse to the presynaptic cells and enhance the secretion of glutamate causing more postsynaptic neurons to be activated. The exact mechanism of LTP and LTD are not yet known. However, it has been proposed that the induction of LTP requires a fast increase of $[Ca^{2+}]$, while LTD is activated by a slow increase of $[Ca^{2+}]$ to a sufficient level (Yang *et al.*, 1999). Recently, it has been demonstrated that overexpression of NR2B in the forebrains of transgenic mice enhanced LTP, and these mice showed better "learning" and "memory" (Tang *et al.*, 1999).

Furthermore, the activity of NMDARs is also inhibited by intracellular Ca^{2+} (Kyrozis *et al.*, 1995; Medina *et al.*, 1995). Although the inhibition of NMDARs is independent the source of Ca^{2+}, the NMDAR-mediated Ca^{2+} influx provides a high $[Ca^{2+}]$ nearby the receptor itself. It has been shown that Ca^{2+} influx from NMDARs is a potent inhibitor of feedback inhibition of NMDARs (Rosenmund *et al.*, 1995).

1.3.2.1.2 α-Amino-3-Hydroxy-5-Methyl-4-Isoxazole Propionic Acid Receptors (AMPARs)

The four AMPAR subunits GluR1-GluR4 have similar size (~900 amino acids) and share 68-73% amino acid sequence identity. Each of the GluR1-GluR4 subunits exits in two different forms generated by alternative splicing of a region preceding the transmembrane segment TM4. These splicing variants are differentially distributed in different cells (Sommer *et al.*, 1990). It has been proposed that the differential expression of the GluR2 in heteromeric channels may produce various AMPARs with different Ca^{2+} permeability (Burnashev *et al.*, 1992). Both homomeric and heteromeric channels have been identified. AMPAR subunits (GluR1, 3, and 4) contain a glutamine residue at the Q/R/N site in M2, called Q-form channels, and show a high Ca^{2+} to monovalent cation permeability ratio of ~2. However, AMPAR subunits (GluR2) contain an arginine residue at the Q/R/N site in M2, giving R-form channels, which show a low Ca^{2+} to monovalent cation permeability ratio of ~0.1 (Jonas and Burnashev, 1995).

AMPARs mediate the fast excitatory postsynaptic currents. As mentioned in the previous section, the elevation of intracellular $[Ca^{2+}]$ (at the glutamatergic synapse) is modulated by the coordination of AMPARs and NMDARs. The activity of AMPARs has been shown to be blocked by intracellular polyamines (Bowie and Mayer, 1995). Further studies have indicated that, during repetitive activation of AMPARs, the amplitude of the current increases because of the release of the activity-dependent block of polyamines (Rozov *et al.*, 1998). Therefore, this

phenomenon may play a critical role in controlling the functions of AMPARs during intense synaptic stimulation.

1.3.2.1.3 Kainate Receptors (KARs)

The kainate receptor family includes KA1, KA2, and GluR5, 6, and 7 subunits. KA1 and KA2 subunits are high-affinity kainate receptors whereas GluR5-7 subunits show low-affinity to kainates. KA1 and KA2 subunits share 70% amino acid identity with each other, but only 37% amino acid homology with GluR1-4 subunits and 43% amino acid homology with GluR5-7 subunits. The GluR5-7 subunits share 75-80% amino acid identity with each other, but only 40% amino acid homology with GluR1-4 subunits (Hollmann and Heinemann, 1994). Both GluR5 and GluR6 subunits can form homomeric channels (Sommer and Seeburg, 1992). Either a glutamine or an arginine residue in the Q/R/N site of the putative channel-lining segment M2 has been identified in GluR5 and GluR6 subunits. Further analysis of the GluR6 subunit has revealed two additional positions, located in transmembrane segment TM1, that are generated by RNA editing (either isoleucine or valine, and tyrosine or cysteine). Thus, there are eight different GluR6 subunits with respect to M2 and TM1 regions (Kohler *et al.*, 1993). For the GluR2 subunit of the AMPAR family, less than 1% of the unedited form was found in rat and mouse brain. However, *GluR5* and *GluR6* mRNA variants are abundant in cells.

The Q- and R-form GluR6 channels show similar sensitivity to polyamine blockade as AMPARs. However, the Ca^{2+} to monovalent cation permeability ratio of Q-form GluR6 channels is lower than that of Q-form AMPARs. The R-form GluR6

channels have an even lower Ca^{2+} permeability, suggesting that in both AMPARs and KARs, positively charged arginine residues reduce Ca^{2+} influx through these channel types. Moreover, TM1 editing also influences the Ca^{2+} permeability of GluR6 channels. The Ca^{2+} permeability of the edited TM1 form of Q-form GluR6 channels was increased compared to the non-edited TM1 form of Q-form GluR6 channels, but the R-form GluR6 is unaffected by TM1 editing (Kohler *et al.*, 1993). The effect of TM1 editing on ion permeation through GluR6 channels indicates that the specific residue in the TM1 region may participate in lining the channel pore.

Although many KAR subunits have been cloned and studied, the functional role of KAR channels in the nervous system is still not very clear. Recently, it has been shown that KARs may be synaptically activated in mossy fiber-CA3 neuron contracts (Castillo *et al.*, 1997; Vignes *et al.*, 1997). The functional role of Ca^{2+} entry through KARs remains to be studied.

1.3.2.2 Nicotinic Acetylcholine Receptors (nAChRs)

The nAChR is proposed to have an extracellular N-terminus, four transmembrane domains and an extracellular C-terminus (Figure 1-2B), which is different from the ionotropic glutamate receptor that contains three transmembrane domains and an intracellular C-terminus (Figure 1-2A). Neuronal nicotinic acetylcholine receptors (nAChRs) subunits are divided into two major subfamilies. The α-type subunits (α_2-α_9) are designated on sequence homology with the α_1 subunit of the muscle nAChRs. The β-type subunits contain three members- β_2, β_3, and β_4, designated after the identification of β_1 subunits from muscle nAChRs. The

α-type subunits apparently require coexpression with other α- and/or β-type subunits to form functional nAChRs. "Duplex" α/β combinations and some "triplex" (i.e. αx/αy/β or α/βx/βy) combinations have been identified (Colquhoun and Patrick, 1997). However, α_7-α_9 subunits may also form homomeric nAChRs (McGehee and Role, 1995). The relative Ca^{2+} to monovalent cation permeability ratio of nAChRs, composed from α/β subunit combinations, ranged from 1 to 1.5 (Costa *et al.*, 1994; Vernino *et al.*, 1992). α_7 homomeric channels in oocytes showed the highest value of ~20 (Seguela *et al.*, 1993), which is about two-fold higher than that of NMDARs. Recently, it has been shown that the human α_5 subunits coassembled with $\alpha_3\beta_2$ or $\alpha_3\beta_4$ subunits increased the Ca^{2+} permeability, with a similar Ca^{2+} to monovalent cation permeability ratio of α_7 homomeric nAChRs (Gerzanich *et al.*, 1998). The structural determinants of Ca^{2+} permeability in nAChRs are located in the second hydrophobic M2 domain as in GluRs, which contributes to the channel-lining pore, thus almost every mutation in M2 affects Ca^{2+} permeability (Bertrand *et al.*, 1993; Ferrer-Montiel and Montal, 1993).

Functional nAChRs have a specific feature in the strong inward rectification of the current-voltage relation. It has recently been shown that, similarly to AMPARs, this rectification arises from the release of the voltage-dependent block by intracellular polyamines (Haghighi and Cooper, 1998). Although there is a fast inward current in brain in response to acetylcholine, there was evidence that the current was not mediated by nAChRs (Edwards *et al.*, 1992). The functional role of nAChRs is controversial. Recently, it has been shown that nicotine can stimulate

glutamatergic synaptic transmission, which is induced by the activation of presynaptic nAChRs (McGehee and Role, 1995).

1.3.2.3 ATP-Gated Channels (Purinoreceptors)

ATP-gated, P2X receptor channels, are widely expressed in the central and peripheral nervous system. Seven subunits of the P2X receptor family ($P2X_{1-7}$) have been cloned. The P2X subunits can form homo- and heteromeric channels (Buell *et al.*, 1996; North, 1996). The Ca^{2+} to monovalent cation permeability ratio is depending on the composition of subunits. For example, the ratio for homomeric $P2X_2$ receptors was 2.5, whereas homomeric $P2X_3$ or heteromeric $P2X_{2/3}$ was 1.2 and 1.3, respectively (Virginio *et al.*, 1998). Although the structural determinants of Ca^{2+} permeability of the ATP-gated channels have not been identified, it is assumed that, like GluRs and nAChRs, they are also located in the channel-lining M2 regions.

P2X receptor channels mediate fast synaptic transmission in peripheral ganglia and the central nervous system (Edwards *et al.*, 1992; Gu and MacDermott, 1997). In dorsal root ganglion neurons, the presynaptic P2X receptors cause the release of dopamine (Gu and MacDermott, 1997). They not only modulate transmitter release but may also initiate sensory signals in CNS without peripheral input. This interesting observation makes presynaptic P2X receptors a possible target for pain therapy.

1.3.2.4 Serotonin 5-HT_3 Receptors

Seven different types of serotonin 5-hydroxytryptamine (5-HT) receptors have been molecularly cloned (Gyermek, 1996). Most are coupled to G proteins, and one, the 5-HT_3 receptor, is a cation channel that is substantially permeable to Ca^{2+}. Similar to many other ligand-gated ion channels, 5-HT_3 receptors are probably composed of five subunits. The exact composition of the receptor is not completely understood, but there is evidence supporting the existence of both homo- and heteromers (Hussy *et al.*, 1994). The function of presynaptic 5-HT_3 receptors is not clear. Recently, it has been shown that presynaptic 5-HT_3 receptors can induce exocytosis by increasing intracellular [Ca^{2+}] (Ronde and Nichols, 1998). Thus, Ca^{2+} influx through 5-HT_3 receptors might be important for presynaptic modulation of neurotransmission.

1.3.3 Receptor-Activated Ca^{2+} Channels (RACCs)

RACCs are defined as "any plasma membrane Ca^{2+} channel opened as a result of the binding of an agonist to its receptor, where the receptor protein is separate from the channel protein and the mechanism of channel opening does not involve depolarisation of the plasma membrane" (Barritt, 1999). There are three major types of RACC: (a) intracellular-messenger-activated non-selective cation channels, (b) non-selective cation channels activated by a trimeric G-protein, and (c) store-operated (capacitative) Ca^{2+} channels (SOCs).

It has been shown that in non-excitable cells, RACCs are regulated by the action of cGMP, cAMP, inositol 1,4,5-trisphosphate (IP_3), inositol 1,3,4,5-tetrakisphosphate (IP_4), and arachidonic acid (or arachidonic acid metabolites) (Finn

et al., 1996; Irvine and Moor, 1986; Kiselyov *et al.*, 1997; Shuttleworth and Thompson, 1998). The most thoroughly studied RACCs are the cGMP-activated non-selective cation channels found in mammalian retinal cells. This kind of channel was also identified in olfactory and gustatory cells (Finn *et al.*, 1996), as well as in heart and kidney (Ahmad *et al.*, 1990).

The cGMP-activated channels in retinal rod and cone photoreceptors have an important role in visual transduction. In darkness, a relatively high concentration of cGMP in the cells maintains cGMP-activated cation channels in the open state. Closure of these channels in response to the absorption of light by rhodopsin, and subsequent decrease in the concentration of cGMP, leads to hyperpolarisation of the plasma membrane and decreases the release of neurotransmitters. An important characteristic of the rod and cone cGMP-activated channels is that they show no desensitisation in the presence of ligand (Yau and Baylor, 1989). This property allows the channels to stay open in darkness, and to be closed only by light.

The olfactory cyclic nucleotide-activated channel has similar properties to those of the rod and cone cGMP-activated channels, except that it is activated by a much lower cyclic nucleotide concentration (Nakamura and Gold, 1987). The photoreceptor channels are activated much more readily by cGMP than cAMP, but the olfactory channel is only slightly more sensitive to cGMP than cAMP. Similar to photoreceptor channels, the olfactory channel is highly permeable to Ca^{2+}. The topology of the cyclic-nucleotide-activated cation channel is shown in Figure 1-3A.

Plasma membrane Ca^{2+} channels activated by inositol 1,4,5-trisphosphate (IP_3) have been found in isolated membrane patches (Kiselyov *et al.*, 1997). There is also

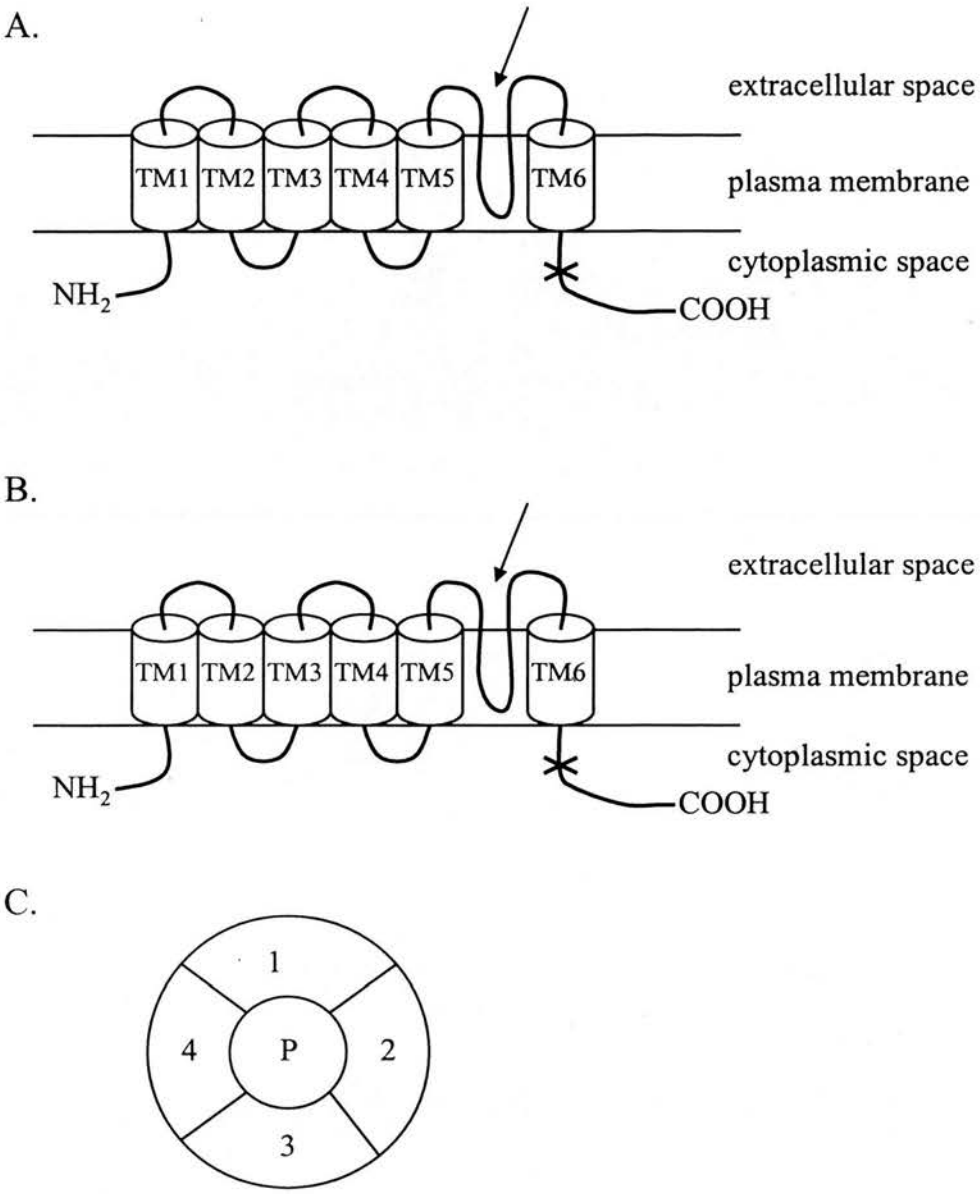

Figure 1-3. The topology of RACCs.

A. The topology of cyclic-nucleotide-activated cation channels containing six transmembrane segments (TM1 to TM6) and a pore-forming loop between TM5 and TM6. The cross shows the cGMP/cAMP binding site. The arrow indicates the pore-forming regions.
B. The topology of *Drosophila* TRP channels is similar to A. The cross shows the calmodulin binding site. The arrow indicates the pore-forming regions.
C. Tetrameric RACCs are formed by four subunits (from 1 to 4), and either homo- or heterotetramers are proposed. P is the channel pore.

other evidence suggesting that some IP_3 receptors (IP_3Rs) are located on the plasma membrane (Khan *et al.*, 1996), although it is very difficult to differentiate between IP_3Rs located in the ER close to the plasma membrane, and IP_3-activated Ca^{2+} channels located in the plasma membrane (Putney, 1997).

IP_4-activated Ca^{2+} channels in the plasma membrane have also been proposed (Parekh and Penner, 1997). There is no clear evidence to show that IP_4 directly activates any plasma membrane Ca^{2+} channels, but it has been assumed that the interaction of IP_4 with either an IP_3R or with an IP_4-binding protein located in the ER near the plasma membrane, or with an IP_4-binding protein in the plasma membrane may exert its effects. Thus, the subsequent interaction of IP_3Rs or IP_4-binding proteins with RACCs in the plasma membrane may open plasma membrane Ca^{2+} channels (Irvine, 1990).

Arachidonic acid or arachidonic acid metabolites can induce the opening of plasma membrane Ca^{2+} channels in many cell types. The generation of the arachidonic acid metabolite leukotriene C4 by epidermal growth factor activates a Ca^{2+} channel with a conductance of ~10 pS (Peppelenbosch *et al.*, 1992). It has been shown that arachidonic acid itself activates plasma membrane Ca^{2+} channels in HEK293 cells when human M3-muscarinic receptors were stably transfected (Shuttleworth and Thompson, 1998). It has also been proposed that arachidonic acid may regulate the activation of some SOCs (Wolf *et al.*, 1997).

It has been shown that guanosine 5'-[γ-thio]trisphosphate, an activator of trimeric G-proteins, activates non-selective cation channels in mast cells (von zur Muhlen *et al.*, 1991). The binding of carbachol to M3-muscarinic receptors leads to

an increase in intracellular Ca^{2+} concentration, which suggests that RACCs are activated by direct interaction with a trimeric G-protein (Singer-Lahat *et al.*, 1996; 1997). It has also been shown that the third cytoplasmic loop of the M3-muscarinic receptor, which associated with G-proteins, is required for the activation of Ca^{2+} inflow but not for the release of Ca^{2+} from the ER. Another example is the *Drosophila* transient receptor potential like (TRPL) non-specific cation channel, which is opened in response to a direct interaction between $G_{11\alpha}$ and the TRPL (Obukhov *et al.*, 1996).

SOCs were first described by Putney (1986), who found that the depletion of intracellular stores activates a calcium entry mechanism at the plasma membrane called "capacitative" calcium entry. Use of patch-clamp techniques provided a way to examine the properties of SOCs. In lymphocytes and mast cells, plasma membrane Ca^{2+} channels could be opened by inducing the release of Ca^{2+} from the ER by adding thapsigargin, IP_3 or ionomycin (Parekh and Penner, 1997). These SOCs were called Ca^{2+}-release-activated Ca^{2+} channels (CRACs), and the current was designated I_{CRAC}. CRACs are very specific to Ca^{2+}, and contain some other distinctive characteristics, including a very low unitary conductance (~ 20 fS) and a dependence of I_{CRAC} on extracellular [Ca^{2+}] (Parekh and Penner, 1997).

One or more subtypes of SOC are present in a wide variety of non-excitable and excitable cells. Channels with the characteristics of CRACs have so far only been detected in lymphocytes and mast cells (Parekh and Penner, 1997). However, other types of SOCs with characteristics similar to CRACs were identified in macrophages, megakaryocytes, MDCK cells, 3T3 fibroblasts, hepatocytes, pancreatic

acinar cells, endothelial cells and *Xenopus* oocytes (Fasolato and Nilius, 1998; Yao and Tsien, 1997). SOCs conduct Ca^{2+} with the exception of those Na^{+} channels that are activated by a decrease in ER [Ca^{2+}] (Krause *et al.*, 1996), and they may play a crucial role in intracellular Ca^{2+} homeostasis.

Transient receptor potential (TRP), a plasma-membrane Ca^{2+} channel, and also TRPL (as memtioned earlier), have been identified from the *Drosophila* photoreceptor cell (Montell, 1997) (Figure 1-3B). The absorption of light by rhodopsin leads to an increase in the open-probability of TRP and TRPL, and the subsequent influx of Na^{+} and Ca^{2+} depolarise the plasma membrane of the photoreceptor cell. In addition, the absorption of light by rhodopsin also leads to the activation of a phospholipase C isoform (encoded by the *Drosophila NorpA* gene) and the formation of IP_3. It has been proposed that the function of the channel protein was regulated directly by IP_3 or through an IP_3-induced Ca^{2+}-release from the ER (Hardie and Minke, 1993). Therefore, TRP and TRPL are considered as possible models for SOCs in animal cells.

Following the discovery of mammalian homologues of *Drosophila* TRP gated by Ca^{2+}-store depletion, they became the channels of choice for studying gating by store depletion. HEK293 cells stably transfected with human TRP3 (hTRP3) have recently been used to demonstrate functional coupling between hTRP3 and IP_3Rs (Kiselyov *et al.*, 1998). The activation of hTRP3 by store depletion was inhibited by the inhibition of IP_3Rs. In excised patches, the regulation of hTRP3 by IP_3 could be "washed away" and then completely reconstituted by incubating the patches with native or partially purified recombinant IP_3Rs. The discovery of hTRP3 channels

forming stable complexes with IP_3Rs, and the specific sequences of the two proteins interacting *in vitro*, provides strong evidence to support the regulation of hTRP3 channels by IP_3Rs (Kiselyov *et al.*, 1999; Vannier *et al.*, 1999). On the basis of these findings, it has been proposed that coupling of SOCs to IP_3Rs provides a molecular mechanism for gating by Ca^{2+}-store depletion.

1.4 Ca^{2+} Efflux from Intracellular Stores

1.4.1 Inositol 1,4,5-Trisphosphate Receptors (IP_3Rs)

Receptors for the second messenger inositol 1,4,5-trisphosphate (IP_3) constitute a family of Ca^{2+} channels responsible for the mobilisation of Ca^{2+} from intracellular Ca^{2+} stores. IP_3 receptors (IP_3Rs) have been purified from a variety of sources (Chadwick *et al.*, 1990; Dasgupta *et al.*, 1997; Mourey *et al.*, 1990; Supattapone *et al.*, 1988) and were first cloned from mouse cerebellum (Furuichi *et al.*, 1989). IP_3Rs are thought to reside in the ER membrane. However, in some tissues, IP_3Rs have been localised to the plasma membrane (Khan *et al.*, 1992) and nuclear membrane (Gerasimenko *et al.*, 1995; Stehno-Bittel *et al.*, 1995). The latter localisation is not surprising, since the outer nuclear membrane is continuous with the ER membrane in cells. Recently, it has been suggested that IP_3Rs may also mediate Ca^{2+} release from secretory vesicles (Petersen, 1996; Yule *et al.*, 1997) and the Golgi apparatus (Pinton *et al.*, 1998). IP_3 induces Ca^{2+} fluxes from biochemical studies and the reconstitution of purified protein in planar lipid bilayers gives rise to Ca^{2+} channels (Ferris *et al.*, 1989; Mayrleitner *et al.*, 1991).

Three distinct *IP_3R* genes (I-III) have been molecularly cloned from rodent and human tissues (Blondel *et al.*, 1993; Furuichi *et al.*, 1989; Harnick *et al.*, 1995; Maranto, 1994; Mignery *et al.*, 1990; Nucifora *et al.*, 1995; Sudhof *et al.*, 1991; Yamada *et al.*, 1994; Yamamoto-Hino *et al.*, 1994) and form both homo- (Hirota *et al.*, 1995) and hetero-tetrameric assemblies (Monkawa *et al.*, 1995; Wojcikiewicz and He, 1995). Two additional isoforms, type IV (De Smedt *et al.*, 1994; Ross *et al.*, 1992) and V (De Smedt *et al.*, 1994), are proposed to exist based on the result of RT-PCR. However, IP_3RIV may be a splice variant of IP_3RII (Parys *et al.*, 1995; Ross *et al.*, 1992). IP_3RI is spliced at three regions, termed S1 (Nakagawa *et al.*, 1991), S2 (Danoff *et al.*, 1991; Nakagawa *et al.*, 1991) and S3 (Nucifora *et al.*, 1995). S2 contains five distinct variants resulting from alternative splicing (Iida and Bourguignon, 1994; Nakagawa *et al.*, 1991). IP_3Rs have also been cloned from *Drosophila* (Sinha and Hasan, 1999; Yoshikawa *et al.*, 1992) and *Xenopus* (Kume *et al.*, 1993). The predicted molecular weight of IP_3Rs is ~300 kDa, but the apparent molecular weight of IP_3Rs from SDS-PAGE is ~260 kDa. Using non-denaturing polyacrylamide gel electrophoresis, the apparent molecular weight of IP_3Rs is approximately four times that estimated under denaturing conditions. This suggests that native IP_3Rs form a tetramer (Supattapone *et al.*, 1988). Both homomeric and heteromeric complexes have been found (Joseph *et al.*, 1995; Monkawa *et al.*, 1995; Wojcikiewicz and He, 1995). From deletion analysis, IP_3Rs are divided into three regions; a large N-terminal IP_3-binding domain, an intervening regulatory domain and a short C-terminal hydrophobic domain (Figure 1-4).

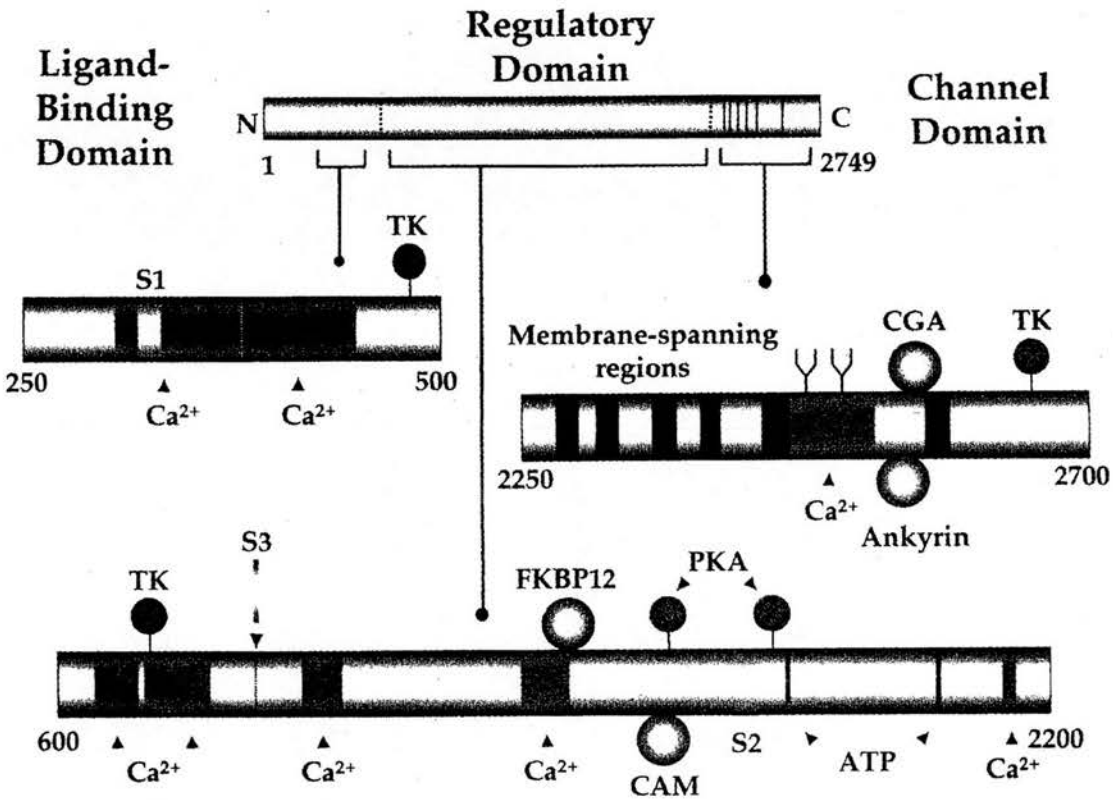

Figure 1-4. Domain structure of the IP_3RI.

The IP_3RI consists of an N-terminal ligand-binding domain, a central regulatory domain and a C-terminal channel domain containing six membrane-spanning regions. Ca^{2+}-binding sites are highlighted throughout the sequence. The accessory proteins, chromogranin A (CGA), ankyrin, FK506-binding protein (FKBP12) and calmodulin (CAM) are depicted as large open circles. Cytosolic phosphorylation sites for cAMP-dependent protein kinase (PKA) and tyrosine kinase (TK) are depicted as small solid circles. ATP-binding regions and sites for N-glycosylation (Ψ) are also shown. S1, S2 and S3 represent the alternative splicing sites. Adapted from Patel *et al.* (1999).

A series of deletion mutants showed that IP_3RI binds IP_3 within the N-terminal 650 amino acids, independently of tetramer formation (Mignery and Sudhof, 1990; Miyawaki *et al.*, 1991). More detailed deletion analysis has defined amino acids 226-578 as the minimal region required for high affinity IP_3 binding (Yoshikawa *et al.*, 1996). Recently, it has been shown that the IP_3-binding pocket consists of two non-covalently but tightly associated structural domains each of which has a discrete function: the C-terminal domain (341-604) alone has low affinity for IP_3, whereas the N-terminus alone (1-343) is incapable of binding but is able to potentiate binding affinity (Yoshikawa *et al.*, 1999).

The regulatory domain contains several Ca^{2+}-binding sites (Sienaert *et al.*, 1996; 1997), two ATP-binding sites and sites for phosphorylation by different protein kinases (Furuichi *et al.*, 1989). In addition, several accessory protein have been identified for the regulation of the IP_3R (see section 1.5). A critical property of the IP_3R is its regulation by cytosolic Ca^{2+}. Many Ca^{2+}-binding sites have been identified throughout the IP_3R (Mignery *et al.*, 1992; Sienaert *et al.*, 1997). Two of these regions (residues 304-381 and 378-450) fall within the IP_3-binding domain, suggesting that Ca^{2+} binding at these sites may exert complex effects on IP_3 binding (Pietri *et al.*, 1990). Biphasic effects of cytosolic Ca^{2+} on IP_3-stimulated Ca^{2+} flux were first described by Iino (Iino, 1990). During sustained exposure to Ca^{2+}, responses to submaximal concentrations of IP_3 are enhanced by modest increases in cytosolic Ca^{2+} ($\leq$300 nM), while more substantial increases in Ca^{2+} concentration inhibit responses to most IP_3 concentrations. Although there are tissues in which IP_3Rs do not show a biphasic effect with Ca^{2+}, there is no doubt that in many tissues

physiological changes in cytosolic Ca^{2+} concentration biphasically modulate IP_3Rs. Changes in ER luminal [Ca^{2+}] may also regulate IP_3R activity (Missiaen *et al.*, 1991; Nunn and Taylor, 1992). The multiple effects of Ca^{2+} have attracted considerable attention, since they are clearly a key element in the modulation of Ca^{2+} oscillations.

ATP also exerts biphasic effects on IP_3Rs. The activity of IP_3Rs is increased by adding ATP to the micromolar concentration range, and decreased when the concentration of ATP reaches millimolar levels (Bezprozvanny and Ehrlich, 1993; Ehrlich and Watras, 1988; Iino, 1991). These effects are thought to be mediated by two independent binding sites (residues 1773-1780 and 2016-2021 of mouse IP_3RI). Because of its high charge, ATP is a competitive antagonist at the IP_3-binding site at higher concentration, exerting inhibitory effects (Nunn and Taylor, 1990; Willcocks *et al.*, 1987).

In addition to the property of autophosphorylation (Ferris *et al.*, 1992), IP_3Rs are substrates for several protein kinases, including cAMP-dependent protein kinase (PKA), cGMP-dependent protein kinase (PKG), protein kinase C (PKC) and Ca^{2+}-calmodulin dependent protein kinase II (CaMKII). In hepatocytes, activation of PKG induces Ca^{2+} oscillations (Rooney *et al.*, 1996). The activation of PKA has similar effects (Burgess *et al.*, 1991). It has been shown that cGMP potentiated the effects of IP_3-forming agonists and increased the sensitivity of intracellular stores to IP_3 (Guihard *et al.*, 1996; Rooney *et al.*, 1996). PKC and CaMKII have been shown to increase the sensitivity of Ca^{2+} flux to IP_3 (Cameron *et al.*, 1995). The activity of IP_3Rs is also regulated by tyrosine phosphorylation (Jayaraman *et al.*, 1996). Following T cell activation, non-receptor tyrosine kinases have been shown to

associate with and phosphorylate IP_3Rs, increasing their open probability. One of these phosphorylation sites falls within the IP_3-binding site. Therefore, the binding of IP_3 may be modulated by tyrosine phosphorylation.

The three major isoforms of the IP_3R can be found in variety of tissues and cell lines with different expression levels (De Smedt *et al.*, 1994; Wojcikiewicz, 1995). Cerebellar Purkinje cells express exclusively IP_3RI, whereas IP_3RII and IP_3RIII predominate in AR4-2J cells (a rat pancreatic acinar cell line) and RIN-5F cells (a rat hepatocyte cell line), respectively. However, most cells express all three isoforms to a different degree. Promoter regions for IP_3Rs have been cloned and analysed (Furutama *et al.*, 1996; Kirkwood *et al.*, 1997; Morikawa *et al.*, 1997). The tissue distribution of a *LacZ* gene fused to the promoter of the IP_3RI in transgenic mice is very similar to that of the native protein (Furutama *et al.*, 1996). Hence, transcriptional regulation of IP_3Rs may underlie the differences in the expression of IP_3Rs observed throughout the body. IP_3Rs can also be down regulated post-transcriptionally. In SH-SY5Y cells (a human neuroblastoma cell line), IP_3R degradation has been proposed to be mediated by the Ca^{2+}-sensitive protease, calpain (Wojcikiewicz and Oberdorf, 1996). Down regulation of IP_3Rs may function to limit the effects of chronic agonist stimulation on Ca^{2+}-release.

1.4.2 Ryanodine Receptors (RyRs)

Ryanodine is an insecticidal plant alkaloid, which affects the function of skeletal and cardiac muscle. Three different ryanodine receptor genes have been identified in mammals, and they are designated as the skeletal, cardiac and brain

ryanodine receptor genes or *ryr1*, *ryr2* and *ryr3*, respectively (McPherson and Campbell, 1993). In fact, skeletal muscle SR contains mainly the RyR1 protein with some RyR3, while RyR2 is predominant in cardiac muscle. Brain contains all three isoforms, which are also widely distributed in other tissues. *ryr1* was specifically localised to region 19q13.1 on the long arm of human chromosome 19 (MacKenzie *et al.*, 1990), whereas *ryr2* was localised to human chromosome 1 (Otsu *et al.*, 1990). *ryr3* was localised to human chromosome 15 at a locus between q14 and q15 (Sorrentino *et al.*, 1993). Each of the three genes encodes an mRNA of ~16 kilobases and a predicted protein of ~5,000 amino acid residues, with an estimated molecular weight of ~560 kDa (Hakamata *et al.*, 1992; Nakai *et al.*, 1990; Otsu *et al.*, 1990; Zorzato *et al.*, 1990).

There are some common features to be found in the three proteins. A motif of ~100 amino acid residues is repeated four times in each protein with unknown function (Hakamata *et al.*, 1992; Nakai *et al.*, 1990; Otsu *et al.*, 1990; Zorzato *et al.*, 1990). An N-terminal signal sequence is not present in any of the proteins, indicating that the N-terminus is cytoplasmic. Four (Takeshima *et al.*, 1989) or twelve (Zorzato *et al.*, 1990) putative transmembrane domains have been proposed near the C-terminus of the proteins. The N-terminus and central part of each protein is hydrophilic, and is therefore believed to form the cytoplasmic "foot process" (Takeshima *et al.*, 1989; Zorzato *et al.*, 1990). Within this region, possible locations of ATP, Ca^{2+} and calmodulin binding sites have been proposed. Many of these sites appear to reside approximately halfway between the N-terminus and the first transmembrane segment (Chen *et al.*, 1992; Otsu *et al.*, 1990; Treves *et al.*, 1990).

In skeletal muscle SR, Ca^{2+}-induced Ca^{2+} release is stimulated by adenine nucleotides and inhibited by Mg^{2+}. The Ca^{2+} dependence of the efflux rate forms a bell-shaped curve with a maximum near pCa 6 (Donoso and Hidalgo, 1993; Kim *et al.*, 1983; Meissner, 1984; Sumbilla and Inesi, 1987). Efflux rates decrease as extravesicular free Ca^{2+} concentration approach a pCa 9 or 3. The rate of Ca^{2+} release from cardiac SR is also a biphasic function of free Ca^{2+} concentration, with a similar maximum at 5-20 μM Ca^{2+} (Chamberlain *et al.*, 1984; Chu *et al.*, 1993; Meissner and Henderson, 1987; Rousseau *et al.*, 1986). The bell-shaped Ca^{2+} dependence of release has been hypothesised to result from different Ca^{2+}-binding sites, a high-affinity site that stimulates Ca^{2+} release and a low-affinity site that inhibits release (Meissner and Henderson, 1987; Nagasaki and Kasai, 1983). The mechanism of Mg^{2+} inhibition (Ashley and Williams, 1990) appears to be a competitive displacement of Ca^{2+} from the high-affinity stimulatory site. In contrast to its effect on skeletal SR, Mg^{2+} in the millimolar range does not completely block Ca^{2+} release in cardiac SR (Meissner and Henderson, 1987; Rousseau *et al.*, 1986). Adenine nucleotides and nonhydrolysable ATP analogues, such as β,γ-methyleneadenosine 5'-triphosphate (AMP-PCP), have been shown to counteract the inhibition by Mg^{2+} (Calviello and Chiesi, 1989; Moutin and Dupont, 1988).

The insecticide ryanodine has been shown to either stimulate or inhibit Ca^{2+} fluxes in skeletal or cardiac SR (Gilchrist *et al.*, 1992; Hasselbach and Migala, 1987; Humerickhouse *et al.*, 1993). At ryanodine concentrations in the range of 0.01-10 μM, Ca^{2+} release was stimulated; whereas, at higher concentration in the range of 10-300 μM ryanodine, release was inhibited. In addition, cyclic ADP ribose (cADPR)

mobilises Ca^{2+} from intracellular stores (Galione *et al.*, 1993). It has been shown that cADPR, like caffeine, potentiated Ca^{2+}-induced Ca^{2+} release in sea urchin eggs (Lee *et al.*, 1993). It has been suggested that cADPR may be an endogenous ligand of the RyR. However, its actions appear to be restricted to regulation of non-skeletal muscle RyRs. For example, high concentrations of cADPR (up to 50 μM) failed to increase the open probability of skeletal RyR in planar bilayers (Morrissette *et al.*, 1993). Another group of Ca^{2+}-release agents that affect RyRs are fatty acids and their metabolites. For example, the glycolipid sphingosine had a dual effect. It induced release at high concentrations but inhibited caffeine-induced Ca^{2+} release at low concentrations (Sabbadini *et al.*, 1992). Arachidonic acid, stearic acid, palmitoyl carnitine and palmitoyl coenzyme A also stimulated Ca^{2+} release from skeletal or cardiac SR (Cardoso and De Meis, 1993; Dettbarn and Palade, 1993; el-Hayek *et al.*, 1993).

In skeletal and cardiac muscle, excitation-contraction (EC) coupling is defined as the process by which an action potential propagated along the surface membrane and the transverse tubules in junctional SR, triggers the rapid release of Ca^{2+} from SR (Martin *et al.*, 1994; Rios *et al.*, 1991). The released Ca^{2+} binds to troponin located in the thin filaments, resulting in activation of the contractile apparatus. Like hTRP3 coupling to the IP_3R, skeletal muscle RyRs couple to DHPRs for EC coupling (Nakai *et al.*, 1996). Depolarisation-induced movements of charged protein domains in DHPRs (see section 1.3.1.2) in the transverse tubule membrane are thought to induce reciprocal movements in charged regions of RyRs in the SR membrane, and subsequent Ca^{2+} release from the SR. However, cardiac muscle RyRs do not couple

to DHPRs. In the heart, EC coupling relies heavily on Ca^{2+}-dependent activation of RyR2 by the Ca^{2+} which enters during the prolonged "plateau" phase of the action potential. This Ca^{2+}-induced Ca^{2+} release (CICR) is also present in many noncontractile and nonexcitable cells, and plays a crucial role in the generation of calcium spikes and calcium waves (Berridge, 1997). Some of the properties of IP_3Rs and RyRs are compared in Table 1-1.

1.5 Accessory Proteins that Regulate Intracellular Ca^{2+} Channels

Calreticulin and calsequestrin are structurally similar Ca^{2+} storage proteins located within the lumen of the SR/ER (Niki *et al.*, 1996). The high-capacity Ca^{2+}-binding property enables them to bind ~40 mole of Ca^{2+} per mole of protein. The binding of Ca^{2+} induces large conformational changes in calreticulin and calsequestrin. It has been shown that calsequestrin plays an important role in mediating Ca^{2+} fluxes in skeletal muscle SR. When RyRs in skeletal muscle SR are activated, there is a transient Ca^{2+} influx preceding the expected Ca^{2+} efflux, suggesting reciprocal coupling between RyRs and intraluminal protein. After calsequestrin is removed from the SR, these changes in intraluminal $[Ca^{2+}]$ disappeared (Gilchrist *et al.*, 1992). From planar lipid bilayer studies, adding calsequestrin to the luminal side of the SR increases the open probability of RyRs (Kawasaki and Kasai, 1994). Thus, it has been proposed that calsequestrin may bind directly to RyRs and regulate Ca^{2+} release. The functional roles of calreticulin in the regulation of Ca^{2+} fluxes from SR/ER are not clear. Calreticulin has been found in the cytoplasm and the nucleus, and modulates integrin function and transcription factors

Property	RyRs	IP_3Rs
Subunit molecular mass (deduced from cDNA)	~565 kDa	~320 kDa
Subunit structure	Homotetrameric	Homo/heterotetrameric
Glycosylation	?No	Yes
Transmembrane segments	At least 4	6
Conductance (50 mM luminal $[Ca^{2+}]$)	100 pS	10-20 pS
Activators	Voltage Ca^{2+} IP_3 (slight) Adenine nucleotides Caffeine cADP-ribose	Ca^{2+} IP_3 Adenine nucleotides (variably)
Inhibitors	Ryanodine Ca^{2+} Ruthenium red	Heparin Ca^{2+} IP_3

Table 1-1. Properties of IP_3Rs and RyRs. Adapted from Ashley (1995).

(Meldolesi *et al.*, 1996). In addition, calreticulin inhibits IP_3-induced Ca^{2+} oscillations when overexpressed in *Xenopus* oocytes, suggesting it is coupled to IP_3Rs (Camacho and Lechleiter, 1995). Calreticulin also increases Ca^{2+} accumulation in intracellular stores when expressed in cells (Mery *et al.*, 1996). However, calreticulin knock-out mice show no detectable change in intracellular Ca^{2+} stores (Coppolino *et al.*, 1997).

Triadin is an integral membrane protein of the junctional SR of skeletal muscle triads. The C-terminus of triadin has been shown to interact with both the intraluminal face of the RyR and with calsequestrin (Guo *et al.*, 1996), but not to DHPRs. Thus, it has been proposed that triadin anchors calsequestrin to the skeletal muscle RyR instead of coupling RyRs to DHPRs. In this way, stored Ca^{2+} is close to channel-opening sites of RyRs, which enables the Ca^{2+} released from RyRs more efficient. The interaction between triadin and calsequestrin is inhibited by increasing $[Ca^{2+}]$, whereas its binding to the RyR is Ca^{2+}-independent. Like triadin, junctin is also an integral membrane protein and interacts with calsequestrin, triadin and RyRs (Zhang *et al.*, 1997). The interaction between junctin and calsequestrin is inhibited by increasing $[Ca^{2+}]$, whereas its interaction with RyRs or triadin is Ca^{2+}-independent. It has been proposed that the RyR, junctin, calsequestrin and triadin form a quaternary complex involved in the accumulation and release of Ca^{2+} from the SR.

FK506-binding proteins (FKBPs) are target proteins for the immunosuppressant drugs FK506 and rapamycin. Although several members of this family have been identified, a 12 kDa isoform known as FKBP12 predominates in many cells and tissues. FKBP12 catalyses peptidylpropyl cis-trans isomerisation,

which is essential for protein folding. However, it has been shown that this isomerase activity is not critical for modulating either RyR or IP_3R function (Timerman *et al.*, 1995). FK506 and rapamycin inhibit this isomerase activity, but they act by altering the association of FKBP12 with RyRs and IP_3Rs, rather than by preventing protein folding (Marks, 1996). For example, the interaction between FKBP12 and RyR1 can be disrupted by treatment with FK506 or rapamycin, and RyR1 then shows long-lasting subconductance states in planar lipid bilayer studies (Brillantes *et al.*, 1994). Addition of FKBP12 or coexpression of FKBP12 with RyRs enables channel gating to fully open or closed states, rather than subconductance states. RyR2 has been found to interact with another FKBP isoforms, FKBP12.6 (Timerman *et al.*, 1996). FKBP12 knock-out mice show apparently normal skeletal muscle, but severe dilated cardiomyopathy (Shou *et al.*, 1998). However, abnormal gating properties were identified in both RyR1 and RyR2. The phenotype may come from the different mechanism in EC coupling between cardiac and skeletal muscle (see section 1.4.2). Thus, FKBP12 is essential for regulation of RyR2, while RyR1 may interact with DHPRs to modulate Ca^{2+} fluxes.

The association of the Ca^{2+}-dependent phosphatase calcineurin with IP_3Rs is inhibited by FK506 or rapamycin, indicating that calcineurin is anchored to IP_3Rs via FKBP12 (Cameron *et al.*, 1995). FKBP12 binds IP_3Rs at residues 1400-1401, a leucine-proline dipeptide that is structurally similar to FK506. Similar motifs are present in all IP_3R and RyR isoforms. Use of the yeast three-hybrid assay suggests the formation of ternary complexes between IP_3Rs, FKBP12 and calcineurin (Cameron *et al.*, 1997). However, the interaction between FKBP12 and RyR1 might

not be dependent on calcineurin, since re-addition of FKBP12 is sufficient to restore normal gating properties after depletion with FK506. It has recently been proposed that binding of FKBP12 causes long-range conformational changes of RyR1 (Wagenknecht *et al.*, 1997).

1.6 Spatial and Temporal Signalling by Ca^{2+}

With advances in imaging technology, it has become possible to see the elementary events which constitute Ca^{2+} signalling. These elementary events have a variety of names often reflecting their spatiotemporal properties, such as "sparks", "puffs", "bumps" and "quantum emission domains" (QEDs) (Klein *et al.*, 1996; Sugimori *et al.*, 1994; Wong *et al.*, 1982; Yao *et al.*, 1995). These specific events have been identified as the spontaneous transient outward currents (STOCs) (Benham and Bolton, 1986; Zholos *et al.*, 1994) or the spontaneous miniature outward currents (SMOCs) (Marrion and Adams, 1992), depending on the property of Ca^{2+} current. As the channel opens, Ca^{2+} diffuses out rapidly to produce a plume, which then dissipates more slowly by diffusion once the channel closes. As described in section 1.4.1 and 1.4.2, the opening and closing of IP_3Rs and RyRs is modulated by the positive and negative feedback effects of Ca^{2+}. The elementary events have at least three basic functions. They are essential to maintaining the resting level of Ca^{2+}. They can also produce highly localised $[Ca^{2+}]$ to regulate many physiological processes such as exocytosis or the activation of ion channels, or they can coordinate with each other for the production of global Ca^{2+} signals to activate more distant sites. It has been shown that the small amount of Ca^{2+} released into the cytoplasm

during each elementary event can exert a critical effect on the resting level of Ca^{2+}. This elevation in Ca^{2+} will enhance the excitability of the intracellular receptors, and thus set up the platform for producing global Ca^{2+} signals (Figure 1-5).

Elementary events generate highly concentrated and localised Ca^{2+} signals that can produce a variety of functions, depending on where they occur. As discussed previously, exocytosis is activated by a Ca^{2+} influx entering through VOCCs (Llinas *et al.*, 1992). In smooth muscle, increases in $[Ca^{2+}]$ arising near the plasma membrane activate K^+ channels, causing the muscle to relax. However, when these elementary events deeper in the cell are coordinated to create a global Ca^{2+} signal, the muscle contracts (Nelson *et al.*, 1995). Therefore, elementary events not only contribute to global Ca^{2+} signals, they may also have very precise localised signalling functions such as relaxation and contraction of smooth muscle or exocytosis of secretory vesicles. In order to produce global Ca^{2+} signalling, the elementary events must be tightly coordinated with each other (Bootman and Berridge, 1995). In muscle cells, channel opening is tightly coupled to an action potential in the plasma membrane. However, in non-excitable cells, channels may coordinate their own activity through CICR. This process is much slower because the signal is Ca^{2+} itself diffusing from one channel to another, usually as Ca^{2+} waves. If cells are connected, such intracellular waves can spread into neighbouring cells and become intercellular waves to coordinate cellular responses within a tissue (Figure 1-5).

Ca^{2+} signalling can also be modulated by the engineering principles of amplitude and frequency modulation (AM/FM). Recently, Dolmetsch *et al.* (1997) have clearly demonstrated that differential gene transcription in B lymphocytes is

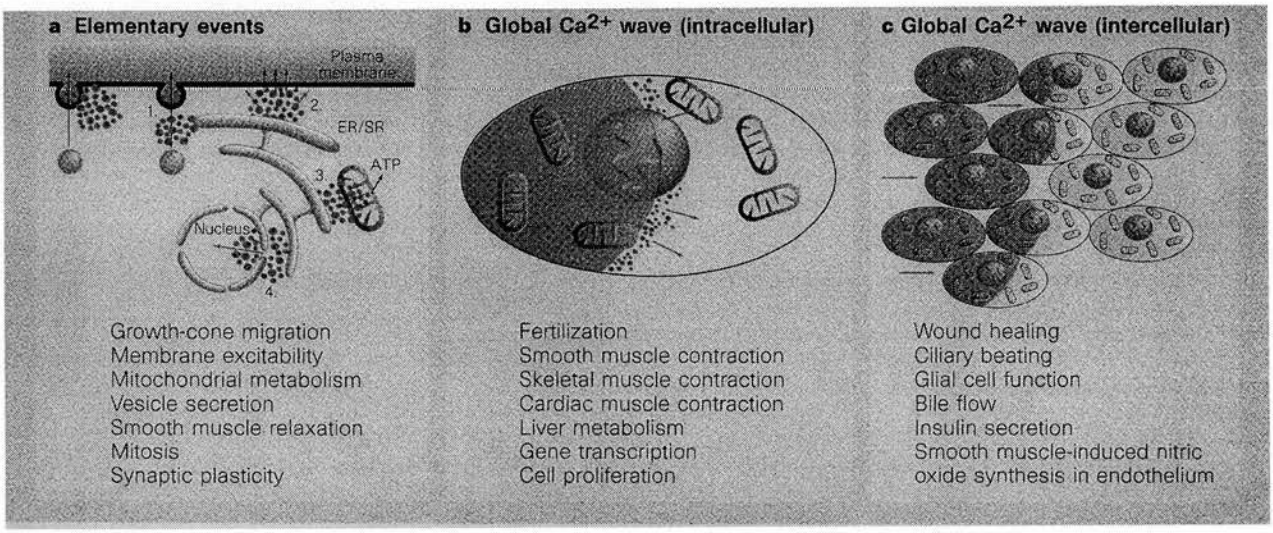

Figure 1-5. Spatial aspects of Ca^{2+} signalling.

a, Elementary events result from the entry of external Ca^{2+} across the plasma membrane or release from internal stores in the ER/SR. They can activate many processes, including export of cellular material (1), opening of K^+ channels (2), metabolism in the mitochondria (3) and Ca^{2+} entry to the nucleus (4). b, Global Ca^{2+} signals are produced by coordinating the activity of elementary events to produce a Ca^{2+} wave. c, The activity of neighbouring cells within a tissue can be coordinated by an intercellular wave. Adapted from Berridge *et al.* (1998).

achieved through amplitude modulation (AM) of the Ca^{2+} signalling system. They found that a low concentration of Ca^{2+} activates the nuclear factor of activated T cells (NF-ATs), whereas a much higher concentration stimulates a different set of transcriptional regulators, such as NF-κB and c-Jun kinase. This differential gene activation using AM signalling mode provides an excellent explanation of how B cells respond differently when they are presented with the same antigen. Naive B cells, which have had no previous contact with the antigen, produce a large Ca^{2+} signal that induces proliferation and positive selection. However, self-tolerant B cells that have responded previously and are thus tolerant to the antigen, generate a much smaller signal which fails to stimulate proliferation. Instead, the cells display negative selection by blocking cell differentiation and antibody secretion.

It was shown some time ago that insect salivary glands use frequency modulation to control fluid secretion (Rapp *et al.*, 1981). In addition, the calmodulin-dependent protein kinase II regulates other enzymes depending on the frequency of $[Ca^{2+}]$ oscillations (De Koninck and Schulman, 1998). Three transcription factors, NF-AT, Oct/OAP and NF-κB, have also been shown to be regulated by $[Ca^{2+}]$ oscillations (Dolmetsch *et al.*, 1998). $[Ca^{2+}]$ oscillations reduced the effective Ca^{2+} threshold for activating transcription factors, thereby increasing signal detection at low levels of stimulation. Rapid Ca^{2+} oscillations stimulated all three transcription factors, whereas infrequent Ca^{2+} oscillations only activated NF-κB.

1.7 Ca^{2+}, Cell Division and Cell Death

There are two major kinds of death process: apoptosis and necrosis. Apoptosis is a tightly regulated process and characterised by some specific events, including chromatin condensation, regular DNA fragmentation pattern, protein degradation by proteases, cell shrinkage and no mitochondria swelling. However, necrosis is poorly regulated and performs different pathological events, including leakage of cell content, cell inflammation and swelling of cytoplasm and mitochondria (Kroemer *et al.*, 1998). Although the relation between apoptosis and necrosis is controversial (Leist and Nicotera, 1997; Raffray and Cohen, 1997), generally apoptosis is a tightly controlled programmed cell death, whereas necrosis happens accidentally because of homeostatic failure.

Ca^{2+} is a versatile second messenger, which regulates a wide variety of molecular, genetic and enzymatic functions during apoptosis. For example, calpains are a family of heterodimeric proteases, which contain Ca^{2+}-binding domains. The importance of calpains is that they act on a very wide range of cellular substrates, including cytoskeletal proteins, membrane-associated proteins, enzymes and transcription factors (Carafoli and Molinari, 1998). Thus, calpain-induced proteolysis may be essential for the regulation of apoptosis.

Chromatin condensation and the nuclear fragmentation are two important events during apoptosis. The precise mechanisms are not fully understood. However, the formation of distinct DNA fragments of 180-200 bp in size is performed by an endogenous Ca^{2+}/Mg^{2+}-dependent endonuclease (e.g. DNase I) which induces the

DNA fragmentation (Hale *et al.*, 1996). Inhibition of its activity reduces the DNA laddering, whereas its overexpression induces nuclear apoptosis.

Mitochondria have been shown to play a central role in apoptosis. The disruption of the mitochondrial membrane potential is an early and irreversible event in apoptosis. This pre-apoptosis event is closely related with the opening of the permeability transition pore (Mignotte and Vayssiere, 1998). Two factors released from mitochondria have been shown to be apoptotic signalling molecules. One is the apoptosis-inducing factor (AIF), a flavoprotein (Susin *et al.*, 1999), and the other factor is cytochrome c. In fact, cytochrome c itself is not a apoptosis inducer, while it can cooperate with other factors to activate caspases and nuclear endonucleases (Liu *et al.*, 1996). Bcl-2 families constitute two groups of apoptosis regulatory proteins that may be either a death antagonist (e.g. Bcl-2) or a death agonist (e.g. Bax, Bak) (Kroemer *et al.*, 1998). The relative amount of these proteins establishes a regulatory switch whose function is determined by selective protein-protein interactions (Sedlak *et al.*, 1995). Bcl-2 is located in the outer mitochondrial membrane and may thus exert its actions through preventing the opening of the permeability transition pore (Murphy *et al.*, 1996).

Mitochondria are an important cellular Ca^{2+} compartment, and respond rapidly to changes in cytosolic [Ca^{2+}]. Limited Ca^{2+} uptake increases the speed of electron transfer through the respiratory chain, providing a functional coupling between cell activation and ATP production. In contrast, larger increases in mitochondrial [Ca^{2+}] lead to an eventual inhibition of the respiratory chain, opening of the permeability transition pore and collapse of ATP production (White and Reynolds, 1996). These

events cause cell death. Ca^{2+} signalling thus controls a variety of cellular processes. However, any of these signalling events can be switched on to activate a programme that leads to cell death. To understand how Ca^{2+} signalling suddenly transforms from "being a signal for life to a signal for death" will be a crucial topic in the future (Berridge *et al.*, 1998).

1.8 Aims of This Study

At the outset of this project, the human IP_3RI had not been cloned and expressed. The IP_3RI is the most abundant IP_3R, and it is also the predominant type in human brain. The main aim of this project was to clone and express a functional IP_3RI from human brain. The first objective was to assemble a full-length human *IP_3RI* from three overlapping cDNA clones. By using *in vitro* or *in vivo* expression systems, the full-length IP_3RI can then be overexpressed, and functionally studied by IP_3 binding assays. Further study of single channel activity of the expressed IP_3RI reconstituted into planar lipid bilayers would also be possible. In addition, FKBP12, a cytosolic protein, which is relatively small (12 kDa) compared to IP_3RI, has been shown to bind to IP_3RI. In addition to cloning and expression experiments with FKBP12 in parallel with IP_3RI, to test the methods used, future coexpression of FKBP12 and IP_3RI would be useful to investigate how FKBP12 affects the function of the Ca^{2+}-release channel.

Chapter 2

Materials and Methods

2.1 Materials and Suppliers

2.1.1 Chemicals and Reagents

All chemicals were the best available grade and supplied by Sigma-Aldrich Company Ltd., Dorset, England except where otherwise stated.

2.1.2 Molecular Biology Reagents

There were obtained from suppliers as follows:

Amersham, Little Chalfont, Bucks, UK.

[α^{35}S]-dATP radiolabelled nucleotides, Hybond-C pure nitrocellulose membrane, ECL detection kit, Sequenase II DNA sequencing kit, D-myo-[^{3}H]inositol 1,4,5-trisphosphate, potassium salt.

Boehringer Mannheim, Lewes, Sussex, UK.

Calf intestinal alkaline phosphatase, Complete protease inhibitor.

Difco Laboratories, Surrey, UK.

All media components for bacterial cell culture.

Flowgen, Staffordshire, UK.

Sequagel polyacrylamide reagent system, SeaKem LE agarose, SeaPlaque agarose.

GIBCO BRL, Paisley, UK.

All reagents and media for cell culture, 1kb DNA ladder, Lipofectin reagent, Lipofectamine reagent.

ICN Pharmaceuticals, Irvine, CA, USA.

TRAN^{35}S-Label.

Invitrogen, Leek, The Netherlands.

MaxBac 2.0 kit, plasmid vector pcDNA3.1.

New England Biolabs, Hitchin, Hertfordshire, UK.

All restriction endonucleases.

OSWEL Ltd., Southampton, UK.

All DNA synthesis and automated DNA sequencing.

Pharmacia Biotech, St. Albans, UK.

dNTPs.

Promega Corporation UK, Southampton, UK.

T4 DNA ligase, *Taq* DNA polymerase, TnT coupled transcription/translation kit, plasmid vectors pCI and pCI-neo.

QIAGEN Ltd, Dorking, Surrey, UK.

Qiagen 500 plasmid purification kit, miniprep spin columns, QIAEX II DNA extraction kit.

Stratagene, La Jolla, CA, USA.

Plasmid vector pBluescript II KS (+/-), E. coli strain XL1-Blue MRF', *Pfu* DNA polymerase.

2.1.3 Antibodies

Calbiochem, Beeston, Nottingham, UK.

Rabbit anti-human IP_3R N-terminal polyclonal antibody

Pierce & Warriner, Chester, UK.

Goat anti-rabbit IgG (H+L), horseradish peroxidase conjugate.

Santa Cruz Biotechnology, USA.

Goat anti-human FKBP12 C-terminal polyclonal antibody.

2.2 Details of *Eschericia coli* strains

XL1-Blue MRF': *Δ(mcrA) 183, Δ(mcrCB-hsdSMR-mrr) 173, endA1, supE44, thi-1, recA1, gyrA96, relA1, lac[F' proAB, lacI^{q}ZΔM15, Tn10]*

JM109: *endA1, recA1, gyrA96, thi, hsdR17, (r_k^-, m_k^+), relA1, supE44, Δ(lac-proAB), [F', tra D36, proAB, lacI^{q}ZΔM15]*

2.3 DNA Protocols

2.3.1 Standard Recombinant DNA Protocols

Standard recombinant DNA protocols followed the procedures described by Sambrook *et al.* (1989), including restriction enzyme digestion of DNA, phenol/chloroform extraction of DNA, ethanol precipitation of DNA, and DNA ligation.

2.3.2 Preparation of Competent Bacterial Cells

A single colony was picked up using a sterile pipette tip from an Luria-Bertani (LB) medium plate containing appropriate antibiotics and inoculated into 5 ml of LB medium containing the same antibiotics, and incubated at 37^{0}C in a shaking incubator overnight with shaking at 250 rpm. The overnight culture was diluted 100 fold in 20 ml culture medium containing antibiotics and incubated at 37^{0}C until the OD_{600} reached 0.5. The culture was centrifuged at 3000 x g for 5 min at 4^{0}C, the

supernatant was discarded, and the pellet was placed immediately on ice. The cell pellet was resuspended very gently with 10 ml of 100 mM ice cold $CaCl_2$ by inverting the tube several times, and incubated on ice for 30 min. The suspension was re-centrifuged at 3000 x g for 5 min at 4°C and the pellet was resuspended in 2 ml ice cold 100 mM $CaCl_2$. Competent cells were used after 1 h incubation on ice or 15% glycerol (v/v) was added before freezing 100 µl aliquots in liquid nitrogen and storing at –70°C for up to six months.

2.3.3 Transformation of Competent Bacterial Cells

Competent bacterial cells taken from one frozen 100 µl aliquot was thawed on ice. 10 ng of DNA were added to the tube and mixed by gently swirling the pipette tip, and incubated on ice for 30 min. The tube was transferred to a 42°C water bath for 1 min, and then placed on ice for 2 min. 800 µl of LB medium were added to the tube and incubated for 45 min at 37°C in a shaking incubator with shaking at 250 rpm. 100 µl of the mixture was added to a LB medium plate containing appropriate antibiotics, and spreaded evenly on the surface of the agar by using glass beads. When the medium were almost absorbed by the agar, the plate was inverted and incubated at 37°C for 12-16 h until the colonies appeared.

2.3.4 Small Scale Plasmid Preparation (Mini-Prep)

Two different methods were used for small-scale plasmid preparation. The first was the alkaline lysis method (Birnboim and Doly, 1979) described in the Protocols and Applications Guide (Promega, 1996, p 47). The second method used a QIAprep

Spin miniprep kit (Qiagen), according to the manufacturer's manual. This method also used the alkaline solution to lyse the bacteria. Instead of the phenol/chloroform extraction and ethanol precipitation of DNA used in method one, this kit included a silica-gel membrane in a spin column for DNA binding, and DNAs were eluted by distilled water.

2.3.5 Large Scale Plasmid Preparation (Maxi-Prep)

The QIAfilter plasmid maxi kit (Qiagen) was used for large-scale plasmid preparation, according to the manufacturer's manual. This method was based on a modified alkaline lysis procedure, followed by binding of plasmid DNA to an anion-exchange resin under appropriate low-salt and pH conditions. RNA, proteins, and low-molecular-weight impurities were removed by a salt wash. Plasmid DNA was eluted in a high-salt buffer, and then concentrated and desalted by isopropanol precipitation.

2.3.6 DNA Gel Electrophoresis

This method was described by Sambrook *et al.* (1989, 6.1-6.62). An agarose gel was used for separating DNA fragments of different lengths. Gel electrophoresis was performed in the tank containing 45 mM Tris-borate and 1 mM EDTA (TBE). Because the DNA is negatively charged, it moved from cathode to anode. DNA was visualised under ultraviolet (UV) light by staining the gel with ethidium bromide, or by adding ethidium bromide directly to the gel.

2.3.7 Purification of DNA Fragments

DNA was digested by restriction endonucleases, and the solution was loaded on agarose gels (0.8-1.2% (w/v), as stated) to separate any undigested circular DNA. When each DNA band was separated clearly, the desired fragments were cut out and purified using the QIAEX II gel extraction kit (Qiagen), according to the manufacturer's manual. This method used silica-gel particles for binding DNAs. The gels were washed before DNAs were eluted by distilled water.

2.3.8 Dephosphorylation of 5'-DNA Ends

The reaction was set up by adding the following components to the digested vector DNA: 5 μl calf intestinal alkaline phosphatase (CIAP) 10 X buffer (0.5 M Tris-HCl, 1 mM EDTA, pH 8.5), 1 μl CIAP (1 U/μl), and distilled water to a final volume of 50 μl. The samples were incubated at 37^0C for 1 h before phenol:chloroform:isoamyl alcohol (25:24:1) extraction and ethanol precipitation. Samples were resuspended in distilled water to give a final concentration of 50 ng/μl.

2.3.9 DNA Sequencing

The Sequenase version 2.0 DNA sequencing kit (Amersham) was used for DNA sequencing. This method was based on the dideoxy-mediated chain termination method described by Sanger *et al.* (1977).

Sequenase version 2.0 is a form of bacteriophage T7 DNA polymerase. It is a genetically engineered form of Sequenase that entirely lacks 3'→ 5' exonuclease activity, is extremely stable, and has a threefold higher specific activity than the

chemically modified enzyme (Tabor and Richardson, 1989). This enzyme also has high processivity and an enhanced rate of polymerisation, making it useful for DNA sequencing. 2',3' ddNTPs differ from conventional dNTPs in that they lack a hydroxyl residue at the 3' position of deoxyribose. The absence of a 3'-hydroxyl residue prevents formation of a phosphodiester bond with the succeeding dNTP. Further extension of the growing DNA chain is therefore impossible. Thus, when a small amount of one ddNTP is included with the four conventional dNTPs in a reaction mixture for DNA synthesis, there is competition between extension of the chain and infrequent, but specific, termination. By using the four different ddNTPs in four separate enzymatic reactions, populations of oligonucleotides are generated that terminate at positions occupied by every A, C, G, or T in the template strand. The sequences can be read by incorporating radiolabelled dNTPs, followed by autoradiography.

DNA (3-5 μg) was denatured by adding 0.1 volumes of 2 M NaOH containing 2 mM EDTA, and incubated for 30 min at 37°C. The mixture was neutralised by adding 0.1 volumes of 3 M sodium acetate (pH 4.5-5.5), and the DNA precipitated with 2-4 volumes of ethanol for 15 min at -70°C. After spinning at 14,000 x g for 20 min, the pelleted DNA was washed with 70% ethanol and dissolved in 7 μl of distilled water. Annealing was carried out by adding 2 μl of reaction buffer and 1 μl of primer (100 ng/μl) to 7 μl of denatured DNA, and the mixture was incubated for 2 min at 65°C on a hot plate. The heating block was then placed at room temperature to cool slowly to below 35°C over 15-30 min. The mixture was then centrifuged briefly and chilled on ice for 5 min. 2.5 μl of each termination mixture was added to

individual, labelled wells in a microtitre plate pre-warmed by floating the plate in a 37^{0}C water bath. The labelling reaction was carried out by adding the following components to the denatured DNA/primer mixture and incubating at room temperature for 5 min: 1 µl, 0.1 M DTT, 2 µl of diluted labelling mix (1:5 dilution in water), 0.5 µl of [^{35}S]dATP and 2 µl of diluted Sequence Polymerase (1:8 dilution, in enzyme dilution buffer). 3.5 µl of labelled reaction mixture was transferred to each well of a microtitre plate and incubated at 37^{0}C for 5 min. The reaction was stopped by adding 4 µl of stop solution (95% (v/v) formamide, 20 mM EDTA, 0.05% (w/v) bromophenol blue, and 0.05% (w/v) xylene cyanol FF) to each well of the microtitre plate.

2.3.10 Denaturing polyacrylamide gel electrophoresis

Polyacrylamide gels were prepared from Sequagel (Flowgen) for DNA sequencing. The components of the system were mixed appropriately to give a uniform 6% (w/v) polyacrylamide gel. Gels were cast in a Bio-Rad Sequi-Gen apparatus, using 0.4 mm uniform spacers and a sharks-tooth comb. The samples to be electrophoresed were heat-denatured before loading by placing the microtitre plate on a heated block at 90^{0}C for 3 min, before chilling quickly on ice. The gels were pre-run in 1 X TBE at a constant power of 75 W for 30 min to equilibrate and pre-warm them. Immediately before loading, the wells of the gel were flushed with 1 X TBE to remove excess urea, and 2.5 µl of each termination reaction was loaded in a separate well. Gels were run at 75 W constant power, maintaining an even gel temperature throughout the run. When the bromophenol blue dye front reached the bottom of the

gel, the run was stopped and the gel was dismantled before fixation in 10% (v/v) methanol, 10% (v/v) acetic acid for 5 min. The gels were then dried under vacuum with a paper backing before autoradiography.

2.4 RNA Protocols

2.4.1 *In vitro* Transcription

The mCAP RNA Capping Kit (Stratagene) was used for *in vitro* transcription, according to the manufacturer's manual.

2.4.2 Denaturing Formaldehyde-Agarose Gel Electrophoresis

The method used was adapted from that of Sambrook *et al.* (1989, pp 7.43-7.45). A 1% (w/v) agarose gel was prepared by melting agarose in 1 X formaldehyde running buffer (FRB), 20 X concentrate comprising: 0.4 M MOPS, 0.1 M sodium acetate, and 0.02 M EDTA by boiling. The gel was allowed to cool to approximately 55^{0}C, and 17 ml of formaldehyde (37% (v/v)) were added, resulting in a final concentration of 2.2 M. The gel was cast and allowed to cool until firmly set. The RNA samples were prepared by incubating at 65^{0}C for 15 min in an equal volume of RNA Loading Buffer (50% (v/v) formamide, 1 X FRB, 2.2 M formaldehyde and 0.01% (w/v) bromophenol blue), and loaded and electrophoresed at 5 V/cm in 1 X FRB, 2.2 M formaldehyde. RNAs moved from cathode to anode. Constant recircularisation of running buffer from the anode to the cathode prevented the generation of a salt gradient. After electrophoresis, the gel was rinsed briefly in diethyl pyrocarbonate (DEPC)-treated distilled water, and stained with ethidium

bromide (0.5 μg/ml in DEPC-treated distilled water) for 15 min. After staining, the gel was destained for 12 h in DEPC-treated distilled water.

2.5 Protein Protocols

2.5.1 Sodium Dodecylsulfate-Polyacrylamide Gel Electrophoresis (SDS-PAGE)

Protein electrophoresis followed the method of Laemmli (1970). The SDS-polyacrylamide gels were poured in a Mini-Protean II system (Bio-Rad), which was assembled according to the manufacturer's instructions. The solutions for separating gels (total volume 10 ml) were prepared in the order shown in Table 2-1. The separating gels were mixed well and then poured between the glass plates of the gel apparatus and overlaid with water. After the gels polymerised (about 20 min), the overlaid water was poured out and the gels were washed three times with water. A 3.5% (w/v) of stacking gel (total volume 5 ml) was prepared and poured over the separating gel (Table 2-2). Before the stacking gels polymerised (about 15 min), a comb was inserted to allow the wells to form. The samples were denatured by heating at 100^{0}C for 5 min in an equal volume of 2 X SDS gel sample buffer (2% (w/v) SDS, 5% (v/v) 2-mercaptoethanol, 10% (v/v) glycerol, 62.5 mM Tris-HCl, pH 6.8), and then placed on ice. Once the stacking gels had polymerised, the comb was carefully removed and the wells were washed with water to remove unpolymerised acrylamide. The samples were loaded and voltage applied to the gel at 8 V/cm until the dye front moved into the stacking gel, and then 15 V/cm until the dye front reached the bottom of the separating gel. Proteins moved from cathode to anode.

	mls added for stated percentage of gels		
component	5%	10%	15%
H_2O	4.79	3.53	2.28
40% (w/v) acrylamide/bisacrylamide	1.25	2.5	3.75
1 M Tris-HCl, pH 8.8	3.76	3.76	3.76
10% (w/v) SDS	0.1	0.1	0.1
10% (w/v) ammonium persulphate	0.1	0.1	0.1
TEMED	0.01	0.01	0.01

Table 2-1: The composition of separating gels in SDS-PAGE

component	mls added
H_2O	3.2
0.5 M Tris-HCl, pH 6.8	1.25
40% (w/v) acrylamide/bisacrylamide	0.44
10% (w/v) SDS	0.05
10% (w/v) ammonium persulphate	0.05
TEMED	0.005

Table 2-2: The composition of stacking gels in SDS-PAGE

2.5.2 Staining and Destaining of Protein Gels

SDS-polyacrylamide gels were stained in a solution containing 0.25% (w/v) Coomassie Brilliant Blue R250, 90% (v/v) methanol:H_2O (1:1 v/v), and 10% (v/v) glacial acetic acid for 30 min at room temperature. The gels were then destained by immersing them in 90% (v/v) methanol:H_2O (1:1 v/v) and 10% (v/v) glacial acetic acid for 24 h, changing the destaining solution twice. To make a permanent record, the gels were dried on a vacuum gel drier (Hoefer), according to the manufacturer's manual.

2.5.3 Western Blotting

Proteins were sized fractionated using 5% (w/v) SDS-PAGE then transferred to Hybond C-Pure nylon membranes (Amersham) using a wet transfer apparatus (Hoefer) at a constant current of 300 mA for 2 h. Proteins transferred from gel to membrane in the direction of cathode to anode. Membranes were incubated with blocking buffer (5% (w/v) skimmed milk in PBS) overnight at 4^0C. Rabbit anti-human IP_3R N-terminal antibodies (Calbiochem) were added at 1:2000 dilution in blocking buffer. After 2 h incubation at room temperature, membranes were washed 4 times for 5 min each time, with gentle agitation, with 50 ml PBS, and incubated at room temperature for 1 h with goat anti-rabbit IgG-horseradish peroxidase conjugate at 1:1000 dilution in blocking buffer. After 1 h incubation, membranes were washed 4 times for 5 min each time, with gentle agitation, with 50 ml PBS. Signals were detected using the ECL method (Amersham), followed by exposure to photographic film.

2.5.4 *In vitro* Translation

The *in vitro* transcription/translation reactions were performed using either a TnT Coupled Reticulocyte Lysate System (Promega), or a TnT Quick Coupled Transcription/Translation System (Promega), according to the manufacturer's instruction. The scale of the reaction was reduced to 25 µl.

2.5.5 Preparation of Microsomal Membranes

The method followed the procedures described by Yoneshima *et al.* (1997) with some modifications. Three 90 mm plates of transfected cells were homogenised in 3 ml homogenisation buffer (0.32 M sucrose, 5 mM Tris-HCl, pH 7.4, 0.2 mM 4-(2-aminoethyl) benzenesulfonyl fluoride (AEBSF), 1 µg/ml leupeptin, 0.5 µg/ml pepstatin, 0.5 µg/ml aprotinin, 10 µg/ml trypsin inhibitor, 150 µg/ml benzamidine). After 30 strokes using a tight-fitting glass-teflon homogeniser, the homogenates were centrifuged in a TLA-100.3 rotor using a TL-100 centrifuge (Beckman) at 1,000 x g for 10 min at 4^{0}C. The supernatant was re-centrifuged at 105,000 x g for 45 min at 4^{0}C. The pellet was resuspended in 80 µl homogenisation buffer to be used immediately or quick frozen in liquid nitrogen then stored at –70^{0}C.

2.6 Cell Culture Protocols

2.6.1 Mammalian Cell Culture

COS7 cells (a transformed monkey fibroblast cell line) (Gluzman, 1981) and HEK293 cells (a transformed human embryonic kidney cell line) (Graham *et al.*,

1977) were cultured in DMEM (Gibco BRL) supplemented with 10% (v/v) foetal calf serum (Gibco BRL), 2 mM L-glutamine, 2 mM sodium pyruvate, 100 units penicillin, and 100 μg/ml streptomycin. Cells were cultured and passaged according to standard procedures (Doyle *et al.*, 1994).

2.6.2 Transfection of Mammalian Cells

Transfection was performed by using liposomes including Lipofectin (Gibco BRL), Tfx-20 (Promega), Lipofectamine (Gibco BRL), or electroporation (Bio-Rad) and the manufacturer's instruction were followed pre*cis*ely.

2.6.3 Insect Cell Culture

Sf9 cells derived from fall armyworm ovaries (Myers *et al.*, 1992) were cultured in supplemented Grace's medium (Gibco BRL) including 10% (v/v) foetal bovine serum (Gibco BRL), 2.5 μg/ml Fungizone (Gibco BRL), 100 units penicillin, and 100 μg/ml streptomycin. Sf21 cells (Vaughn *et al.*, 1977) were cultured in Sf-900 II medium (Gibco BRL) including 2.5 μg/ml Fungizone (Gibco BRL), 100 units penicillin, and 100 μg/ml streptomycin. Insect cells were passaged by gently tapping the culture flasks and using a stream of medium from a 10 ml pipette to dislodge the cells from the surface.

2.6.4 Transfection of Insect Cells

Insect cells were transfected by using the MaxBac 2.0 Transfection kit (Invitrogen). The day before transfection, cells were plated in a 60 mm dish to give

~60% confluence. The transfection mixture was prepared by adding the following components to a 1.5 ml screw-capped tube containing 10 μl (0.5 μg) of Bac-N-Blue DNA:

Recombinant transfer plasmid (1 μg/μl)	4 μl
Grace's medium (without supplements or FBS)	1 ml
InsectinPlus liposomes	20 μl

The mixture was vortexed and incubated at room temperature for 15 min. The medium was removed without disrupting the monolayer and the cells were washed with 2 ml of fresh Grace's medium, without supplements or FBS. The transfection mixture was added dropwise to the cells, and the dishes were incubated at room temperature for 4 h on a side-to-side, rocking platform (about 2 side-to-side motions per minute). Following the 4 h incubation period, 1 ml of complete Grace's medium was added to the dish and the dish was incubated at 28^{0}C for 4-5 days. After 5 days, the supernatant was collected and stored at 4^{0}C for screening the recombinant virus.

2.6.5 Plaque Assay

The day before plaque assay, six 10 mm plates were seeded with insect cells to give ~70% confluence. The transfection viral stock was diluted to 1 in 10^{-2}, 1 in 10^{-3}, and 1 in 10^{-4} in 2 ml of complete medium. The medium was removed from the cells to leave only about 2 ml. One ml of each viral dilution was added to the plates, and the plates were incubated at room temperature on a slowly rocking platform (about 2 side-to-side motions per minute) for 1 h. During the 1 h incubation period, a 37^{0}C water bath was placed in a tissue culture hood. 3% (w/v) SeaPlaque low melting

temperature agarose (Flowgen) was prepared by adding 0.69 g of agarose to 23 ml of distilled water, and melted completely by microwaving then incubated at 37^{0}C in the water bath. 207 µl of 50 mg/ml 5-bromo-4-chloro-3-indolyl-β-D-galactopyranoside (X-gal) was added to 46 ml of complete medium and this was pre-warmed to 37^{0}C. The molten 3% (w/v) SeaPlaque agarose and complete medium were mixed to produce 1% (w/v) agarose. Following the 1 h incubation period, the inoculums were aspirated and the cells were carefully overlaid with 10 ml of 1% (w/v) agarose mixture. After the agarose had solidified, the plates were sealed with parafilm and incubated at 28^{0}C until plaques were well-formed (about 5-7 days).

2.6.6 Preparation of Primary Virus Stock

Insect cells were plated in 12-well culture plate to give ~50% confluence. Well-separated plaques were picked up by sucking a plug of agarose from above the plaque into a Pasteur pipette, and these plaques were transferred to each well of the plate. After 5 to 6 days, the medium was collected and centrifuged at 3000 x g for 10 min. The supernatant was collected and stored at 4^{0}C as "primary virus stock".

2.6.7 Extraction of Viral DNAs

100 µl of the primary virus stock were mixed with 350 µl of TE buffer (10 mM Tris-HCl, pH 7.8, 1 mM EDTA) and 50 µl of 10% (w/v) SDS. 500 µl of phenol:chloroform:isoamyl alcohol (25:24:1) were added to extract viral DNA followed by ethanol precipitation. The DNA pellet was resuspended in 50 µl of TE buffer.

2.6.8 Amplification of Virus Stock

The day before amplification, the insect cells were plated in a 75 cm^2 flask to give ~70% confluence. 100 µl of the primary virus stock was added and the flask was incubated at 28°C for 5 to 6 days until more than 90% cells were lysed. The cell debris was removed by centrifugation at 3000 x g for 10 min. The supernatant was collected and stored at 4°C. This give the "high titre", small-scale virus stock. Large-scale virus stock was obtained by infection of a 150 cm^2 flask of cells with 150 µl of small-scale virus stock, following the same procedures.

2.6.9 End Point Dilution Assay

Insect cells were seeded at ~30% confluence in each well of a 12-well plate. For each virus titre to be tested, 100, 10, and 1 µl of virus stock were added to each well, and cells were incubated at 28°C for three days. Control wells contained no virus stock. Successful transfections and high titre virus stock resulted in uniformly large infected cells in the 100, 10, and 1 µl experimental wells. The cells in the control wells did not appear infected, and remained as normal controls.

2.6.10 Indirect Immunofluorescence

HEK293 cells were cultured in a six-well tissue culture plate containing 10 mm^2 glass coverslips. This permitted the transfer of cells adhered to coverslips to other vessels for fixation and antibody binding. After 48 h of transfection, the culture medium was removed from cells by aspiration. Cells were washed 3 times with 3 ml

of PBS. Coverslips with cells attached to them were transferred to a well of a six-well tissue culture plate. 3 ml of 4% (w/v) paraformaldehyde in PBS, pH 7.0 was added to fix cells and incubated at room temperature for 10 min. After the incubation, the solution was removed by aspiration, and the fixed cells were washed 3 times with 3 ml of PBS. The cells were then incubated in 3 ml of 50 mM NH_4Cl in PBS for 10 min to quench potential autofluorescence. The cells were again washed 3 times with 3 ml of PBS, and 3 ml of 0.1% (v/v) Triton X-100 in PBS were added and incubated for 5 min to permeabilise the cells. After 3 times washes with 3 ml of PBS, the coverslips were inverted onto 100 µl of antibody (diluted 1:100 in 0.2% (v/v) fish skin gelatin in PBS) on a piece of parafilm and incubated for 1 hr. The coverslips were washed 3 times with 3 ml of 0.2% (v/v) fish skin gelatin in PBS for over 5 min, followed by 3 times washes with 3 ml of PBS. The coverslips were then inverted onto 100 µl of fluorochrome-labelled secondary antibody (rhodamine-conjugated anti-rabbit IgG diluted 1:400 in 0.2% (v/v) fish skin gelatin in PBS), and incubated at room temperature for 1 hr. The coverslips were washed 3 times with 3 ml of 0.2% (v/v) fish skin gelatin in PBS and 3 times with 3 ml of PBS. The cells were also stained with the dye Di-O-C_5(3), by placing them in 50 µl of 1 µg/ml dye in ethanol for 20 min. After the incubation, the coverslips were washed 3 times with 3 ml of PBS. The coverslips were mounted using 20 µl of Aquamount (BDH) and allowed them to set for 2 hr before examination using a Leitz Ortholux fluorescence microscope with standard FITC/rhodamine block. Photographs were taken using confocal fluorescence microscope and analysed by Paint Shop Pro (Jasc Software).

2.7 Other Protocols

2.7.1 IP_3 Binding Assay

Protein samples were incubated with 10 nM [^{3}H]IP_3 in the binding buffer (50 mM Tris-HCl, pH 8.8, 1 mM EDTA, 1 mM DTT, 100 mM NaCl) for 10 min at 4^{0}C. The IP3/protein mixture was added to 4 µl of γ-globulin (50 mg/ml) and 100 µl of polyethylene glycol (PEG) precipitation buffer (30% (w/v) PEG6000, 1 mM EDTA, 50 mM Tris-HCl, pH 8.8) and incubated for 5 min at 4^{0}C. The protein-PEG complexes were pelleted by centrifugation at 18,000 x g for 10 min at 4^{0}C. The pellet was quickly washed with 100 µl of binding buffer and resuspended in 200 µl of dH_2O. The radioactivity of the samples was measured by mixing 3.5 ml of Ultimagold (Packard) followed by counting in a liquid scintillation counter (Packard 1900CA). The specific binding was defined as total binding minus non-specific binding that was measured in the presence of 25 µM cold IP_3.

2.7.2 Planar Lipid Bilayer Reconstitution

The bilayer set-up is similar to those described by Williams (1995) and shown in Figure 2-1. 7.5 µl each of 50 mg/ml phosphatidyl ethanolamine and phosphatidyl serine (Avanti Polar Lipids) prepared in chloroform was mixed, and the chloroform was evaporated under a stream of nitrogen. 25 µl of n-decane was then added to the dried phospholipids to give a final phospholipid concentration of 30 mg/ml. A small amount of phospholipid (~3 µl) was painted using a flexible plastic stick around the 300 µm hole of the cup. This "primed" cup was then used for bilayer reconstitution. The block containing the *trans* chamber and the circular hole into which the cup

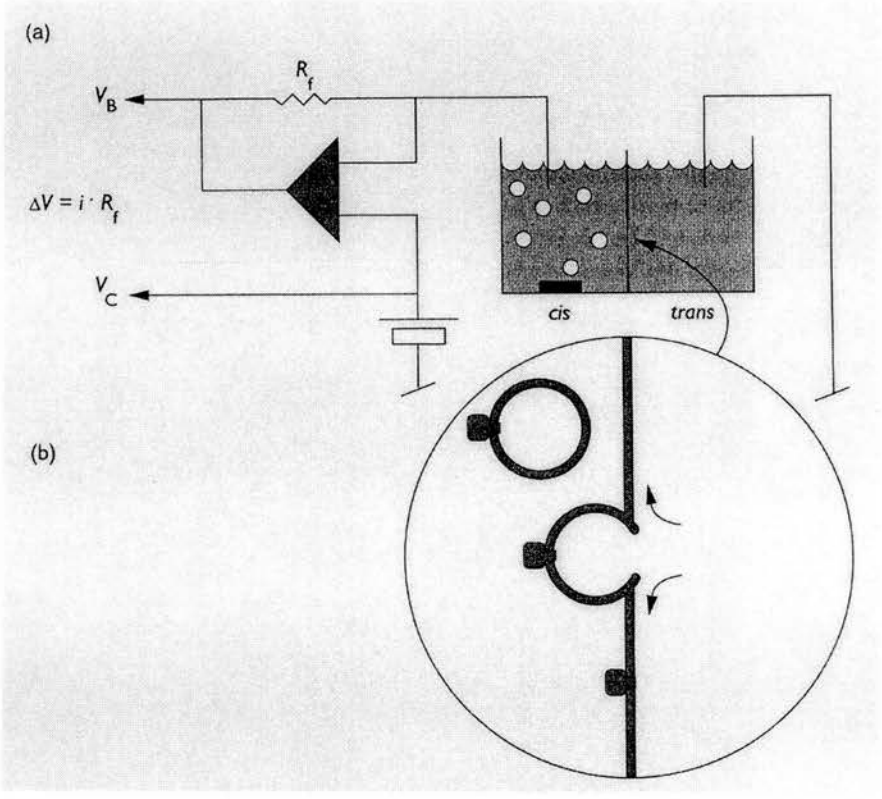

Figure 2-1. Reconstitution of IP_3RI in planar lipid bilayer

(a) The set-up of a planar lipid bilayer. The *cis* chamber is voltage-clamped at a given potential (V_C) relative to the *trans* chamber, which is grounded. The transmembrane currents are measured by (minus)$[V_B-V_C]/R_f$ (Ohm's law). A stirbar and vesicles are also shown in the *cis* chamber.
(b) Microscopic view of membrane/vesicle fusion, with a single channel property, is shown. Adapted from Ashley (1995).

containing *cis* chamber fits. Block and "primed" cup were assembled, and electrodes and bridges were connected with each chamber. 600 μl of 110 mM Tris-HCl, 250 mM HEPES, pH 7.35 was added to each chamber, and ~1 μl of phospholipid was drawn across the hole. Bilayers formed spontaneously as observed by monitoring the increase in membrane capacitance which accompanied thinning. The bilayer capacitance was measured using a triangle wave of 100 Hz at 100 mV. All the bilayers used had a capacitance of >250 pS. The *cis* chamber was voltage clamped at a potential relative to the *trans* chamber using a Biologic RK-300 patch clamp amplifier (Intracel). The relative potential applied across the bilayer was termed the "holding potential" or "voltage clamp potential". The current was filtered and digitally recorded.

After an ideal bilayer formed, the *trans* chamber was perfused with 3 ml of 250 mM HEPES, 53 mM $Ba(OH)_2$, pH 7.35. To incorporate channels, 5 μl of microsomes were added to the *cis* chamber in the presence of a salt gradient containing 800 mM KCl, 2 mM $CaCl_2$. After the incorporation were identified, the *cis* chamber was perfused with 6 ml of 110 mM Tris-HCl, 250 mM HEPES, pH 7.35, 0.2 μM free Ca^{2+} buffered with 1 mM EGTA and 0.7 mM $CaCl_2$, 1 mM ATP, and 2 μM IP_3. Single channel currents were recorded and analysed using pClamp (Axon Instruments).

Chapter 3

Assembly and *In vitro* Expression of Human Type I IP_3R cDNA

3.1 Introduction

IP_3 produced via the hydrolysis of phosphatidylinositol 4,5-bisphosphate by phospholipase C (PLC) acts as an intracellular second messenger that triggers the release of Ca^{2+} from cell stores. There are two pathways for PLC activation (Berridge, 1993): (1) activation of G protein-linked seven-membrane-spanning receptors for neurotransmitters, neuropeptides, odorants, or light, followed by activation of a G protein which then activates PLC-β1, and (2) activation of tyrosine kinase-linked receptors for growth factors and neurotrophins, followed by the activation of PLC-γ1. Therefore, IP_3 signalling is involved in diverse cellular responses to many kinds of extracellular information.

IP_3 is physiologically effective only on the IP_3R. The IP_3R transduces this intermediate signal to a Ca^{2+} signal. Three distinct *IP_3R* genes (I-III) have been molecularly cloned from both rodent and human tissues. Within this family, IP_3RI is the best characterised (Ferris and Snyder, 1992; Mikoshiba, 1993), and it is the predominant type in brain.

The IP_3RI is structurally divided into three domains: a large N-terminal cytoplasmic domain (~83% of the receptor), six putative membrane-spanning-domains (MSDs) clustered near the C-terminus, and a short C-terminal cytoplasmic domain (~5%) (Furuichi *et al.*, 1989; Mignery *et al.*, 1990). The N-terminal tip (~650 amino acids) is the ligand-binding domain for IP_3 (Mignery and Sudhof, 1990; Miyawaki *et al.*, 1991; Yoshikawa *et al.*, 1999). The central portion is the modulatory domain containing binding sites for various modulators, including: Ca^{2+} (Sienaert *et al.*, 1996; 1997), calmodulin (CaM) (Yamada *et al.*, 1995), and ATP

(Furuichi *et al.*, 1989); two sites phosphorylated by cyclic AMP-dependent protein kinase (PKA) (Ferris *et al.*, 1991; Supattapone *et al.*, 1988); one site phosphorylated by cyclic GMP-dependent protein kinase (PKG) (Komalavilas and Lincoln, 1994); and potential phosphorylation sites for Ca^{2+}/Calmodulin-dependent protein kinase II (CaMKII) (Ferris *et al.*, 1991) and protein kinase C (PKC) (Ferris *et al.*, 1991; Matter *et al.*, 1993). Autophosphorylaton of IP_3RI has also been reported (Ferris *et al.*, 1992). In addition, this central portion probably functions as the transducing domain involved in the transduction of IP_3 binding to channel opening (Mignery and Sudhof, 1990).

Three alternative splicing sites (SI, SII, and SIII) have been identified in *IP_3RI* mRNA (Danoff *et al.*, 1991; Mignery *et al.*, 1990; Nakagawa *et al.*, 1991; Nucifora *et al.*, 1995). The splice variants are found unequally in various mouse and human tissues. SI splicing, in the middle of the ligand-binding domain, may alter IP_3 binding activity. SII splicing, which occurs between the two PKA phosphorylation sites, probably affects PKA phosphorylation kinetics and PKA-dependent sites. SIII splicing may create an additional consensus protein kinase C phosphorylation site (Figure 1-4).

3.2 Assembly of Full-Length Human *IP_3RI* cDNA

Three overlapping cDNAs cloned from a human brain cDNA library (Stratagene, #936212) and encoding the entire human *IP_3RI* cDNA (SI^- SII^+ $SIII^+$) were obtained from Professor C. A. Ross (Nucifora *et al.*, 1995, Genbank accession number U23850). This is the first *IP_3RI* cDNA cloned from human brain, and it also

contains a novel SIII splicing site, which may be important in regulating channel activity. These three clones comprised: 5'-3 L11 in pcDNA3 (ligation product of "HCB-5'-3" and "HCX-L11"), HGB-6 in pGEM, and HC-8 in pBlueScript. The most 5'-clone was obtained using PCR with total RNA extracted from human cerebellum as a template. These cDNAs were assembled using the procedures shown in Figure 3-1, using a strategy optimised with Lasergene software (DNASTAR). The single line diagram of each clone was also shown in Fig 3-2. 5'-3 L11 was digested with *Kpn*I and *Xba*I to remove the insert from the pcDNA3 vector, and *Sal*I was subsequently used to digest the vector into two fragments in order to separate it from the insert. The 5.4 kbp insert (5'*Kpn*I→*Xba*I 3') was extracted from a 0.8% (w/v) agarose gel using the QIAEX II (Qiagen) and ligated with *Kpn*I and *Xba*I-digested pBlueScript-SK. This ligation product was called pBS1. Dideoxy sequencing using a T7 sequencing primer was carried out to check the sequence around the start codon. This was found to be ACCCATG, which is not a "good" Kozak consensus sequence for the initiation of transcription (Kozak, 1987a; 1987b), i.e. A/GCCATG. It was also different from the published sequence (the changes were: G18T, T21C, A79G). A pair of primers of the "correct" sequence were designed in order to match the Kozak consensus sequence: forward primer: 5'-TGGGGTACCATGTCTGACAAAA TGTCTAGCTTCC-3'; reverse primer: 5'-CAGTTGATGGCTGCTAGCATG-3', and PCR was used to produce a 600 bp fragment. The PCR reaction was set up as follows:

10 X reaction buffer	5 μl
dNTPs (10 mM)	1 μl

Figure 3-1. Assembly of full-length human *IP3R1* cDNA

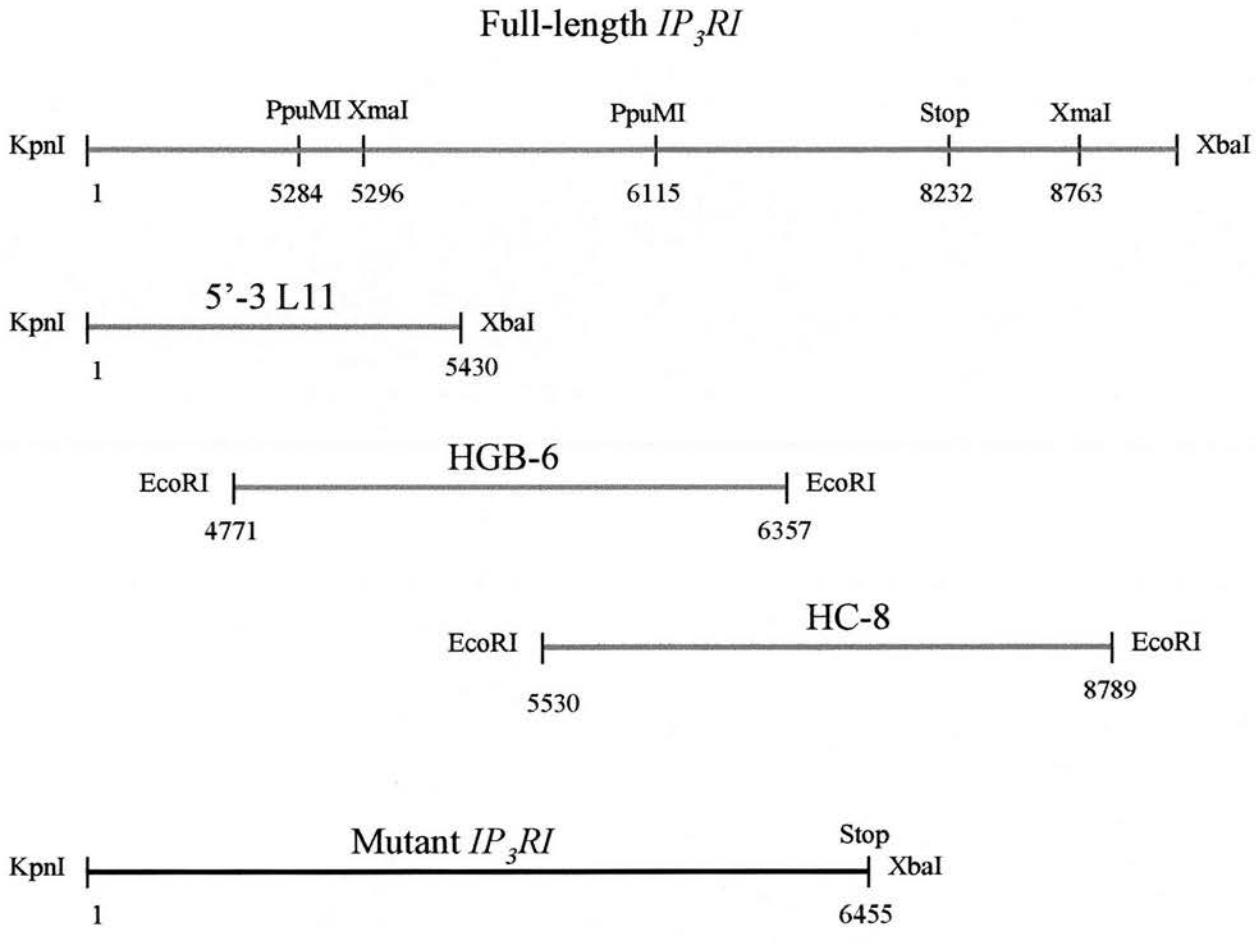

Figure 3-2. Single line diagram of full-length and mutant IP_3RI

The assembly procedures of full-length IP_3RI from plasmid 5'-3 L11, HGB-6, and HC-8 were shown in Figure 3-1. Here it shows that each plasmid corresponds to the position of full-length IP_3RI. The translation of mutant IP_3RI stops at position 6455.

forward primer (10 μM)	1 μl
reverse primer (10 μM)	1 μl
dsH_2O	36 μl
pBS1 (1 ng/μl)	5 μl
Pfu (2.5 U/μl)	1 μl

All the reagents were well mixed and the thermocycler was set as follows:

94°C, 2 min	1 cycle
94°C, 30 sec; 45°C, 30 sec; 72°C, 1 min 30 sec	2 cycles
94°C, 30 sec; 50°C, 30 sec; 72°C, 1 min	28 cycles

Pfu DNA polymerase was used for its high fidelity (the error rate of *Pfu* DNA polymerase is significantly lower than for other proofreading enzymes, DNA polymerase mixtures, and *Taq* DNA polymerase) (Cline *et al.*, 1996). 10 X reaction buffer contains 200 mM Tris-HCl, pH 8.8, 20 mM $MgSO_4$, 100 mM KCl, 100 mM $(NH_4)_2SO_4$, 1% (v/v) Triton X-100, 1 mg/ml BSA. The annealing temperature of the first two cycles was set at 45°C to enable the two overhanging primers to anneal to the template DNA properly in order to produce the desired template for subsequent PCR cycles.

This 600 bp fragment was then digested with *Kpn*I and *Nhe*I to recreate these sites and ligated with *Kpn*I and *Nhe*I-digested pBS1. The ligation product was called pBS2, and the ligation site was again checked by manual sequencing. HGB-6 was digested with *Ppu*MI and the 832 bp insert (from position 5284 to 6115) was ligated to the *Ppu*MI-digested HC-8. The ligation product TK1 was digested with *Xma*I and *Sca*I and the 3468 bp insert (from position 5296 to 8763) was ligated to *Xma*I-

digested pBS2. Using either *BglI* digestion or PCR to check the orientation of the inserts, a full-length human *IP_3RI* cDNA was cloned in pBlueScript-SK. This was called pBS-IP3. The exact sequence of the inserts is: 5'-*Kpn*I 1→8763 + 5296→5430 *Xba*I-3'.

3.2.1 Creation of Additional Expression Constructs

pBlueScript-SK was chosen as a basic cloning vector because it contains both T3 and T7 promoters for *in vitro* transcription of RNA. pBS-IP3 was digested with *Kpn*I and *Xba*I and subcloned into pcDNA3. This was called pcDNA3-IP3.

pcDNA3 is a mammalian expression vector that contains the cytomegalovirus (CMV) enhancer-promoter for high level expression (Andersson *et al.*, 1989; Boshart *et al.*, 1985; Nelson, 1987), a bovine growth hormone (BGH) polyadenylation signal and transcription termination sequence to enhance mRNA stability (Goodwin and Rottman, 1992), the SV40 origin for episomal replication and simple vector rescue in cell lines expressing the large T antigen (i.e. COS 1 and COS 7), and a T7 RNA polymerase promoter. pcDNA3-IP3 was digested with *Kpn*I and *Not*I and subcloned into pCI. This was called pCI-IP3.

pCI is also a mammalian expression vector. It also contains the human cytomeglovirus (CMV) immediate-early enhancer/promoter for strong expression, a chimeric intron composed of the 5'-splice site from the β-globin intron and the 3'-splice site from an IgG intron for increased expression levels of cDNAs, the SV40 late polyadenylation signal for efficient RNA processing, and a T7 RNA polymerase promoter. pCI-IP3 was digested with *Sal*I and *Not*I and subcloned into pCITE. This

was called pCITE-IP3.

pCITE contains both T7 and SP6 RNA polymerase promoters and a copy of the encephalomyocarditis virus (EMC) RNA 5' non-coding region, which functions as an internal entry point for initiation of translation by eukaryotic ribosomes (Duke *et al.*, 1992; Elroy-Stein *et al.*, 1989; Kaminski *et al.*, 1990; Parks *et al.*, 1986). This Cap-Independent Translation Enhancer (CITE) sequence has been shown to increase reporter gene expression up to 10-fold in transfected mammalian cells, and has a similar effect when used in the translation of synthetic RNA *in vitro* by rabbit reticulocyte lysates (Elroy-Stein *et al.*, 1989).

None of the constructs contained 5'-UTR sequence, which could be important for transcription. The sequence of the corresponding mouse 5'-UTR is known (Furuichi *et al.*, 1989; Miyawaki *et al.*, 1991), and in order to add mouse 5'-UTR to the cDNA encoding human *IP_3RI*, two primers were designed (forward primer: 5'-AACCGCTCGAGGCTGAAGCGTTTCCTCAAGC-3'; reverse primer: 5'-CGGGGTACCGTCCGTGTTGGAAAGCCTG-3'). Using mouse *IP_3R* cDNA (obtained as a gift from Professor K. Mikoshiba) as a template for PCR (as described previously), a 328bp fragment was purified from a 1% (w/v) agarose gel and digested with *Xho*I and *Kpn*I and subcloned into pCI-IP3. This construct was called pCI-IP3-UTR.

3.3 *In vitro* Expression of Full-Length Human IP_3RI mRNA and Protein

3.3.1 Introduction to *In vitro* Expression

The rabbit reticulocyte *in vitro* translation system, originally described by Pelham and Jackson (1976) has become a standard tool for *in vitro* expression of proteins from cloned genes. The primary advantage of *in vitro* translation over *in vivo* protein expression is that *in vitro* systems allow the use of a defined template to direct protein synthesis. In this way, it is possible to greatly reduce or eliminate the background resulting from endogenous RNA that occurs with *in vivo* systems. *In vitro* systems also allow the specific labelling of gene products so that individual proteins can be monitored in complex reaction mixtures. In addition, *in vitro* systems provide a very rapid means for protein analysis as templates need not necessarily be cloned before expression.

There are two basic approaches to *in vitro* translation: programming systems that use RNA templates (two-step transcription/translation), and programming systems using DNA templates (coupled transcription/translation). Protein production in these systems can be monitored in a variety of ways. Usually, a radioactive amino acid is added to the translation reaction and, after incorporation, the gene product is identified by autoradiography following SDS-polyacrylamide gel electrophoresis (SDS-PAGE). Alternatively, a non-radioactive labelling method may be used. If antibodies to the protein are available, then techniques such as immunoblotting or immunoprecipitation can be used to identify products directly from the *in vitro* translation reaction.

3.3.2 Two-Step Transcription/Translation Expression

All eukaryotic mRNAs have a methylated cap structure at the 5' end. This is formed by hydrolysing a phosphate group from the first nucleotide, usually a purine (A or G). The diphosphate 5' end then attacks the α phosphorus atom of GTP to form a very unusual 5'-5' trisphosphate linkage. This special terminus is called a cap. The N-7 nitrogen of the terminal guanine is then methylated by S-adenosyl-methionine to form cap 0. The adjacent riboses may be methylated to form cap 1 or cap 2. Caps contribute to the stability of mRNAs by protecting their 5' ends from phosphatases and nucleases. In addition, caps enhance the translation efficiency of mRNA both by rabbit reticulocyte lysates and by micro-injected *Xenopus* oocytes (Nielsen and Shapiro, 1986).

3.3.2.1 *In vitro* mRNA Synthesis and Translation

The mCAP mRNA capping kit (Stratagene) was used for *in vitro* RNA synthesis. The kit contained a cap analogue, $M^7G(5')ppp(5')G$, which was incorporated at the 5' end of the RNA molecules. The reaction was set up as follows:

5 X transcription buffer	5 µl
linearised pBS-IP3 or pcDNA3-IP3 (1 µg/µl)	1 µl
rNTPs	2 µl
cap analogue	5 µl
0.75 M DTT	1 µl
T7 RNA polymerase (10 U/µl)	1 µl
RNasin (40 U/µl)	0.5 µl

RNase-free H_2O	to a final volume of	25 µl

5 X transcription buffer contained 200 mM Tris-HCl, pH 7.5, 250 mM NaCl, 40 mM $MgCl_2$, and 10 mM spermidine. rNTPs contained 10 mM rUTP, 10 mM rCTP, 10 mM rATP, and 3 mM rGTP. The mixture was incubated at 37°C for 1 h. The DNA template was removed by adding 10 U of RNase-free DNase I directly to the reaction mixture after 1 h incubation and incubated at 37°C for 5 min. 100 µl of RNase-free dH_2O were added to the mixture followed by phenol/chloroform extraction and ethanol precipitation. The RNA was resuspended in 25 µl of RNase-free 10 mM Tris-HCl, pH 7.5 and 0.1 mM EDTA (TE) buffer. 10 µl of RNA were loaded on a 1% (w/v) denaturing formaldehyde-agarose gel (as shown in chapter 2) and visualised by UV light (Figure 3-3). Both pBS-IP3 and pcDNA3-IP3 produced full-length *IP_3RI* RNAs (~9 kbp).

A Flexi rabbit reticulocyte lysate system (Promega) was used for the *in vitro* translation of this RNA. The reaction was set up as follows:

Flexi rabbit reticulocyte lysate		16.5 µl
Amino acid mixture minus methionine (1 mM)		0.5 µl
^{35}S-methionine (10 mCi/ml)		1 µl
MgOAc (25 mM)		0.5 µl
KCl (2.5 M)		0.7 µl
DTT (100 mM)		0.5 µl
RNasin (40 U/µl)		0.5 µl
RNA substrate		2 µl
RNase-free H_2O	to a final volume of	25 µl

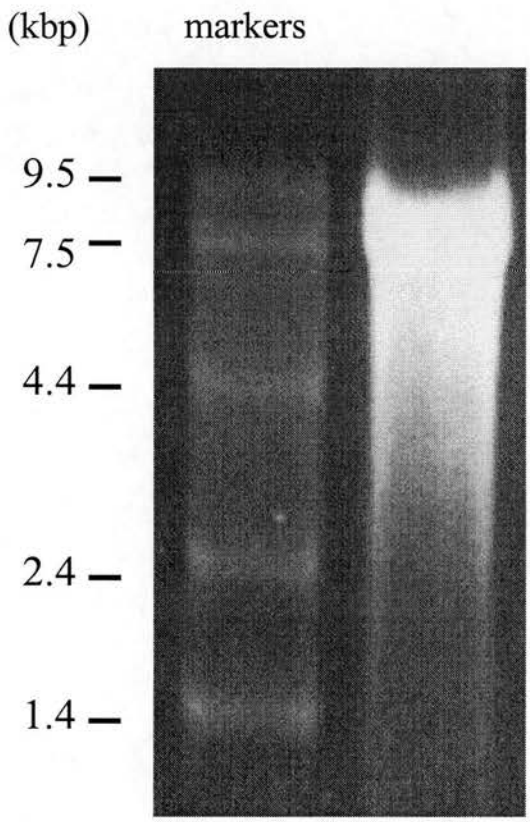

Figure 3-3. *In vitro* transcription of human IP_3RI cDNA.

RNA was prepared from pBS-IP3 using the mCAP mRNA Capping Kit (Stratagene) and resolved on a 1% (w/v) denaturing formaldehyde-agarose gel at 5V/cm for 5 h. After eletrophoresis, the gel was stained with ethidium bromide for 15 min. After staining, the gel was destained for 12 h in DEPC-treated water and visualised using UV light. Size markers are also shown.

The mixture was incubated at 30°C for 2 h. 5 µl of reaction mixture were loaded onto a 5% (w/v) SDS-polyacrylamide gel, and after electrophoresis this was dried and autoradiographed (Figure 3-4). Full-length IP_3RI has an apparent molecular weight of 260 kDa on gels. However, only partial-length products were obtained, even in the presence of anti-proteases. Several measures were taken to optimise the reaction, including varying MgOAc between 0, 1, and 2 µl, changing KCl from 0.7 to 1 µl, and omitting adding DTT. The amount of product changed, but the overall result was still the same. In order to investigate this further, a coupled transcription/translation system was used.

3.3.3 Coupled Transcription/Translation Expression

pBS-IP3, pcDNA3-IP3, and pCI-IP3 were expressed *in vitro* using a TNT T7 coupled transcription/translation system (Promega), following the manufacturer's manual. The following reagents were mixed in a 1.5 ml RNase-free microcentrifuge tube in the order:

TNT rabbit reticulocyte lysate		12.5 µl
TNT reaction buffer		2 µl
TNT T7 RNA polymerase		0.5 µl
amino acid mixture minus methionine (1 mM)		0.5 µl
^{35}S-methionine (10 mCi/ml)		2 µl
RNasin ribonuclease inhibitor (40 U/µl)		0.5 µl
DNA template (1 µg/µl)		0.5 µl
Nuclease-free H_2O	to a final volume of	25 µl

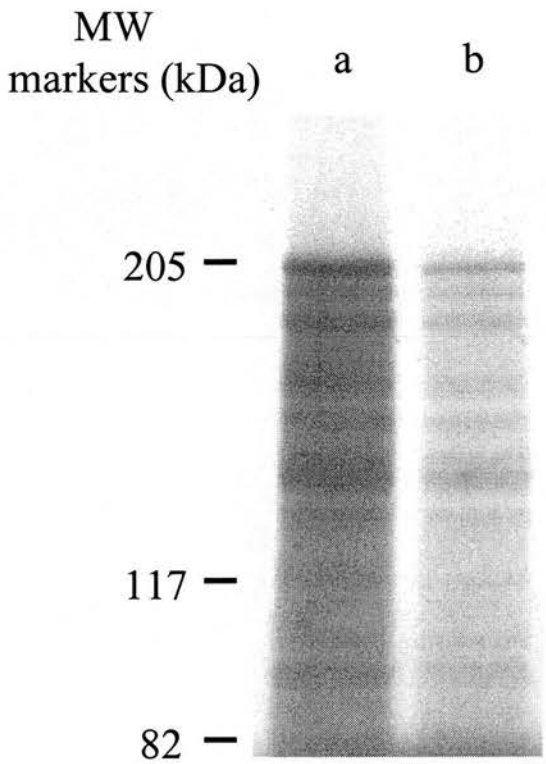

Figure 3-4. SDS-PAGE of [^{35}S]methionine labeled proteins after two-step transcription/translation of human *IP_3RI* cDNA.

Lane a: pBS-IP3, Lane b: pcDNA3-IP3.
RNA was produced by using the mCAP mRNA capping kit (Stratagene).
This was used to perform the Flexi rabbit reticulocyte lysate system (Promega).
After incubation at 30^{0}C for 2 h, 5 µl of lysate was resolved on 5% (w/v)
SDS-PAGE followed by autoradiography. The position of MW markers is shown.

After incubation at 30°C for 60-120 min, 5 μl of the lysate was resolved using 5% (w/v) SDS-PAGE. Electrophoresis was continued until the bromophenol blue marker dye ran off the bottom of the gel, and the gel was then dried and autoradiographed. Typical results are shown in Figure 3-5. The calculated molecular weight of full-length IP_3RI is ~310 kDa, but as mentioned previously the apparent molecular weight from SDS-PAGE is normally ~260 kDa. However, expression from all these three vectors only produced ~200 kDa products and some truncated fragments. This was similar to the two-step procedure. The reaction was optimised by increasing the incubation time to 180 min, adding up to 1 μl of the amino acid mixture, and adding protease inhibitor (as discussed in the microsome preparation, chapter 2), but the same results were obtained.

These findings could be consistent with the occurrence of transcription from alternative start sites in the coding sequence. There are a total of 71 ATGs in the coding sequence, and 9 of these contain a "good" Kozak consensus sequence (position 439, 2467, 3802, 4705, 6928, 7135, 7189, 8020, and 8095), where translation could start instead of at the first ATG. Because pCITE contains an internal entry point for initiation of translation by eukaryotic ribosomes, this construct should ensure that translation of the IP_3RI started from the internal AUG codon in the plasmid vector, instead of other AUGs in subsequent positions. However, the results remained the same (Figure 3-5). Finally, because the 5'-untranslated region (5'-UTR) of DNAs is important for RNA polymerase binding and processing (Breathnach and Chambon, 1981; Bucher, 1990), pCI-IP3-UTR was also constructed (as described earlier), and expressed *in vitro*. Again, full-length

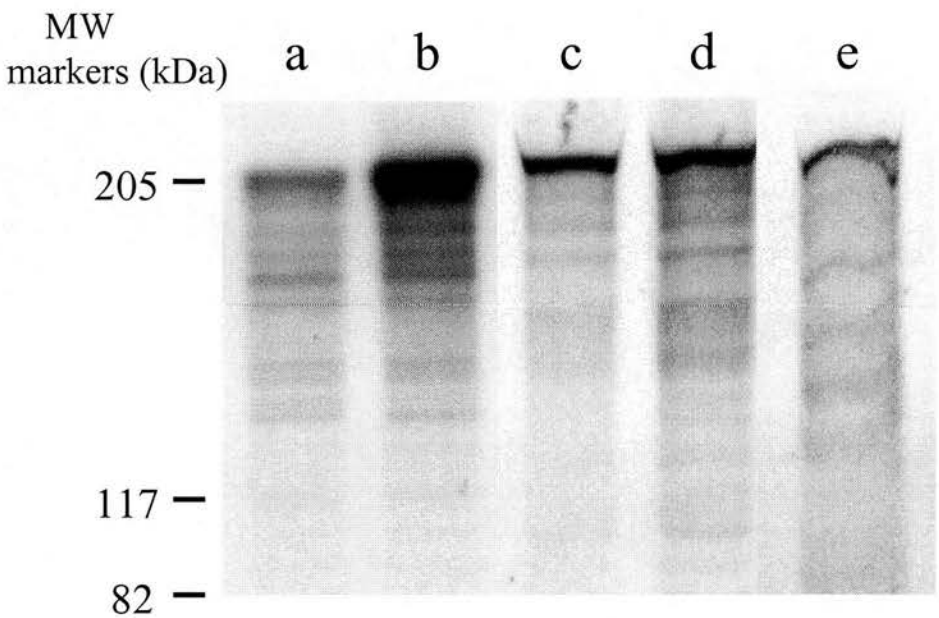

Figure 3-5. SDS-PAGE of [^{35}S]methionine labeled proteins after coupled transcription/translation of human *IP_3RI* cDNA.

Lane a: pBS-IP3, Lane b: pcDNA3-IP3, Lane c: pCI-IP3,
Lane d: pCITE-IP3, Lane e: pCI-IP3-UTR.
In vitro transcription/translation was carried out using the TNT T7 Coupled system (Promega). After incubation at 30^{0}C for 90 min, 5 μl of lysate was resolved on 5% (w/v) SDS-PAGE. The gel was then dried and exposed to X-ray film. The position of MW markers is shown.

IP_3RI could still not be obtained (Figure 3-5).

As a result of these studies it was hypothesised that the production of the short, truncated proteins might arise from: (1) the limitations of the *in vitro* transcription/translation system for producing large products, (2) errors in the DNA sequence leading to premature termination. Three constructs were made to test this second idea in the coupled *in vitro* transcription/translation system. They were all in pBlueScript, and included pIP3-1 (position 1 to 2161, MW 82 kDa), pIP3-2 (position 1 to 2539, MW 96 kDa), and pIP3-3 (position 1 to 5430, MW 206 kDa). When these constructs were expressed *in vitro*, full-length products were obtained from each reaction although some additional truncated proteins were found from pIP3-3 expression (Figure 3-6). From this result, it was clear that the system could transcribe and translate *IP_3RI* cDNAs up to 5430 bp long. Why did translation fail at some point after position 5430? The simplest explanation was that the sequence following this position contained an error, causing the production of stop or "nonsense" codons, so that translation stopped before a full-length product was produced.

3.4 Automated Sequencing and Sequence Correction

In order to establish whether coding errors had occurred, *IP3RI* cDNAs were sent to Oswel (Southampton, UK) for single-stranded automated sequencing. Where ambiguous sequences were found, a reverse primer was designed and that region was re-sequenced in the opposite direction. After a total of 19 rounds of sequencing, 8 nucleotides were found to be different from the published sequence (G18T, T21C, A79G, A679G, G682A, A721T, C1290T, and G7297T). This caused 5 amino acids

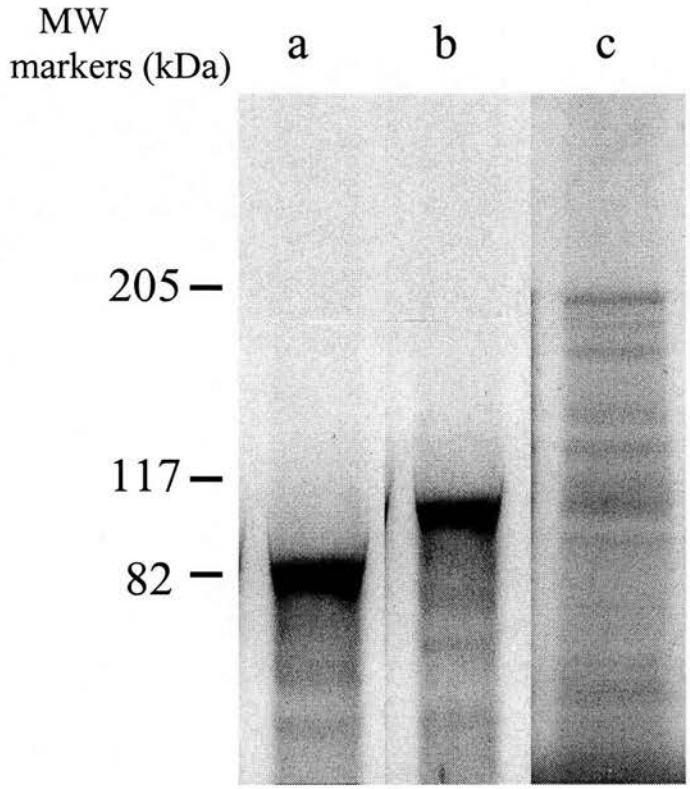

Figure 3-6. *In vitro* expression of three different human IP_3RI cDNA constructs.

Lane a: pIP3-1 (nucleotides 1 to 2161)
Lane b: pIP3-2 (nucleotides 1 to 2539)
Lane c: pIP3-3 (nucleotides 1 to 5430)
The experiment was carried out as described for Figure 3-5.

to be changed (I27V, S227G, D228N, R241W, and A2433S). In addition, a single base deletion was found at position 6429 (AGGAA to AGAA), and this was confirmed by manual sequencing (Figure 3-7). Because of this mutation the reading frame was shifted and a stop codon was generated at position 6455. The original plasmid HC-8 was checked by manual sequencing, but contained no mutation. Therefore, the mutation occurred during the assembly of full-length *IP$_3$RI*, although this was carried out by subcloning (not PCR).

In order to correct this mutation, HC-8 was double-digested with *Eco*47III and *Xba*I and the inserts were ligated to pcDNA3-IP3 double-digested with the same enzymes. The sequences around the mutation site were confirmed to be correct by manual sequencing. When using the *in vitro* coupled transcription/translation system to express the correct version of *IP$_3$RI* in pcDNA3, full-length products were obtained although some truncated proteins remained (Figure 3-8).

3.5 Discussion

DNA replication in prokaryotic and eukaryotic organisms is a highly accurate process, with only one error being committed per 10^9 to 10^{10} incorporated nucleotides (Drake, 1991). This high fidelity of DNA replication is achieved by at least three critical steps: (1) the insertion of the correct nucleotides by DNA polymerase; (2) 3'→5' exonuclease activity of DNA polymerase, allowing proofreading of the incorporated nucleotides; (3) postreplicative DNA mismatch repair (Echols *et al.*, 1983; Schaaper, 1993). Because DNA is a structurally dynamic molecule, it is able to adopt a variety of conformations. This flexibility provides a significant opportunity

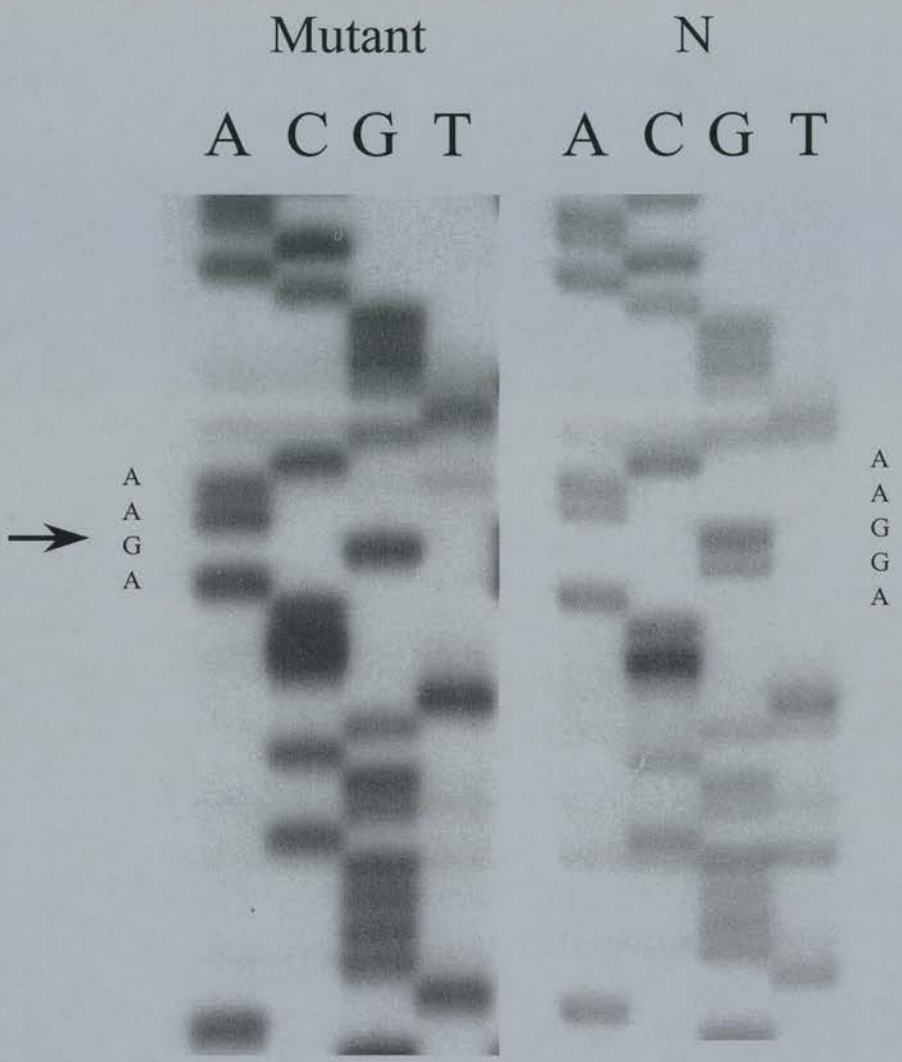

Figure 3-7. Dideoxy sequencing shown the mutation of human *IP$_3$RI* cDNA.

N is the correct *IP$_3$RI* cDNA. A single nucleotide deletion was found. The arrow shows that the sequence was changed from AGGAA to AGAA in the mutant.

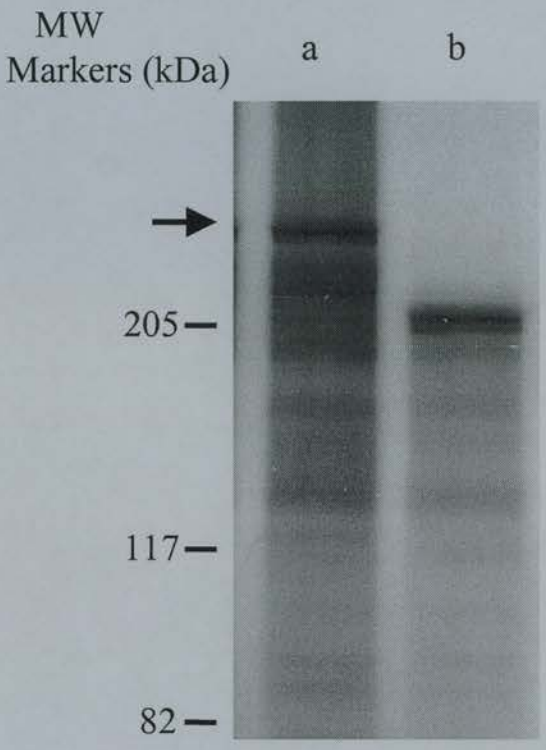

Figure 3-8. SDS-PAGE of [^{35}S]methionine labelled proteins after coupled transcription/translation of human "corrected" *IP_3RI* cDNA.

Lane a: corrected *IP_3RI* cDNA in pcDNA3
Lane b: mutant *IP_3RI* cDNA in pcDNA3
The arrow shows full-length IP_3RI (~260 kDa). The experiment was carried out as described for Figure 3-5.

for errors due to misalignment of strands. There are two major types of mutation, base-substitutions and frame-shifts (Kunkel, 1990) (Figure 3-9). The assay was performed by constructing a double-stranded DNA substrate with a 390-nucleotide single-stranded gap from a circular bacteriophage M13mp2 DNA. The gap contains the reporter gene for DNA synthesis errors, the wild-type *lacZ* gene sequence encoding the N-terminal amino acids (α-peptide) of the enzyme β-galactosidase. Correct polymerisation will fill the gap and produce functional gene. When this was transformed into an appropriate *E. coli.* strain, dark blue plaques formed on plates containing X-gal. The error DNAs formed lighter blue or colourless plaques. Since this assay measured loss of a gene function that is not essential for phage production, a wide variety of sequence mutations at many different sites could be analysed and sequenced.

Several factors mediated the mutations, including the nature of the DNA polymerase, the position and composition of DNA, and the processivity of the DNA polymerase. These factors may work together in a complicated manner. In addition, de Boer and Ripley (1988) found that the GC rich sequences adjacent to the 3' direction of the mutation sites increased the mutation frequencies. GC rich sequences are found in both 5' and 3' direction around the base deletion site of the *IP_3RI* cDNA. Therefore, this might be a factor in the occurrence of mutant *IP_3RI*. The *IP_3RI* cDNA is also very long (~9 kbp) compared to other known cDNAs, so this also increases the possibility of misalignment of DNA and mutation.

In vitro expression systems are a very useful and convenient tool to investigate the function and properties of genes, but they are not as useful as either mammalian

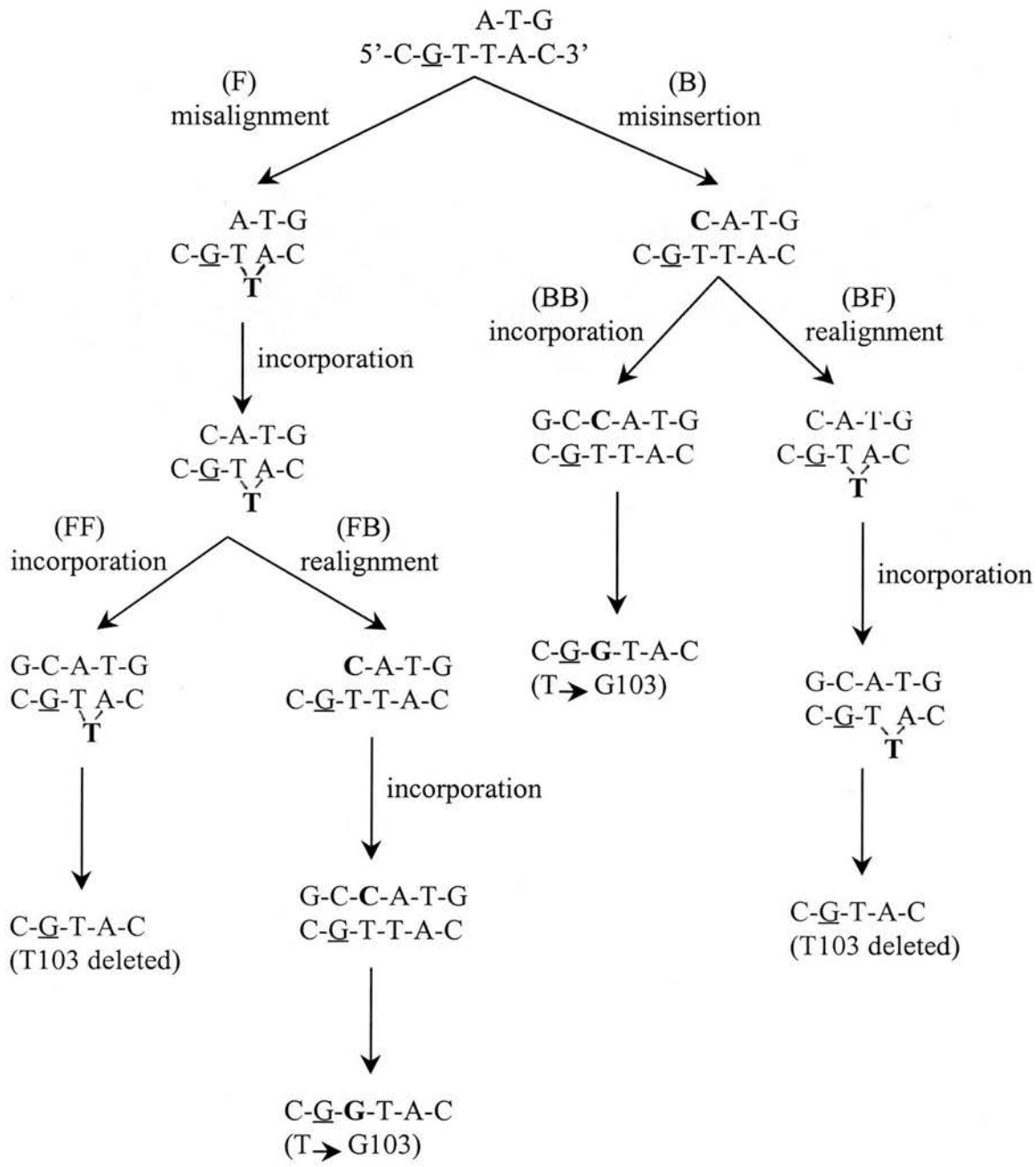

Figure 3-9. Pathways for single-base errors during DNA synthesis.

F = frame shift, B = base substitution. The underlined base is position 102, where position 1 is the first transcribed base of the *lacZ* gene. Adapted from Kunkel (1990).

or insect cell expression systems for expressing high molecular weight proteins like the IP_3R (Mignery *et al.*, 1990; Yoneshima *et al.*, 1997). Canine pancreatic microsomal membranes can be added into the *in vitro* expression system for studying the post-translational processing of expressed proteins (Walter *et al.*, 1984), although the patterns of the modification might be different from the original cells. In order to match cellular expression conditions as close as possible, *in vivo* expression systems were used as discussed in the following chapter.

Chapter 4

In vivo Expression of Human IP_3RI and FKBP12

4.1 Expression of Human IP_3RI in Mammalian HEK293 Cells

Mammalian cells have been used in the production of recombinant proteins, antibodies, and viruses (Walker, 1998). In addition to being used for commercial purpose, mammalian cell expression systems has served as a means for studying many important cellular processes, including gene replication, transcription, translation, and post-translational processing of proteins. Important features of mammalian cells include their ability to perform post-translational modifications, and to secret glycoproteins in correctly folded forms. In contrast, *E. coli* does not possess any glycosylation machinery, and yeast tends to produce hypermannose-type glycosylation, which is different from sialyl glycoforms produced by mammalian cells. Moreover, the production of intracellular proteins like IP_3R in *E. coli* leads to accumulation of the protein in insoluble refractile bodies, requiring subsequent denaturation and refolding.

Partial-length human *IP_3RI* cDNA (the truncated pcDNA-IP3 construct) was transiently expressed in HEK293 cells. 48 h after transfection using either Tfx-20 (DNA/Tfx-20 ratio of 15 μg/45 μl per 100 mm culture dish) or Lipofectin (DNA/Lipofectin ratio of 4 μg/40 μl per 100 mm culture dish), both cytosolic and membrane fractions were purified and resolved using 5% (w/v) SDS-PAGE. A typical Western blot result is shown in Figure 4-1. Although the truncated IP_3RI does not have the C-terminus containing all transmembrane regions, it was found in membrane fractions. The cytosolic fraction of transfected cells showed no detectable signal from Western blot. pCI-IP3 and pCI-IP3-UTR were also transfected into HEK293 cells. As described in section 3.2.1, pCI-IP3 contains the same CMV

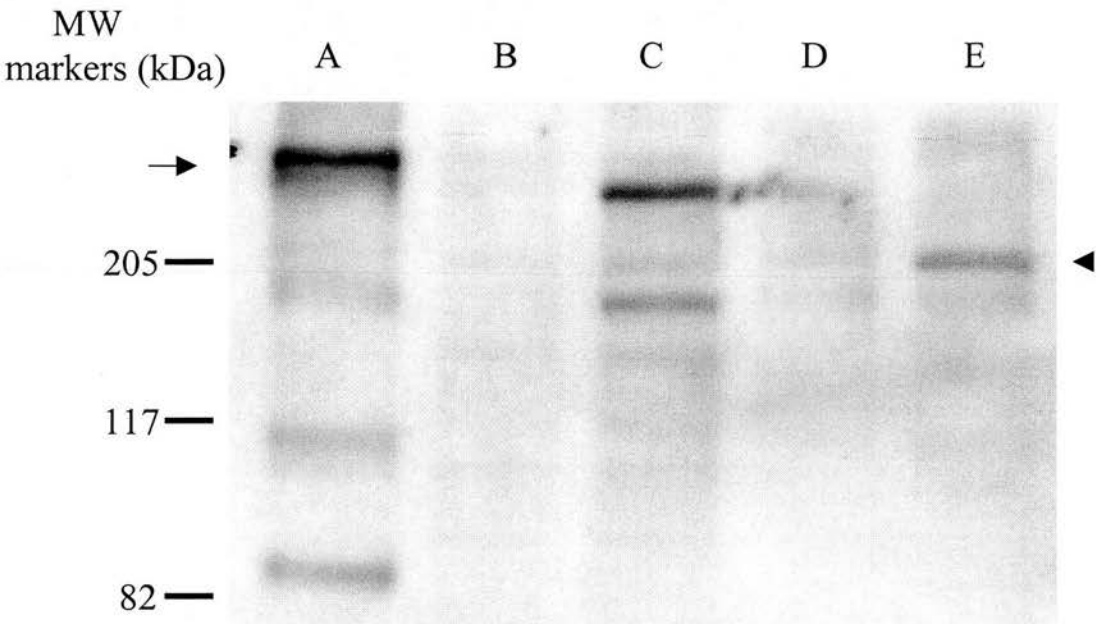

Figure 4-1. Western blot of human *IP_3RI* expressed in HEK293 cells

Lane A: membrane fractions of rabbit brain (positive control)
Lane B: membrane fractions of HEK293 cells (negative control)
Lane C: membrane fractions of HEK293 cells transfected with full-length pcDNA-IP3
Lane D: cytosolic fractions of HEK293 cells transfected with truncated pcDNA-IP3
Lane E: membrane fractions of HEK293 cells transfected with truncated pcDNA-IP3
The arrow shows full-length IP_3RI (~260 kDa). The arrow head shows truncated IP_3RI (~200 kDa). Anti-IP_3R N-terminal Ab was used and followed by the standard protocol described in section 2.5.3.

promoter as pcDNA-IP3, and a heteromeric intron for high-level expression. pCI-IP3-UTR is the same as pCI-IP3, except that mouse 5'-UTR was inserted before the first start codon of *IP_3RI*. The expression of these two constructs gave similar results to pcDNA-IP3 (data not shown).

pcDNA-IP3 (full-length) was also transfected into HEK293 cells using Lipofectamine. A DNA/Lipofectamine ratio of 7 μg/35 μl per 100 mm culture dish was used for transfection, followed by standard membrane purification and Western blotting. The result is shown in Figure 4-1. The full-length IP_3RI was identified, with some proteolytic products.

4.2 Indirect Immunofluorescence of Human IP_3RI in HEK293 Cells

Indirect immunofluorescence is a very useful technique to localise expressed proteins to specific compartments of cells. Because the primary antibody of the target protein is not conjugated to a fluorochrome, a fluorochrome-labelled (e.g. fluorescein, rhodamine or R-phycoerythrin) secondary antibody is required to bind the primary antibody, and thus enable the expressed proteins to be detected using a fluorescence microscope.

In this study, HEK293 cells were transfected with pcDNA3-IP3 (full-length). After 48 h of transfection, rabbit anti-IP_3RI polyclonal antibodies and rhodamine-conjugated goat anti-rabbit IgG secondary antibodies were added, followed the procedure described in section 2.6.10. The result is shown in Figure 4-2A. The localisation of IP_3RI (red) around the nucleus and spreading in a "reticular" fashion into the cytoplasm suggests it is in the ER. To confirm the ER localisation, Di-O-

A.

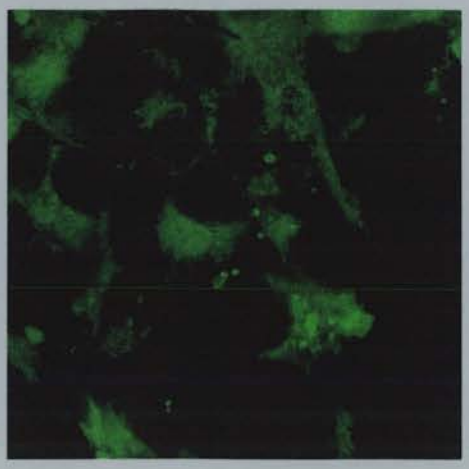

B.

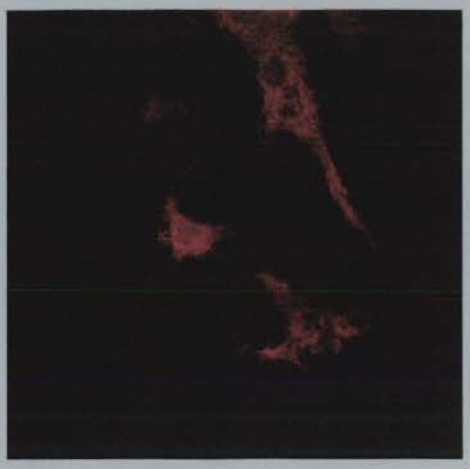

C.

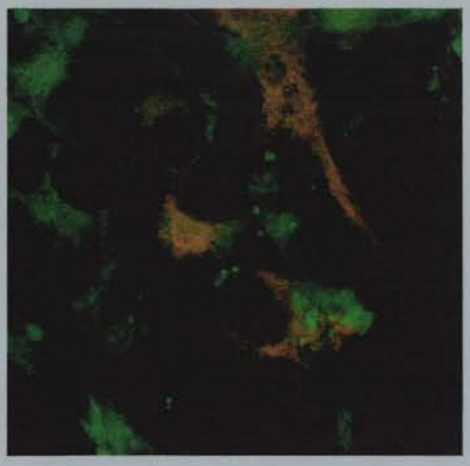

Figure 4-2. Indirect immunofluorescence of human IP_3RI expressed in HEK293

A. The ER membrane of HEK293 cells were labelled by Di-O-C_5(3). (green)
B. IP_3RI was localised by TRITC-conjugated secondary antibodies. (red)
C. Super-imposition of A and B using Paint Shop Pro (Jasc Software). (yellow)
The experiment was carried out as described in section 2.6.10.

$C_5(3)$ (Molecular Probe), which binds to the ER, was also used to identify the ER membrane (Figure 4-2B). After superimposing these two figures by Paint Shop Pro (Jasc Software), a clear match (yellow) can be observed (Figure 4-2C). Thus, recombinant IP_3RI was confirmed to reside in the ER membrane.

4.3 IP_3 Binding and Planar Lipid Bilayer Reconstitution of IP_3RI Expressed in HEK293 Cells

An IP_3 binding assay was used to measure the binding ability of expressed IP_3RI in HEK293 cells (see section 2.7.1 for detailed procedures). Both truncated and full-length IP_3RI were used to detect IP_3 binding activity. However, very low IP_3 binding activity (~0.1 pmol/mg of proteins) could be detected (Figure 4-3). Furthermore, full-length IP_3RI was also failed to form specific IP_3RI channels when reconstituted in planar lipid bilayer (see section 2.7.2 for bilayer reconstitution procedures). The reason may be due to low level of IP_3RI expressed in HEK293 cells following transient expression.

4.4 Production of HEK293 Cells Stably Transfected with IP_3RI

In order to get high level expression of IP_3RI in HEK293 cells, a stably transfected cell line was tried to establish. As mentioned earlier, 48 h after transfection of pcDNA-IP3 using Lipofectamine in a 100 mm culture dish, cells were split into 3 x 100 mm culture dish containing 1.2 mg/ml of G418 in DMEM medium. The medium was changed every 5 days with that containing the same concentration of G418. After 4 weeks, several positive clones were found and collected for further

A.

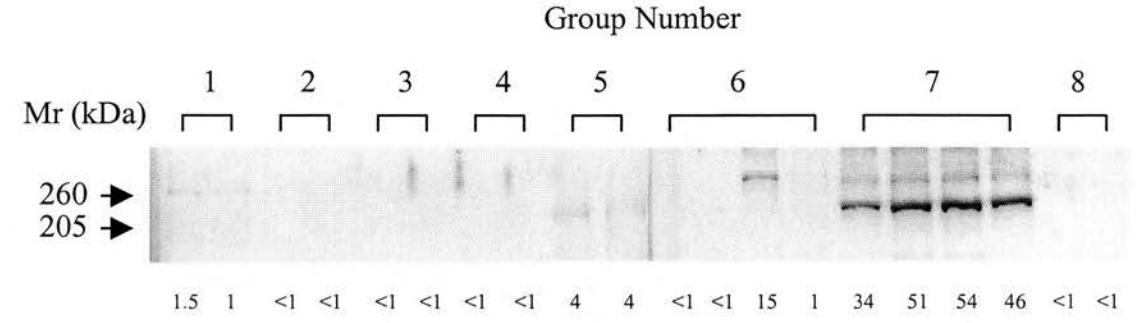

B.

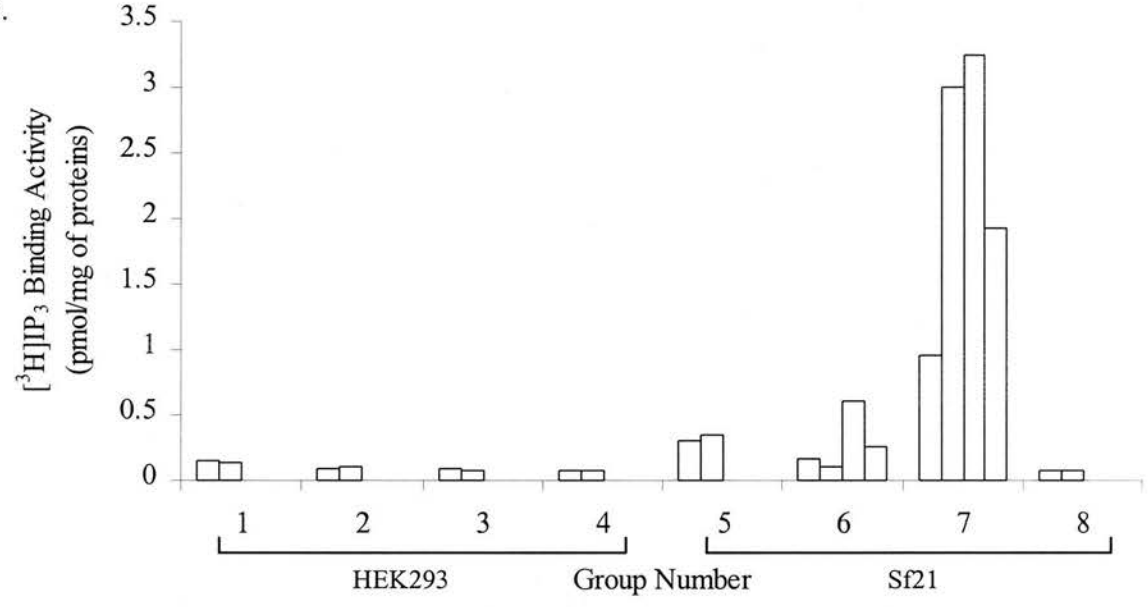

HEK293 only				+				
Sf21 only								+
M/full-length IP_3RI	+					+		
M/truncated IP_3RI		+					+	
C/truncated IP_3RI			+		+			
unit of intensity per IP_3 binding activity	-	-	-	-	~13	~25	~25	-

Figure 4-3. [^{3}H]IP_3 binding activity of IP_3RI expressed in HEK293 and Sf21 cells

A. Western blot of expressed IP_3RI in HEK293 or Sf21 cells. 25 μg samples in groups 1 to 5 and 6 to 8 were loaded on the same gels, respectively. Anti-IP_3R N-terminal Ab was used as described previously followed by ECL. Each number under the blot shows relative intensity of each band (analysed by phosphorimager).
B. Corresponding [^{3}H]IP_3 binding activity of IP_3RI.
M/full-length IP_3RI : membrane fractions of full-length IP_3RI
M/truncated IP_3RI : membrane fractions of truncated IP_3RI
C/truncated IP_3RI : cytosolic fractions of truncated IP_3RI
Each column represents an independent binding assay.

identification of IP_3RI expression. However, the expression level of IP_3RI was similar to untransfected HEK293 cells (data not shown). Thus, a baculovirus expression vector system was used for high-level expression of IP_3RI.

4.5 Expression of Human IP_3RI in Insect Cells

4.5.1 Introduction

The Baculovirus Expression Vector System (BEVS) is one of the most powerful eukaryotic expression systems available (O'Reilly *et al.*, 1992). It has been used to express heterologous genes in insect cells from many different sources, including viruses, mammals, fungi, plants and bacteria. The baculovirus belongs to a family of double-stranded DNA virus called the *Baculovirinae*, which infects many different species of insects. They are highly specific and are not known to infect any non-arthropod hosts. This family can be divided into two subfamilies, occluded baculoviruses (*Eubaculovirinae*) and non-occluded baculoviruses (*Nudibaculovirinae*). The two *Eubaculovirinae* most commonly used in expressions are *Autographa californica* nuclear polyhedrosis virus (AcNPV) and *Bombyx mori* nuclear polyhedrosis virus (BmNPV). They have a large circular genome of ~130 kbp. AcNPV is the most commonly used for heterologous expression in insect cells, and its entire genome has been sequenced (Ayres *et al.*, 1994). Several AcNPV genes, which are nonessential in the tissue culture life cycle (e.g. polyhedrin and p10), can be replaced by heterologous genes. Since the entire genome of AcNPV is too large to directly insert foreign genes by cloning, the gene of interest is cloned into a transfer vector. Co-transfection of the transfer vector containing foreign genes with

linearised AcNPV DNA into Sf9 insect cells makes use of homologous recombination in the nucleus, which transfers the heterologous gene from the transfer vector to the AcNPV DNA. Recombinant proteins can be produced by the polyhedrin promoter at levels ranging between 30% and 50% of the total insect protein. The system was used in an attempt to obtain high-level expression of recombinant human IP_3RI.

The life cycle of the baculovirus is shown in Figure 4-4. The name baculovirus refers to the rod shaped capsid of viral particles. Because the capsid is flexible, it can accommodate large genomes generated by the insertion of a foreign gene. During viral infection, two forms of viral progeny are produced, budded virus particles and occluded virus particles. Budded virus particles contain a loose membrane capsid and are processed by migrating through the plasma membrane during 10-12 h of postinfection. Occluded virus particles are embedded in viral inclusions called polyhedrin produced after 18-24 h of postinfection, and are processed by acquiring a membrane from the nuclear membrane. This creates a stable membrane capsid that protects viruses from desiccation in the environment. Both occluded and budded viruses are found in wild-type AcNPV infected cells. However, recombinant AcNPV viruses which lack the polyhedrin gene do not display polyhedrin occlusion bodies. Budded viruses are the only types of virus found in recombinant AcNPV infected cells.

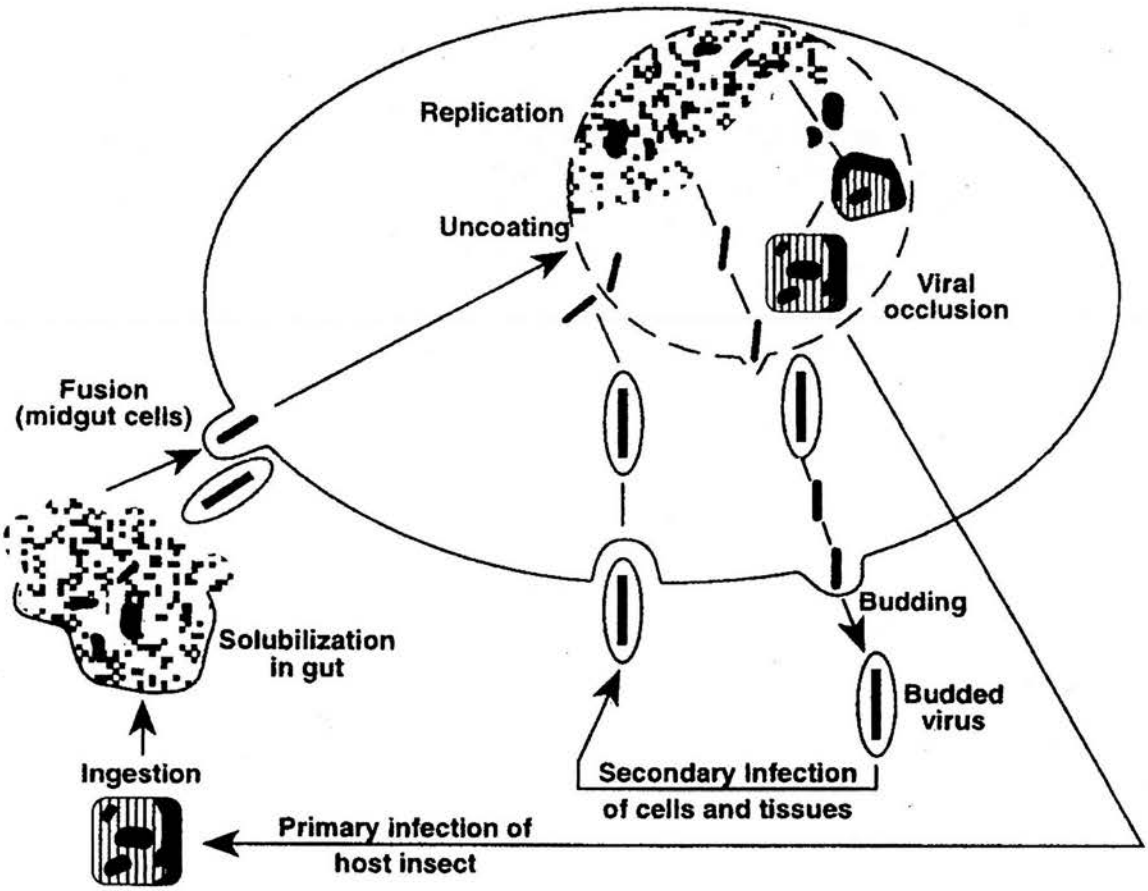

Figure 4-4. The life cycle of the baculovirus

See previous page for description. Adapted from Summers and Smith (1985).

4.5.2 p10 Locus-Based Expression of Truncated Human IP_3RI

The transfer vector pAcUW43 (Pharmingen) was chosen for the expression of human IP_3RI. pAcUW43 is a p10 locus-based vector which contains the polyhedrin gene promoter inserted downstream of and in tandem with the p10 gene promoter. A copy of the SV40 transcription termination sequences between the two promoters has been inserted to prevent "read through" into the polyhedrin gene promoter. Therefore, two different genes can be expressed at the same time in insect cells.

pcDNA-IP3 was double digested with *Kpn*I and *Not*I and the insert was subcloned into pAcUW43 double digested with the same restriction enzymes. This ligated product was called pAcUW43-IP3. The linearised AcUW1.lacZ DNA (Pharmingen) is a modified AcNPV DNA in which the *lacZ* gene replaces the p10 gene and is driven by the p10 promoter. This was used for cotransfection with pAcUW43-IP3. Homologous recombination disabled the *lacZ* gene, so that recombinant AcUW1.lacZ DNA could be colour selected by plaque assay on X-gal plates. Non-recombinant viruses expressing the *lacZ* gene gave blue plaques, whereas recombinant viruses did not express the *lacZ* gene and produced colourless plaques. Since the polyhedrin gene was still retained in the AcUW1.lacZ DNA, both non-recombinant and recombinant viruses were occlusion body positive. The cotransfection reaction was set up in a 1.5 ml microcentrifuge tube as follows:

Linearised AcUW1.lacZ	5 µl
pAcUW43-IP3 (0.1 µg/µl)	5 µl
ds H_2O	40 µl
Lipofectin (0.1 µg/µl)	50 µl

The mixture was mixed thoroughly and incubated at room temperature for 15 min. During the incubation, a 60 mm tissue culture dish with 50% confluent Sf9 insect cells was washed with 2 ml of serum-free Grace's medium, and then 1.5 ml of serum-free medium were added. The DNA-Lipofectin mixture were added dropwise to the culture dish and incubated at 28^{0}C for 4 h. 1.5 ml of 10% (v/v) FBS in Grace's medium were added to the culture dish which was incubated at 28^{0}C for a further 4 to 5 days until occlusion bodies were identified under the microscope. The medium was then collected and a plaque assay was performed to isolate pure recombinant virus from non-recombinant virus (as described in Chapter 2).

As described earlier, the recombinant viruses formed colourless plaques on X-gal plates. The identification of colourless plaques was found to be difficult, and an "end point dilution assay" (EPDA) was also used to identify recombinant virus. Four serial ten-fold dilutions from 10^2-fold to 10^5-fold containing a final concentration of 150 μg/ml X-gal were prepared, and each dilution was used to infect 24 wells in a 96 well plate. This initial screen produced at least one dilution where the infection rate was lower than one virus per well. Wells that were infected at this limiting dilution were generally the result of a single "plaque forming unit" (pfu). Because of the X-gal added to the serial dilutions, the colourless wells which contained recombinant viruses could be distinguished from the blue coloured wells. Nine colourless wells from 10^3-fold dilutions were chosen and the cells were collected for identification by further Western blot analysis. Unfortunately, there were no positive results from Western blotting (data not shown). The reason may have been a low population of recombinant virus (~30%), and difficulty in isolating recombinant viruses from non-

recombinant viruses. In order to increase the homologous recombination frequency, the MaxBac 2.0 system (Invitrogen) was used. This is described in the following section.

4.5.3 Polyhedrin Locus-Based Expression of Truncated Human IP_3RI

The MaxBac 2.0 system (Invitrogen) was used for the expression of human IP_3RI. The truncated pcDNA-IP3 construct was doubled digested with *Kpn*I and *Xba*I, and the insert was subcloned into the transfer vector pBlueBac4.5 (Invitrogen) double digested with the same restriction enzymes. The ligation product was called pBac-IP3 (truncated). pBlueBac4.5 contains the polyhedrin promoter for the expression of the foreign gene, and the 5' end sequences of the *lacZ* gene driven by the early-to-late promoter for the synthesis of β-galactosidase as a reporter gene (Crawford and Miller, 1988). The linearised Bac-N-Blue DNA is a modified AcNPV DNA, which contains only the 5' end sequences of ORF1629 and the 3' end sequences of the *lacZ* gene. When pBac-IP3 is cotransfected with Bac-N-Blue DNA, homologous recombination occurs at ORF1629 and the *lacZ* gene, which enables the production of viable viruses. Non-recombinant viruses are not viable, because the 3' end sequences of the ORF1629, which has been shown to be essential for viral propagation, are deleted in Bac-N-Blue DNA (Kitts and Possee, 1993). Thus, the population of recombinant virus is over 90%. The recombination events between Bac-N-Blue DNA and pBlueBac4.5 transfer vector are shown in Figure 4-5.

pBac-IP3 was cotransfected with Bac-N-Blue DNA into Sf9 insect cells following the standard procedure (section 2.6.4). 6 days after transfection, ~90% of

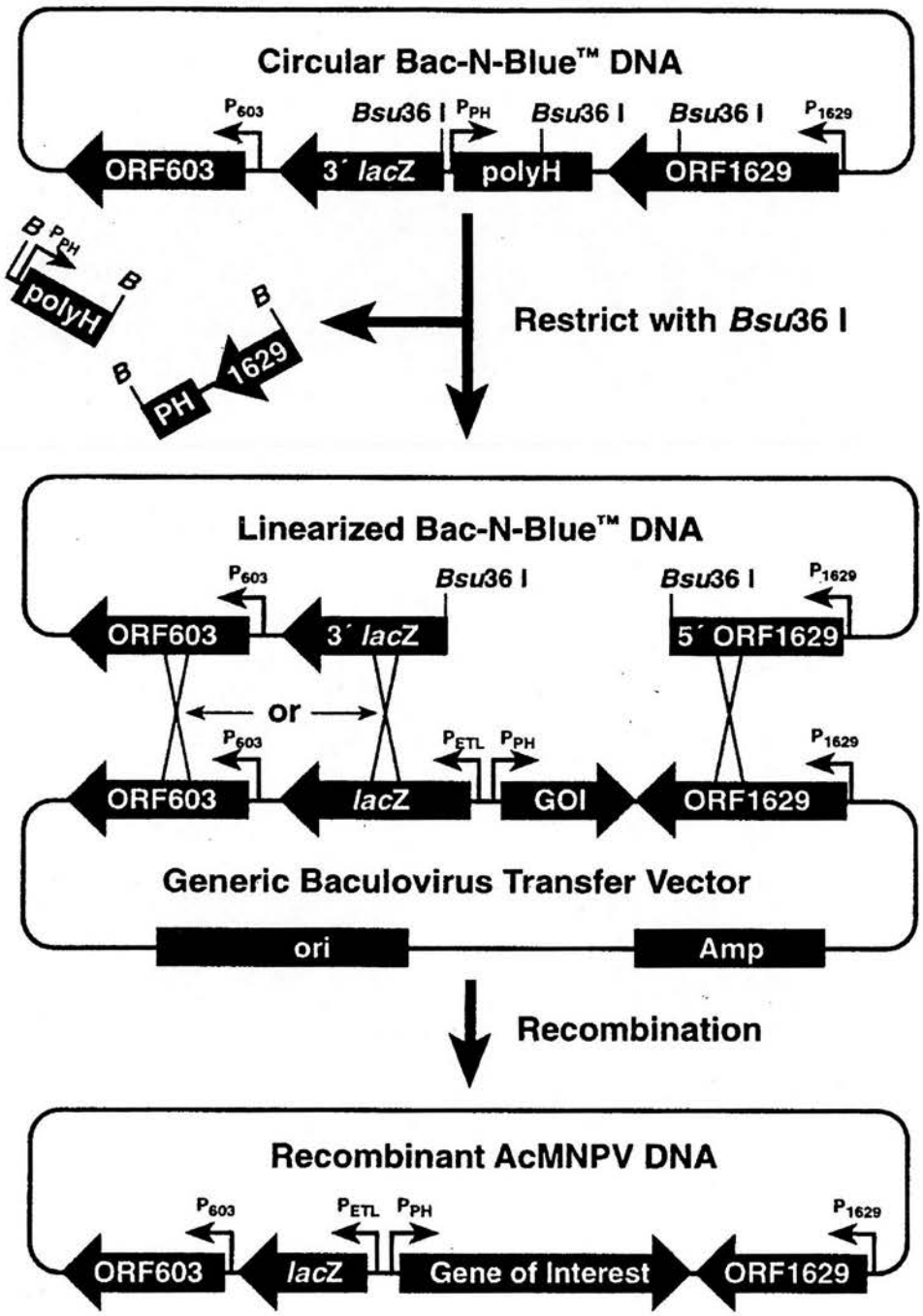

Figure 4-5. Homologous recombination of modified baculovirus DNA and the transfer vector.

See previous page for description. Adapted from the manual of MaxBac 2.0 baculovirus transfer vectors (Invitrogen).

cells were lysed and the medium was collected. Some cells contained occlusion bodies. This may have been due to the small amount of uncut circular viral DNA in Bac-N-Blue DNA. Although the amount of uncut viral DNA is very low, it transfects ~10,000-fold better than linearised Bac-N-Blue DNA. It was very important to separate the recombinant viruses from any wild-type viruses, since the wild-type viruses infect and replicate more efficiently than recombinant viruses, causing the dilution of recombinant viruses over time. Therefore, a plaque assay was performed to purify the recombinant virus (section 2.6.5). Ten blue plaques were picked up, followed by the preparation of primary virus stock (section 2.6.6). The DNA was extracted from 100 µl of each primary virus stock, and analysed by PCR to rule out "false positive" plaques that contained the mixture of recombinant and non-recombinant viruses. One set of primers (Bac-For: 5'-TTTACTGTTTTC GTAACAGTTTTG-3', Bac-Rev: 5'-CAACAACGCACAGAATCTAGC-3') was designed to flank the polyhedrin region (839 bp), and another set of primers (T5583: 5'-AGGCGCTCAGGCAAGTTC-3', T2631: 5'-GGCATTGTTCTTCAGTTCTAA-3') was designed to produce a 1,076 bp fragment corresponding to positions 5180 to 6255 of *IP_3RI* cDNA. Thus, the pure recombinant viruses should produce only the 1,076 bp band, while the virus stock containing both wild-type and recombinant viruses should produce 1,076 bp and 839 bp bands. The PCR reaction was set up as follows:

10X reaction buffer	5 µl
$MgCl_2$ (25 mM)	5 µl
dNTP (10 mM)	1 µl

Bac-For or T5583 (20 μM)	1 μl
Bac-Rev or T2631 (20 μM)	1 μl
ds H_2O	31.5 μl
DNA	5 μl
Taq polymerase	0.5 μl

The PCR cycle was set as follows:

94°C, 2 min	1 cycle
94°C, 30 sec; 55°C, 1 min; 72°C, 2 min	28 cycles

A typical PCR result is shown in Figure 4-6. No. 8 virus stock was selected and amplified to produce high titre virus stock for protein expression (section 2.6.8). High titre virus stock was obtained by several rounds of infection with low multiplicity of infection (MOI), normally below 1. MOI (virions/cell) = titre of virus (virions/ml) x ml of inoculum / number of cells. At a low MOI, cells cannot be infected simultaneously, which allows an exponential increase in the virus titre. A high MOI (from 5 to 10) is usually used for protein expression, because when all cells are synchronously infected, the maximal amount of recombinant protein can be harvested at a given time point. Although the titre of virus is very important for protein expression, it has been found that the exact titre of virus is difficult to obtain by plaque assay, meaning that the exact MOI cannot be predicted. Instead of measuring the titre of virus stock, different amount of high titre virus measured by end-point dilution assay (EPDA) were added to Sf9 insect cells, and maximal protein expression was determined by Western blotting. Sf9 cells were collected after 48 h of infection, and the membrane fraction was purified and resolved on 5% (w/v) SDS-

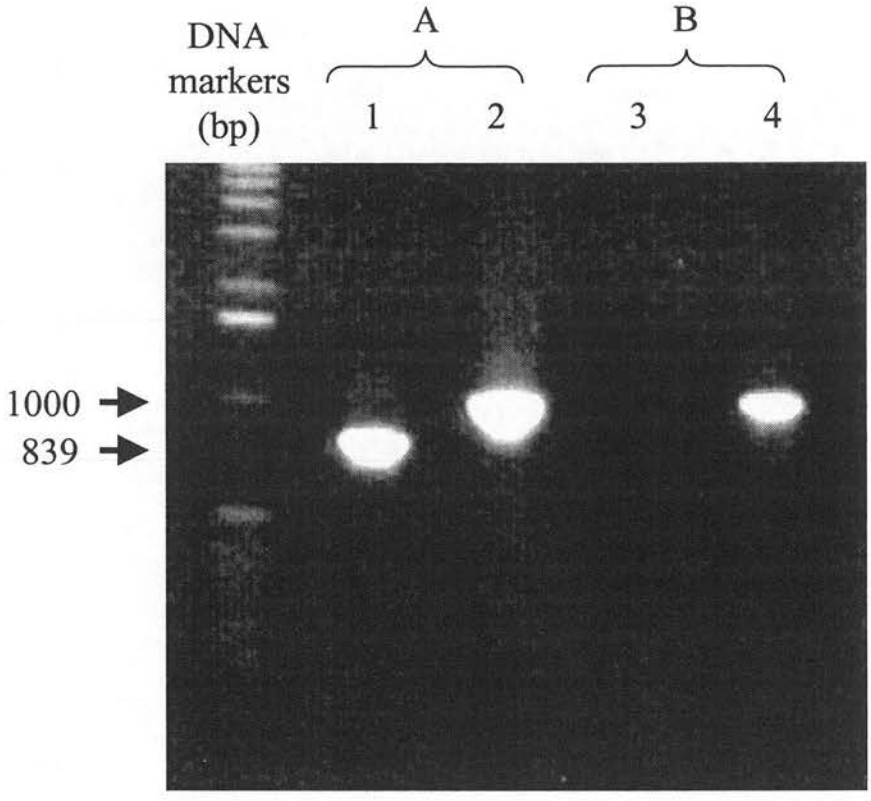

Figure 4-6. PCR analysis of recombinant *IP_3RI* viral clones

PCR analysis of clone A and clone B is shown. Lane 1 and 3 use the primer pair Bac-For and Bac-Rev for detecting wild-type virus DNA (839 bp). Lane 2 and 4 use the primer pair T5583 and T2631 for detecting *IP_3RI*. Clone A is a mixture of recombinant and wild-type virus, and clone B is a pure recombinant virus containing *IP_3RI*.

PAGE. A typical Western blot result was shown in Figure 4-7. The addition of No. 8, passage 4 virus stock from 0.75 ml to 1.5 ml shows almost the same strong signals. Infection time of 24 h and 48 h shows similar results, but after 72 h of infection shows weaker signals (result not shown). This may have been due to the degradation of IP_3RI, because most cells were lysed and released proteases from intracellular compartments at this time point. As expected, the size of the expressed protein is only ~200 kDa.

4.5.4 Polyhedrin Locus-Based Expression of Full-Length Human IP_3RI

The full-length pcDNA-IP3 construct was double digested with *Kpn*I and *Xba*I, and the insert was subcloned into the transfer vector pBlueBac4.5 (Invitrogen) double digested with the same restriction enzymes. The ligation product was called pBac-IP3 (full-length). Followed the same procedures described in 4.3.3, two high titre virus stock 1-2 P4 and 1-6 P4 were used for the production of recombinant human IP_3RI in Sf9 or Sf21 cells. The addition of different amount of 1-2 P4 or 1-6 P4 virus stock to Sf21 cells showed a similar IP_3RI expression level 48 h after infection (Figure 4-8). The expression level of IP_3RI in Sf21 was higher than in Sf9 (Figure 4-9). 48 h of infection produced more recombinant proteins than 72 h (Figure 4-10). In addition, membrane samples mixed with SDS-PAGE loading buffer without boiling at 100^0C for 5 min displayed a ~260 kDa band on Western blotting, whereas boiled samples showed an intense band on the top of separating gels. This suggests that boiling caused recombinant IP_3RI to aggregate. In contrast, truncated IP_3RI represented the same mobility independent of the boiling procedure (Figure 4-11).

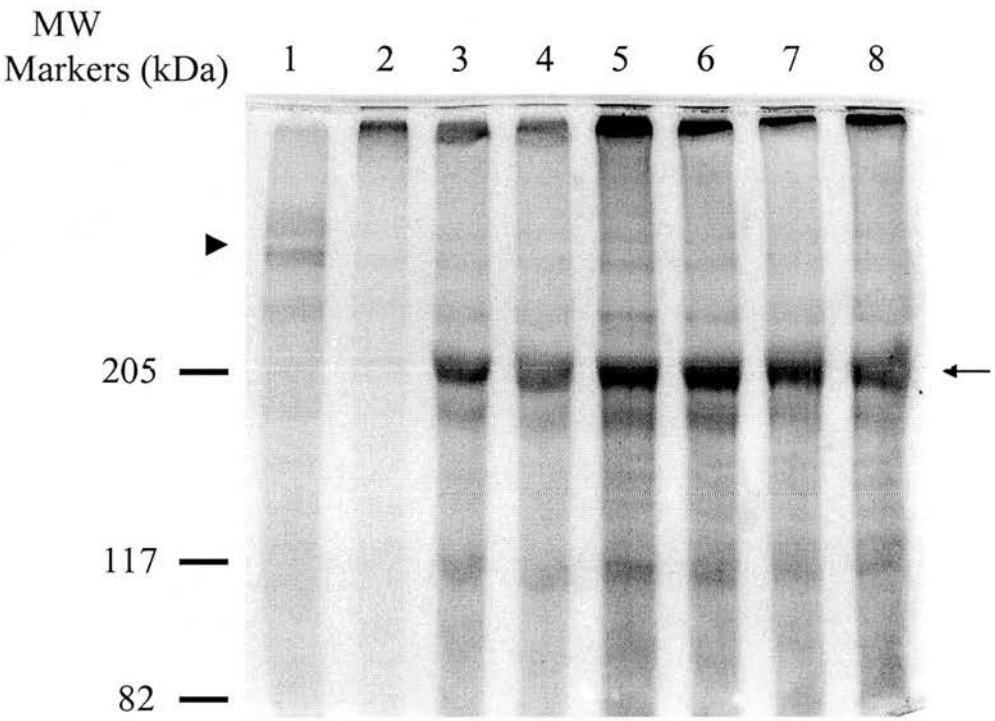

Figure 4-7. Western blot of human IP_3RI expressed in Sf9 cells

Lane 1: rabbit brain membrane fractions (positive control)
Lane 2: Sf9 membrane fractions (negative control)
Lane 3-8: 0.75, 0.9, 1.05, 1.2, 1.35, and 1.5 ml of No. 8, P4 virus stock were added, respectively.
48 h after infection, membrane fractions were purified using the standard method and resolved using 5% (w/v) SDS-PAGE followed by Western blotting using anti-IP_3R N-terminal Ab. The arrow shows truncated IP_3RIs (~200 kDa). The arrow head shows full-length IP_3RIs (~260 kDa).

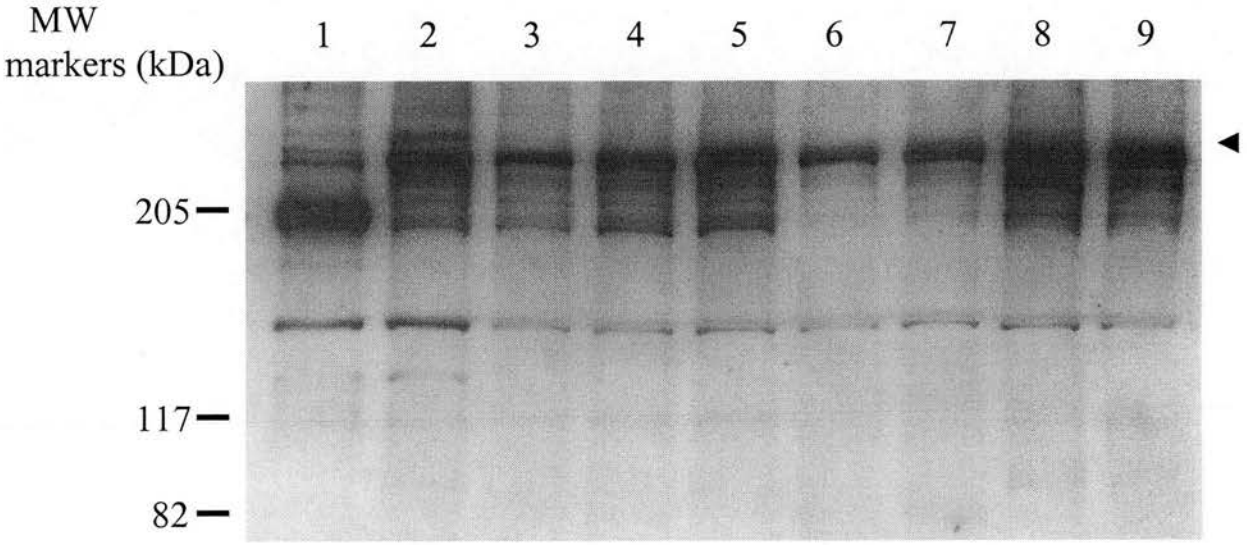

Figure 4-8. Western blot of the full-length IP_3RI expressed in Sf21

Lane 1: truncated IP_3RI expressed in Sf21
Lane 2-5: 1, 2, 3 and 4 ml of 1-2 P4 virus stock were added to Sf21 cells, respectively, and membrane fractions were purified after 48 h of infection.
Lane 6-9: 1, 2, 3 and 4 ml of 1-6 P4 virus stock were added to Sf21 cells, respectively, and following the same procedure as described above. 5 μl (~25 μg) of proteins were mixed with 5 μl of 2 X SDS-PAGE sample-loading buffer and loaded on 5% (w/v) SDS-PAGE without boiling followed by Western blotting. The full-length IP_3RI was identified in lane 2-9 (arrow head), and shown a similar expression level.

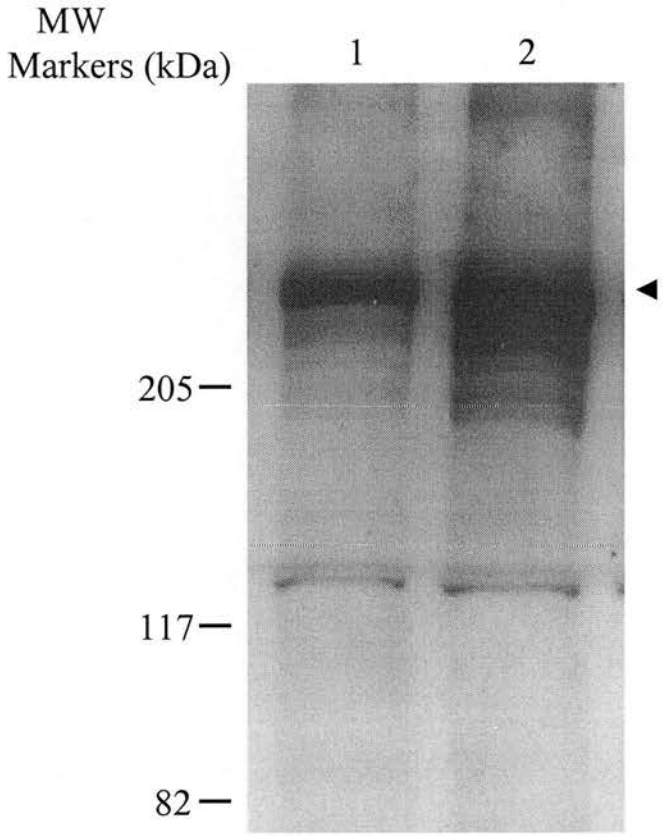

Figure 4-9. The expression level of full-length IP_3RI in insect cells

Lane 1: 1 ml of 1-2 P4 virus stock was added to Sf9 cells
Lane 2: 1 ml of 1-2 P4 virus stock was added to Sf21 cells
48 h of infection, membrane fractions were purified and resolved using 5% (w/v) SDS-PAGE (without boiling samples) followed by Western blotting. The arrow head shows full-length IP_3RI (~260 kDa). The expression level of IP_3RI in Sf21 was higher than that in Sf9, although the expression level of some lower MW proteins (possibly proteolytic fragments) was also increased in Sf21.

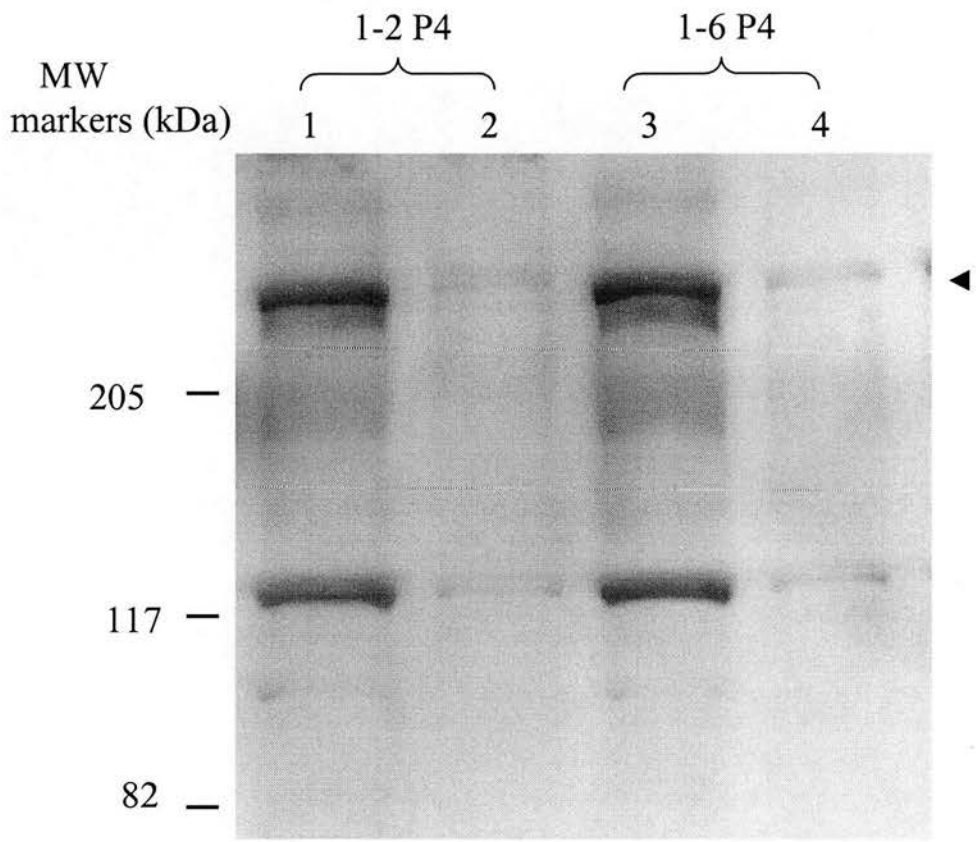

Figure 4-10. The expression level of full-length IP_3RI in Sf21 cells

1 ml of 1-2 P4 and 1-6 P4 was added to Sf21 cells, respectively. After 48 h (lane 1 and 3) or 72 h (lane 2 and 4) of infection, membrane fractions were purified and resolved using 5% (w/v) SDS-PAGE (without boiling samples) followed by Western blotting as described previously. The arrow head shows full-length IP_3RI (~260 kDa). 48 h of infection shows higher expression level than 72 h in both virus stock.

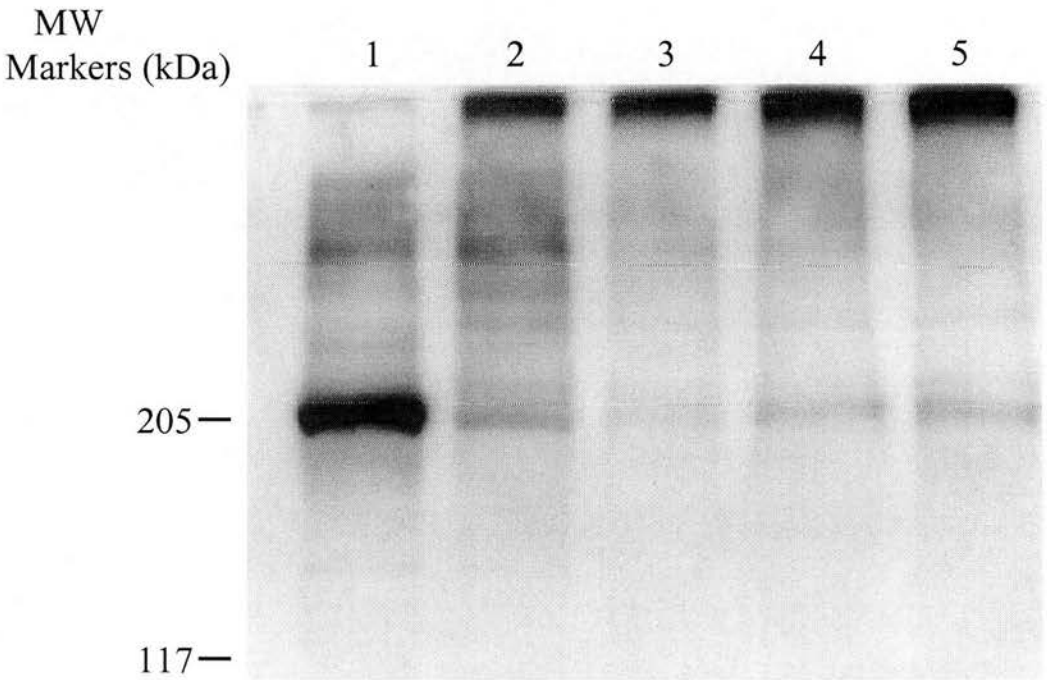

Figure 4-11. Western blot of full-length IP_3RI expressed in Sf21 cells

Lane 1: truncated IP_3RI expressed in Sf21
Lane 2-5: 1, 2, 3 and 4 ml of 1-6 P4 were added in Sf21, respectively, and the membrane fractions were purified after 48 h of infection. 5 μl (~25 μg) of membranes were mixed with 5 μl of loading buffer and then loaded on 5% (w/v) SDS-PAGE after boiling at 100^0C for 5 min followed by Western blotting. The expressed full-length IP_3RI aggregated on the top of the gel, whereas the truncated IP_3RI was at correct position.

4.6 Expression of Human FKBP12 in HEK293 Cells

FKBP12 is a soluble cytosolic protein with a molecular weight of 12 kDa (see section 1.5). It binds IP_3Rs and RyRs and regulates their activities (Marks, 1996).

The full-length human *FKBP12* cDNA (obtained as a gift from Prof. M. D. Walkinshaw, Genbank accession number M92422) was used as template, and a set of primers (forward primer: 5'-CGGGGTACCATGGGAGTGCAGGTGGAAACCA TC-3', reverse primer: 5'-CCGGAATTCTCATTCCAGTTTTAGAAGCTCCAC-3') was designed for a PCR reaction, set up as follows:

10 X reaction buffer	5 μl
dNTPs (10 mM)	1 μl
forward primer (10 μM)	1 μl
reverse primer (10 μM)	1 μl
dsH_2O	36 μl
template (1 ng/μl)	5 μl
Pfu (2.5 U/μl)	1 μl

All the reagents were well mixed and the thermocycler was set as follows:

94°C, 2 min	1 cycle
94°C, 30 sec; 45°C, 30 sec; 72°C, 1 min 30 sec	2 cycles
94°C, 30 sec; 50°C, 30 sec; 72°C, 1 min	28 cycles

A ~350 bp fragment was obtained and double digested with *Kpn*I and *Eco*RI. After purified from a 1% (w/v) agarose gel, it was ligated to pcDNA3 double digested with *Kpn*I and *Eco*RI. The ligation product was called pcDNA-FKBP.

pcDNA-FKBP was then transfected into HEK293 cells using Lipofectamine. A DNA/Lipofectamine ratio of 7 μg/35 μl per 100 mm culture dish was used for transfection. 48 h after transfection, 3 x 100 mm of cells were homogenised in 3 ml of homogenisation buffer (see 2.5.5). After 20 strokes using a tight-fitting glass-Teflon homogeniser, the homogenates were centrifuged at 1,000 x g for 10 min at 4°C. The supernatant was then concentrated using Centricon-10 (Amicon) to a concentration of ~5 mg/ml of proteins containing expressed FKBP12. The Western blot result is shown in Figure 4-12.

4.7 Expression of Human FKBP12 in Sf9 Cells

The same PCR product described in previous section was used for assembling human FKBP12 cDNAs in Baculovirus expression vector pBlueBac4.5. The fragment was double digested with *Kpn*I and *Eco*RI, and it was then subcloned into pBlueBac4.5 double digested with the same enzymes. The ligation product was called pBac-FKBP. Following the standard procedures described in Chapter 2, a recombinant virus was obtained by plaque assay. The primer set (Bac-For and Bac-Rev) was used by PCR for identifying pure FKBP12 virus stock. As shown in Figure 4-13, pure recombinant virus stock contains only one fragment (~760 bp), while recombinant virus with wild-type virus stock produces two bands (~760 and ~840 bp). Two high titre virus stocks No. 6 P4 and No. 8 P4 were obtained after 3 rounds of infection of Sf9 cells. 48 h of infection with 1.5 ml of No. 6 P4 high titre virus, cells were treated as the same procedure described in previous section. The Western blot result is shown in Figure 4-14.

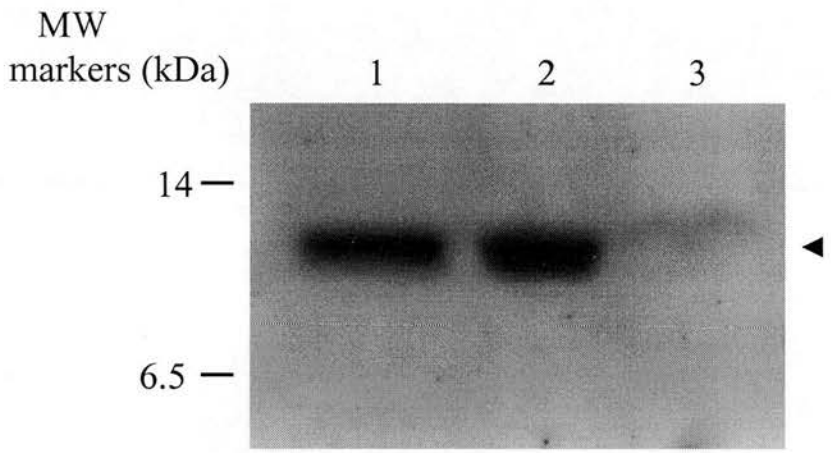

Figure 4-12. Western blot of FKBP12 expressed in HEK293 cells

Lane 1: human FKBP12 (positive control)
Lane 2: recombinant FKBP12 expressed in HEK293
Lane 3: HEK293 alone
10 μg of human FKBP12, 25 μg of recombinant FKBP12 and 25 μg of cytosolic fractions of HEK293 cells were loaded on 15% (w/v) SDS-PAGE followed by Western blotting using anti-FKBP12 C-terminal Ab. The arrow head shows FKBP12 (12 kDa). Some intrinsic FKBP12 was found in HEK293 cells.

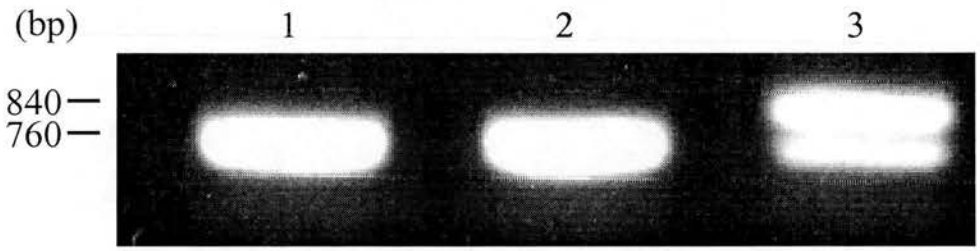

Figure 4-13. PCR analysis of recombinant FKBP12 viral clones

A typical PCR result is shown. Clone 1 and 2 contained only a 760 bp fragment, which meant that they were pure FKBP12 viral clones. Clone 3 contained both 840 bp and 760 bp fragments, which meant that it contained wild-type virus.

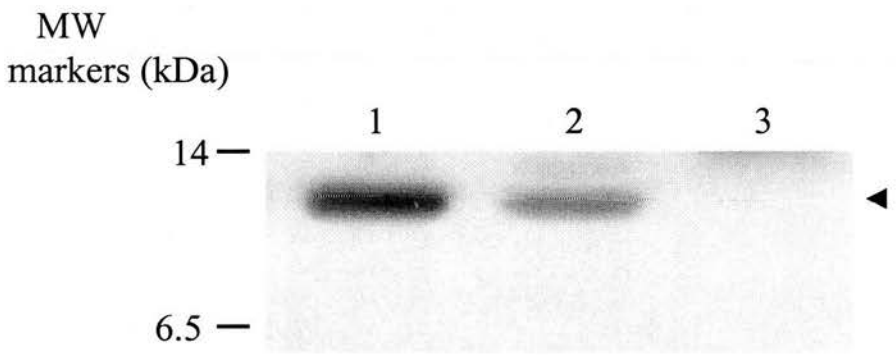

Figure 4-14. Western blot of FKBP12 expressed in Sf21

Lane 1: human FKBP12 (positive control)
Lane 2: recombinant FKBP12 expressed in Sf21
Lane 3: Sf21 alone (negative control)
1.5 ml of No. 6 P4 virus stock were added to Sf21. After 48 h of infection, cytosolic fractions of Sf21 cells were purified and resolved using 15% (w/v) SDS-PAGE followed by Western blotting as described previously. The arrow head shows FKBP12 (12 kDa).

4.8 IP_3 Binding and Planar Lipid Bilayer Reconstitution of IP_3RI Expressed in Insect Cells

An IP_3 binding assay was used to measure the binding ability of expressed human IP_3RI. Although optimised conditions were used for the expression of full-length IP_3RI in Sf9 or Sf21 cells, IP_3 binding activity was still variable from each membrane preparation, with a maximum value of about 0.6 pmol/mg of microsomes, which is much lower than that previously reported (Cardy *et al.*, 1997; Yoneshima *et al.*, 1997). The result is summarised in Figure 4-3. The membrane fraction of Sf9 or Sf21 infected with virus containing truncated IP_3RI construct had a normal IP_3 binding activity of about 3 pmol/mg of microsomes, whereas the cytosolic fraction displayed a low IP_3 binding activity (Figure 4-3). ~25 units of intensity per IP_3 binding activity were found in membrane fraction of Sf21 (full-length or truncated IP_3RI). However, only ~13 units of intensity per IP_3 binding activity were found in cytosolic fraction (truncated IP_3RI). Attempts were also made to reconstitute the full-length IP_3RI in planar lipid bilayer, but no specific IP_3RI channels were found.

4.9 Topology of Truncated IP_3RI Expressed in Sf21 Cells

It has been shown that the IP_3RI without the C-terminus was mostly found as soluble cytosolic proteins when expressed in COS1 cells (Galvan *et al.*, 1999). Although the truncated IP_3RI did not have the C-terminus previously though to contain all the transmembrane regions, the membrane fraction of infected Sf21 cells showed similar IP_3 binding activity as full-length IP_3RI previously reported. This

suggested that truncated IP_3RI may contain other transmembrane regions before the C-terminus, or associate with other membrane-bound proteins as an extrinsic protein when expressed in Sf21 cells. To test the second possibility, the membrane fraction of Sf21 cells infected with recombinant virus containing truncated IP_3RI was dissolved in 100 mM Na_2CO_3, pH 11.4 to a protein concentration of 1.5 mg/ml at 4^0C for 30 min, and the mixture was then centrifuged at 100,000 x g for 30 min. Both precipitate and supernatant fractions were collected and resolved on 5% (w/v) SDS-PAGE followed by Western blotting. The result is shown in Figure 4-15. Most of truncated IP_3RI still remained in the membrane fraction.

4.10 Discussion

Although the human IP_3RI (truncated or full-length) could be overexpressed in HEK293 cells, it did not show measurable IP_3 binding activity. Full-length IP_3RI expressed in HEK293 cells also did not have channel activity when reconstituted in planar lipid bilayer. The reason might be the low expression level of IP_3RI in HEK293 following transient expression. Therefore, attempts were made to establish a stable cell line expressing full-length IP_3RI. However, this attempt was not successful. Only a stable cell line that was resistant to antibiotic G418 was obtained, but it did not express IP_3RI. A baculovirus expression vector system was therefore used to obtain high level expression. It has been shown that IP_3RI could be overexpressed in Sf9 cells using baculovirus expression vector system (Cardy *et al.*, 1997; Yoneshima *et al.*, 1997). However, the expressed full-length IP_3RI could only be detected from Western blot without boiling in SDS sample loading buffer, which

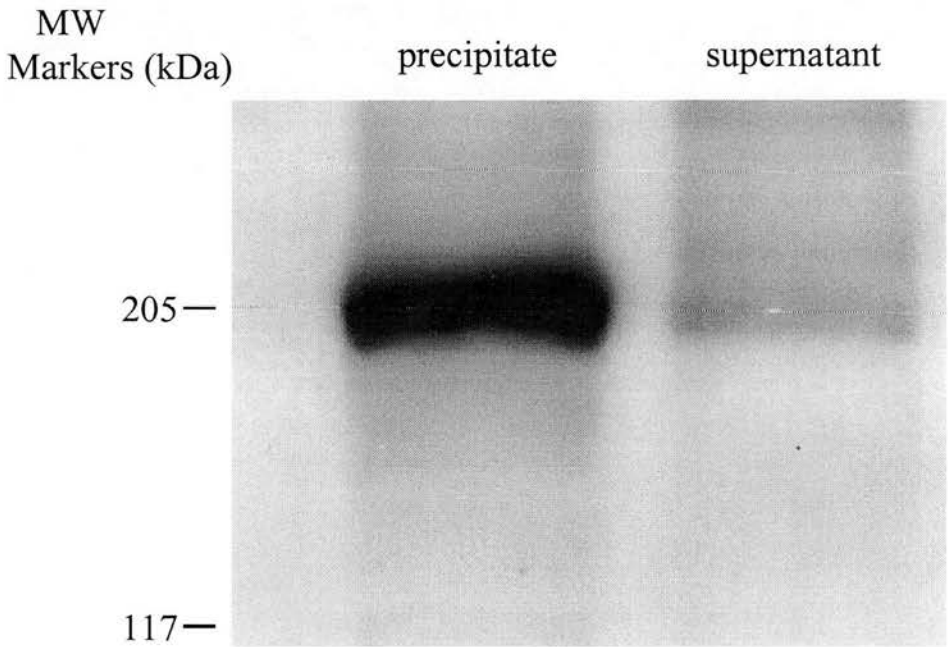

Figure 4-15. Localisation of truncated IP_3RI expressed in Sf21 cells.

Membrane fractions of Sf21 cells infected with 1 ml, No. 8 P4 virus stock containing truncated IP_3RI were dissolved in 100 mM Na_2CO_3, pH 11.4 to a protein concentration of 1.5 mg/ml, and incubated at 4^0C for 30 min. The mixture was then centrifuged at 100,000 x g for 30 min. Both precipitate and supernatant were collected and resolved on 5% (w/v) SDS-PAGE followed by Western blotting as described. The results showed that most of the truncated IP_3RI still remained in the membrane.

is different from published results. The expression of full-length IP_3RI in HEK293 cells did not show this property. The expressed full-length human IP_3RI optimised in Sf9 or Sf21 cells displayed an IP_3 binding activity of up to ~0.6 pmol/mg of microsomes, which is much lower than that previously reported (Cardy *et al.*, 1997; Yoneshima *et al.*, 1997), and it also did not have measurable channel activity. This suggests that further optimisation of the expression of full-length IP_3RI is required. However, the truncated IP_3RI expressed in Sf9 or Sf21 cells showed IP_3 binding activity of about 3 pmol/mg of microsomes, which is similar to published results (Cardy *et al.*, 1997; Yoneshima *et al.*, 1997). The unit of intensity (from phosphorimager) per IP_3 binding activity was similar (~25 unit/binding activity). The truncated IP_3RI does not have the C-terminus containing all the putative membrane-spanning domains, but most of them still remain in the membrane fraction and have similar IP_3 binding activity as full-length receptors. This suggests that there may be other membrane-spanning domains before C-terminal part of human IP_3RI not previously described in other IP_3Rs. However, it has been shown that truncated IP_3RI without the C-terminus expressed in COS1 cells was mostly found in cytoplasmic instead of membrane fraction (Galvan *et al.*, 1999). Another possibility is that the truncated IP_3RI is an extrinsic protein, which associates with intracellular membrane by way of other membrane bound proteins. It has been found that after adding 100 mM Na_2CO_3, pH 11.4 to a protein concentration of 1.5 mg/ml, most of the truncated IP_3RI still remained in the membrane. However, because of no proper positive control including in the experiment, the real location of truncated IP_3RI is uncertain.

FKBP12 is a relatively small (12 kDa) and soluble cytosolic protein. In this study, FKBP12 could be successfully expressed in HEK293 or Sf9/Sf21 cells. It has been identified that FKBP12 binds a leucine-proline dipeptide located at the N-terminus of IP_3RI (Cameron *et al.*, 1997). Moreover, it also binds ryanodine receptors and regulates their channel function (Brillantes *et al.*, 1994). In future studies, coexpression of FKBP12 and IP_3RI will be useful to study how FKBP12 modifies the function of recombinant human IP_3RI.

Chapter 5

Conclusions and Future Studies

In this work, the full-length human *IP$_3$RI* containing SII and novel SIII alternative splicing sites (Nucifora *et al.*, 1995) was assembled from three overlapping cDNAs cloned from a human brain cDNA library. The SII splice site is located between two PKA phosphorylation sites, and is the most divergent region between rodent and human species. There are seven amino acids differences in a total of only twenty-four amino acids. It has been shown that SII splice site alters the phosphorylation of the two consensus PKA phosphorylation sites (Danoff *et al.*, 1991). The novel SIII splice site, which contains nine amino acids, located near the IP_3 binding core may not directly effect IP_3 binding, but could modulate IP_3 binding through a charge to charge interaction (Mourey *et al.*, 1993).

The rabbit reticulocyte *in vitro* translation system is a very convenient and useful expression system for the study of protein functions. From the initial study of *in vitro* expression of assembled *IP$_3$RI*, a ~200 kDa truncated protein, together with some smaller proteins, was identified. It suggested that there might be a mutation causing premature termination. However, three constructs containing different regions of the *IP$_3$RI* (position 1 to 2161, 1 to 2539 and 1 to 5430) could be expressed *in vitro*, all with full-length products. Therefore, the mutation was located after position 5430. After automated sequencing of the assembled *IP$_3$RI* cDNA, a nucleotide deletion was identified at position 6429. In addition, eight nucleotides were found to be different from the published sequence. This caused five amino acids to be changed (section 3.4). After the mutation was corrected by subcloning, a full-length human IP_3RI could be obtained from *in vitro* expression, although some

truncated proteins still remained. Following this, a mammalian cell expression system was chosen for the functional expression of IP_3RI.

Mammalian cell expression systems have become the most popular method for the study of heterologously expressed proteins. The truncated and full-length human IP_3RI could be transiently overexpressed in HEK293 cells. However, their membranes did not have measurable IP_3 binding activity. The reason might be the low expression level following transient expression. Attempts were made to establish a stable cell line expressing IP_3RI, but these were not successful. The baculovirus expression vector system was then used for high-level expression of human IP_3RI.

The baculovirus expression vector system is one of the most powerful eukaryotic expression systems currently available (O'Reilly *et al.*, 1992). Using this, both truncated and full-length IP_3RI were successfully overexpressed in insect Sf9/Sf21 cells. From IP_3 binding assays, full-length IP_3RI had a low IP_3 binding activity of up to ~0.6 pmol/mg of microsomes, compared to published results (Cardy *et al.*, 1997; Yoneshima *et al.*, 1997). It suggests that a further optimisation is required. However, the membrane fraction of insect cells infected with virus containing truncated IP_3RI showed a IP_3 binding activity of ~3 pmol/mg of microsomes, which is similar to that previously reported, whereas the cytosolic fraction of infected cells showed an IP_3 binding activity of only ~0.3 pmol/mg of cytoplasmic protein. The unit of intensity per binding activity was similar (~25 unit/binding activity) in membrane fraction (full-length or truncated IP_3RI), but it was only half (~13 unit/binding activity) in cytosolic fraction (truncated IP_3RI). It has been found that IP_3Rs without their C-terminus (containing six transmembrane

segments, like the truncated IP_3RI), remain as a soluble monomer, and have the same IP_3 binding activity as full-length IP_3Rs (Mignery and Sudhof, 1990). In this study, most of the truncated IP_3RI still remained in microsomes, and showed similar IP_3 binding activity to full-length IP_3Rs. This suggests that the truncated IP_3RI may contain some extra transmembrane regions before the C-terminus, or associate with other membrane-bound proteins. A preliminary experiment showed that the truncated IP_3RI was not an extrinsic protein. However, further studies are required to firmly identify this novel transmembrane region.

FKBP12 is a ubiquitous soluble protein found in almost every kind of cell. It has a molecular weight of 12 kDa, and is the target protein of immunosuppressant drug FK506 and rapamycin (Marks, 1996). It has been shown that IP_3Rs, FKBP12 and calcineurin form a ternary complex (Cameron *et al.*, 1997). In addition, the interaction between FKBP12 and RyR1 can be disrupted by FK506 or rapamycin, and RyR1 then displays unstable subconductance states (Brillantes *et al.*, 1994). In this study, human FKBP12 was successfully expressed in HEK293 and Sf9 cells. In future work, coexpression of FKBP12 and IP_3RI will be useful to investigate how FKBP12 interacts with IP_3RI and modifies its channel functions.

As mentioned earlier, Ca^{2+} is a signal for life and also a signal for death (Berridge *et al.*, 1998). Cells must tightly control $[Ca^{2+}]$ in response to a variety of stimuli from the environment. If cells cannot maintain their $[Ca^{2+}]$ homeostasis, they will die either from necrosis or apoptosis (Kroemer *et al.*, 1998). Apoptosis (programmed cell death) is regulated by a series of cellular events involving the activation of caspases, which in turn cleave specific intracellular proteins resulting in

cell death. It has been shown that IP_3Rs played an important role in apoptosis (Jayaraman and Marks, 1997; Sugawara *et al.*, 1997). Recently, Hirota *et al.* (1999) reported that IP_3RI was a caspase-3 substrate, and caspase-3 cleaved IP_3RI at a consensus DEVD motif during apoptosis. Future studies of how the IP_3R channel is regulated during apoptosis may lead to important new insights into cell function.

Bibliography

Ahmad, I., Redmond, L. J., and Barnstable, C. J. (1990). Developmental and tissue-specific expression of the rod photoreceptor cGMP-gated ion channel gene. Biochem Biophys Res Commun *173*, 463-70.

Andersson, S., Davis, D. L., Dahlback, H., Jornvall, H., and Russell, D. W. (1989). Cloning, structure, and expression of the mitochondrial cytochrome P-450 sterol 26-hydroxylase, a bile acid biosynthetic enzyme. J Biol Chem *264*, 8222-9.

Ashley, R. H., and Williams, A. J. (1990). Divalent cation activation and inhibition of single calcium release channels from sheep cardiac sarcoplasmic reticulum. J Gen Physiol *95*, 981-1005.

Ashley, R. H. (1995). Intracellular calcium channels. Essays Biochem 30, 97-117.

Ayres, M. D., Howard, S. C., Kuzio, J., Lopez-Ferber, M., and Possee, R. D. (1994). The complete DNA sequence of *Autographa californica* nuclear polyhedrosis virus. Virology *202*, 586-605.

Babcock, D. F., and Hille, B. (1998). Mitochondrial oversight of cellular Ca^{2+} signaling. Curr Opin Neurobiol *8*, 398-404.

Bading, H., Ginty, D. D., and Greenberg, M. E. (1993). Regulation of gene expression in hippocampal neurons by distinct calcium signaling pathways. Science *260*, 181-6.

Barritt, G. J. (1999). Receptor-activated Ca^{2+} inflow in animal cells: a variety of pathways tailored to meet different intracellular Ca^{2+} signalling requirements. Biochem J *337*, 153-69.

Bean, B. P. (1989). Multiple types of calcium channels in heart muscle and neurons. Modulation by drugs and neurotransmitters. Ann N Y Acad Sci *560*, 334-45.

Benham, C. D., and Bolton, T. B. (1986). Spontaneous transient outward currents in single visceral and vascular smooth muscle cells of the rabbit. J Physiol (Lond) *381*, 385-406.

Bennett, J. A., and Dingledine, R. (1995). Topology profile for a glutamate receptor: three transmembrane domains and a channel-lining reentrant membrane loop. Neuron *14*, 373-84.

Berridge, M. J. (1997). Elementary and global aspects of calcium signalling. J Physiol (Lond) *499*, 291-306.

Berridge, M. J. (1993). Inositol trisphosphate and calcium signalling. Nature *361*, 315-25.

Berridge, M. J. (1998). Neuronal calcium signaling. Neuron *21*, 13-26.

Berridge, M. J., Bootman, M. D., and Lipp, P. (1998). Calcium-a life and death signal. Nature *395*, 645-8.

Bertrand, D., Galzi, J. L., Devillers-Thiery, A., Bertrand, S., and Changeux, J. P. (1993). Mutations at two distinct sites within the channel domain M2 alter calcium permeability of neuronal alpha 7 nicotinic receptor. Proc Natl Acad Sci U S A *90*, 6971-5.

Bezprozvanny, I., and Ehrlich, B. E. (1993). ATP modulates the function of inositol 1,4,5-trisphosphate-gated channels at two sites. Neuron *10*, 1175-84.

Birnboim, H. C., and Doly, J. (1979). A rapid alkaline extraction procedure for screening recombinant plasmid DNA. Nucleic Acids Res *7*, 1513-23.

Bliss, T. V., and Collingridge, G. L. (1993). A synaptic model of memory: long-term potentiation in the hippocampus. Nature *361*, 31-9.

Blondel, O., Takeda, J., Janssen, H., Seino, S., and Bell, G. I. (1993). Sequence and functional characterization of a third inositol trisphosphate receptor subtype, IP_3R-3, expressed in pancreatic islets, kidney, gastrointestinal tract, and other tissues. J Biol Chem *268*, 11356-63.

Bootman, M. D., and Berridge, M. J. (1995). The elemental principles of calcium signaling. Cell *83*, 675-8.

Boshart, M., Weber, F., Jahn, G., Dorsch-Hasler, K., Fleckenstein, B., and Schaffner, W. (1985). A very strong enhancer is located upstream of an immediate early gene of human cytomegalovirus. Cell *41*, 521-30.

Bowie, D., and Mayer, M. L. (1995). Inward rectification of both AMPA and kainate subtype glutamate receptors generated by polyamine-mediated ion channel block. Neuron *15*, 453-62.

Breathnach, R., and Chambon, P. (1981). Organization and expression of eukaryotic split genes coding for proteins. Annu Rev Biochem *50*, 349-83.

Brillantes, A. B., Ondrias, K., Scott, A., Kobrinsky, E., Ondriasova, E., Moschella, M. C., Jayaraman, T., Landers, M., Ehrlich, B. E., and Marks, A. R. (1994). Stabilization of calcium release channel (ryanodine receptor) function by FK506-binding protein. Cell *77*, 513-23.

Bucher, P. (1990). Weight matrix descriptions of four eukaryotic RNA polymerase II promoter elements derived from 502 unrelated promoter sequences. J Mol Biol *212*, 563-78.

Buell, G., Collo, G., and Rassendren, F. (1996). P2X receptors: an emerging channel family. Eur J Neurosci *8*, 2221-8.

Burgess, G. M., Bird, G. S., Obie, J. F., and Putney, J. W., Jr. (1991). The mechanism for synergism between phospholipase C- and adenylylcyclase-linked hormones in liver. Cyclic AMP-dependent kinase augments inositol trisphosphate-mediated Ca^{2+} mobilization without increasing the cellular levels of inositol polyphosphates. J Biol Chem *266*, 4772-81.

Burnashev, N., Monyer, H., Seeburg, P. H., and Sakmann, B. (1992). Divalent ion permeability of AMPA receptor channels is dominated by the edited form of a single subunit. Neuron *8*, 189-98.

Calviello, G., and Chiesi, M. (1989). Rapid kinetic analysis of the calcium-release channels of skeletal muscle sarcoplasmic reticulum: the effect of inhibitors. Biochemistry *28*, 1301-6.

Camacho, P., and Lechleiter, J. D. (1995). Calreticulin inhibits repetitive intracellular Ca^{2+} waves. Cell *82*, 765-71.

Cameron, A. M., Nucifora, F. C., Jr., Fung, E. T., Livingston, D. J., Aldape, R. A., Ross, C. A., and Snyder, S. H. (1997). FKBP12 binds the inositol 1,4,5-trisphosphate receptor at leucine-proline (1400-1401) and anchors calcineurin to this FK506-like domain. J Biol Chem *272*, 27582-8.

Cameron, A. M., Steiner, J. P., Roskams, A. J., Ali, S. M., Ronnett, G. V., and Snyder, S. H. (1995). Calcineurin associated with the inositol 1,4,5-trisphosphate receptor- FKBP12 complex modulates Ca^{2+} flux. Cell *83*, 463-72.

Carafoli, E., and Molinari, M. (1998). Calpain: a protease in search of a function? [published erratum appears in Biochem Biophys Res Commun 1998 Aug 19;249(2):572]. Biochem Biophys Res Commun *247*, 193-203.

Cardoso, C. M., and De Meis, L. (1993). Modulation by fatty acids of Ca^{2+} fluxes in sarcoplasmic-reticulum vesicles. Biochem J *296*, 49-52.

Cardy, T. J., Traynor, D., and Taylor, C. W. (1997). Differential regulation of types-1 and -3 inositol trisphosphate receptors by cytosolic Ca^{2+}. Biochem J *328*, 785-93.

Castillo, P. E., Malenka, R. C., and Nicoll, R. A. (1997). Kainate receptors mediate a slow postsynaptic current in hippocampal CA3 neurons. Nature *388*, 182-6.

Catterall, W. A. (1998). Structure and function of neuronal Ca^{2+} channels and their role in neurotransmitter release. Cell Calcium *24*, 307-23.

Chadwick, C. C., Saito, A., and Fleischer, S. (1990). Isolation and characterization of the inositol trisphosphate receptor from smooth muscle. Proc Natl Acad Sci U S A *87*, 2132-6.

Chamberlain, B. K., Volpe, P., and Fleischer, S. (1984). Inhibition of calcium-induced calcium release from purified cardiac sarcoplasmic reticulum vesicles. J Biol Chem *259*, 7547-53.

Chen, S. R., Zhang, L., and MacLennan, D. H. (1992). Characterization of a Ca^{2+} binding and regulatory site in the Ca^{2+} release channel (ryanodine receptor) of rabbit skeletal muscle sarcoplasmic reticulum. J Biol Chem *267*, 23318-26.

Chu, A., Fill, M., Stefani, E., and Entman, M. L. (1993). Cytoplasmic Ca^{2+} does not inhibit the cardiac muscle sarcoplasmic reticulum ryanodine receptor Ca^{2+} channel, although Ca^{2+}-induced Ca^{2+} inactivation of Ca^{2+} release is observed in native vesicles. J Membr Biol *135*, 49-59.

Clapham, D. E. (1995). Calcium signaling. Cell *80*, 259-68.

Cline, J., Braman, J. C., and Hogrefe, H. H. (1996). PCR fidelity of *Pfu* DNA polymerase and other thermostable DNA polymerases. Nucleic Acids Res *24*, 3546-51.

Colquhoun, L. M., and Patrick, J. W. (1997). Alpha3, beta2, and beta4 form heterotrimeric neuronal nicotinic acetylcholine receptors in *Xenopus* oocytes. J Neurochem *69*, 2355-62.

Coppolino, M. G., Woodside, M. J., Demaurex, N., Grinstein, S., St-Arnaud, R., and Dedhar, S. (1997). Calreticulin is essential for integrin-mediated calcium signalling and cell adhesion. Nature *386*, 843-7.

Costa, A. C., Patrick, J. W., and Dani, J. A. (1994). Improved technique for studying ion channels expressed in *Xenopus* oocytes, including fast superfusion. Biophys J *67*, 395-401.

Crawford, A. M., and Miller, L. K. (1988). Characterization of an early gene accelerating expression of late genes of the baculovirus *Autographa californica* nuclear polyhedrosis virus. J Virol *62*, 2773-81.

Curtis, B. M., and Catterall, W. A. (1985). Phosphorylation of the calcium antagonist receptor of the voltage-sensitive calcium channel by cAMP-dependent protein kinase. Proc Natl Acad Sci U S A *82*, 2528-32.

Curtis, B. M., and Catterall, W. A. (1984). Purification of the calcium antagonist receptor of the voltage-sensitive calcium channel from skeletal muscle transverse tubules. Biochemistry *23*, 2113-8.

Curtis, B. M., and Catterall, W. A. (1983). Solubilization of the calcium antagonist receptor from rat brain. J Biol Chem *258*, 7280-3.

Danoff, S. K., Ferris, C. D., Donath, C., Fischer, G. A., Munemitsu, S., Ullrich, A., Snyder, S. H., and Ross, C. A. (1991). Inositol 1,4,5-trisphosphate receptors: distinct neuronal and nonneuronal forms derived by alternative splicing differ in phosphorylation. Proc Natl Acad Sci U S A *88*, 2951-5.

Dasgupta, S., Dasgupta, D., Chatterjee, A., Biswas, S., and Biswas, B. B. (1997). Conformational changes in plant Ins(1,4,5)P_3 receptor on interaction with different myo-inositol trisphosphates and its effect on Ca^{2+} release from microsomal fraction and liposomes. Biochem J *321*, 355-60.

De Boer, J. G., and Ripley, L. S. (1988). An *in vitro* assay for frameshift mutations: hotspots for deletions of 1 bp by Klenow-fragment polymerase share a consensus DNA sequence. Genetics *118*, 181-91.

De Jongh, K. S., Warner, C., and Catterall, W. A. (1990). Subunits of purified calcium channels. Alpha 2 and delta are encoded by the same gene. J Biol Chem *265*, 14738-41.

De Koninck, P., and Schulman, H. (1998). Sensitivity of CaM kinase II to the frequency of Ca^{2+} oscillations. Science *279*, 227-30.

De Smedt, H., Missiaen, L., Parys, J. B., Bootman, M. D., Mertens, L., Van Den Bosch, L., and Casteels, R. (1994). Determination of relative amounts of inositol trisphosphate receptor mRNA isoforms by ratio polymerase chain reaction. J Biol Chem *269*, 21691-8.

Dettbarn, C., and Palade, P. (1993). Arachidonic acid-induced Ca^{2+} release from isolated sarcoplasmic reticulum. Biochem Pharmacol *45*, 1301-9.

Dolmetsch, R. E., Lewis, R. S., Goodnow, C. C., and Healy, J. I. (1997). Differential activation of transcription factors induced by Ca^{2+} response amplitude and duration [published erratum appears in Nature 1997 Jul 17;388(6639):308]. Nature *386*, 855-8.

Dolmetsch, R. E., Xu, K., and Lewis, R. S. (1998). Calcium oscillations increase the efficiency and specificity of gene expression. Nature *392*, 933-6.

Donoso, P., and Hidalgo, C. (1993). pH-sensitive calcium release in triads from frog skeletal muscle. Rapid filtration studies. J Biol Chem *268*, 25432-8.

Doyle, A., Griffiths, J. B., and Newell, D. G. (1994). Cell and Tissue Culture: Laboratory Procedures (Chichester, USA: John Wiley & Sons).

Drake, J. W. (1991). Spontaneous mutation. Annu Rev Genet *25*, 125-46.

Duke, G. M., Hoffman, M. A., and Palmenberg, A. C. (1992). Sequence and structural elements that contribute to efficient encephalomyocarditis virus RNA translation. J Virol *66*, 1602-9.

Dunlap, K., Luebke, J. I., and Turner, T. J. (1995). Exocytotic Ca^{2+} channels in mammalian central neurons. Trends Neurosci *18*, 89-98.

Echols, H., Lu, C., and Burgers, P. M. (1983). Mutator strains of *Escherichia coli*, mutD and dnaQ, with defective exonucleolytic editing by DNA polymerase III holoenzyme. Proc Natl Acad Sci U S A *80*, 2189-92.

Edwards, F. A., Gibb, A. J., and Colquhoun, D. (1992). ATP receptor-mediated synaptic currents in the central nervous system. Nature *359*, 144-7.

Ehrlich, B. E., and Watras, J. (1988). Inositol 1,4,5-trisphosphate activates a channel from smooth muscle sarcoplasmic reticulum. Nature *336*, 583-6.

el-Hayek, R., Valdivia, C., Valdivia, H. H., Hogan, K., and Coronado, R. (1993). Activation of the Ca^{2+} release channel of skeletal muscle sarcoplasmic reticulum by palmitoyl carnitine. Biophys J *65*, 779-89.

Elroy-Stein, O., Fuerst, T. R., and Moss, B. (1989). Cap-independent translation of mRNA conferred by encephalomyocarditis virus 5' sequence improves the performance of the vaccinia virus/bacteriophage T7 hybrid expression system. Proc Natl Acad Sci U S A *86*, 6126-30.

Fasolato, C., and Nilius, B. (1998). Store depletion triggers the calcium release-activated calcium current (I_{CRAC}) in macrovascular endothelial cells: a comparison with Jurkat and embryonic kidney cell lines. Pflugers Arch *436*, 69-74.

Ferrer-Montiel, A. V., and Montal, M. (1993). A negative charge in the M2 transmembrane segment of the neuronal alpha 7 acetylcholine receptor increases permeability to divalent cations. FEBS Lett *324*, 185-90.

Ferris, C. D., Cameron, A. M., Bredt, D. S., Huganir, R. L., and Snyder, S. H. (1992). Autophosphorylation of inositol 1,4,5-trisphosphate receptors. J Biol Chem *267*, 7036-41.

Ferris, C. D., Cameron, A. M., Bredt, D. S., Huganir, R. L., and Snyder, S. H. (1991). Inositol 1,4,5-trisphosphate receptor is phosphorylated by cyclic AMP-dependent protein kinase at serines 1755 and 1589. Biochem Biophys Res Commun *175*, 192-8.

Ferris, C. D., Huganir, R. L., Bredt, D. S., Cameron, A. M., and Snyder, S. H. (1991). Inositol trisphosphate receptor: phosphorylation by protein kinase C and calcium calmodulin-dependent protein kinases in reconstituted lipid vesicles. Proc Natl Acad Sci U S A *88*, 2232-5.

Ferris, C. D., Huganir, R. L., Supattapone, S., and Snyder, S. H. (1989). Purified inositol 1,4,5-trisphosphate receptor mediates calcium flux in reconstituted lipid vesicles. Nature *342*, 87-9.

Ferris, C. D., and Snyder, S. H. (1992). Inositol phosphate receptors and calcium disposition in the brain. J Neurosci *12*, 1567-74.

Finn, J. T., Grunwald, M. E., and Yau, K. W. (1996). Cyclic nucleotide-gated ion channels: an extended family with diverse functions. Annu Rev Physiol *58*, 395-426.

Furuichi, T., Yoshikawa, S., Miyawaki, A., Wada, K., Maeda, N., and Mikoshiba, K. (1989). Primary structure and functional expression of the inositol 1,4,5-trisphosphate-binding protein P400. Nature *342*, 32-8.

Furutama, D., Shimoda, K., Yoshikawa, S., Miyawaki, A., Furuichi, T., and Mikoshiba, K. (1996). Functional expression of the type 1 inositol 1,4,5-trisphosphate receptor promoter-lacZ fusion genes in transgenic mice. J Neurochem *66*, 1793-801.

Galione, A., White, A., Willmott, N., Turner, M., Potter, B. V., and Watson, S. P. (1993). cGMP mobilizes intracellular Ca^{2+} in sea urchin eggs by stimulating cyclic ADP-ribose synthesis. Nature *365*, 456-9.

Galvan, D. L., Borrego-Diaz, E., Perez, P. J., and Mignery, G. A. (1999). Subunit oligomerization, and topology of the inositol 1,4, 5- trisphosphate receptor. J Biol Chem *274*, 29483-92.

Gerasimenko, O. V., Gerasimenko, J. V., Tepikin, A. V., and Petersen, O. H. (1995). ATP-dependent accumulation and inositol trisphosphate- or cyclic ADP-ribose-mediated release of Ca^{2+} from the nuclear envelope. Cell *80*, 439-44.

Gerzanich, V., Wang, F., Kuryatov, A., and Lindstrom, J. (1998). alpha 5 Subunit alters desensitization, pharmacology, Ca^{2+} permeability and Ca^{2+} modulation of

human neuronal alpha 3 nicotinic receptors. J Pharmacol Exp Ther *286*, 311-20.

Gilchrist, J. S., Belcastro, A. N., and Katz, S. (1992). Intraluminal Ca^{2+} dependence of Ca^{2+} and ryanodine-mediated regulation of skeletal muscle sarcoplasmic reticulum Ca^{2+} release. J Biol Chem *267*, 20850-6.

Gluzman, Y. (1981). SV40-transformed simian cells support the replication of early SV40 mutants. Cell *23*, 175-82.

Goodwin, E. C., and Rottman, F. M. (1992). The 3'-flanking sequence of the bovine growth hormone gene contains novel elements required for efficient and accurate polyadenylation. J Biol Chem *267*, 16330-4.

Graham, F. L., Smiley, J., Russell, W. C., and Nairn, R. (1977). Characteristics of a human cell line transformed by DNA from human adenovirus type 5. J Gen Virol *36*, 59-74.

Gu, J. G., and MacDermott, A. B. (1997). Activation of ATP P2X receptors elicits glutamate release from sensory neuron synapses. Nature *389*, 749-53.

Guihard, G., Combettes, L., and Capiod, T. (1996). 3', 5'-cyclic guanosine monophosphate (cGMP) potentiates the inositol 1,4,5-trisphosphate-evoked Ca^{2+} release in guinea-pig hepatocytes. Biochem J *318*, 849-55.

Guo, W., Jorgensen, A. O., and Campbell, K. P. (1996). Triadin, a linker for calsequestrin and the ryanodine receptor. Soc Gen Physiol Ser *51*, 19-28.

Gurnett, C. A., De Waard, M., and Campbell, K. P. (1996). Dual function of the voltage-dependent Ca^{2+} channel alpha 2 delta subunit in current stimulation and subunit interaction. Neuron *16*, 431-40.

Gyermek, L. (1996). Pharmacology of serotonin as related to anesthesia. J Clin Anesth *8*, 402-25.

Haghighi, A. P., and Cooper, E. (1998). Neuronal nicotinic acetylcholine receptors are blocked by intracellular spermine in a voltage-dependent manner. J Neurosci *18*, 4050-62.

Hagiwara, S., Ozawa, S., and Sand, O. (1975). Voltage clamp analysis of two inward current mechanisms in the egg cell membrane of a starfish. J Gen Physiol *65*, 617-44.

Hakamata, Y., Nakai, J., Takeshima, H., and Imoto, K. (1992). Primary structure and distribution of a novel ryanodine receptor/calcium release channel from rabbit brain. FEBS Lett *312*, 229-35.

Hale, A. J., Smith, C. A., Sutherland, L. C., Stoneman, V. E., Longthorne, V., Culhane, A. C., and Williams, G. T. (1996). Apoptosis: molecular regulation of cell death. Eur J Biochem *237*, 884.

Hardie, R. C., and Minke, B. (1993). Novel Ca^{2+} channels underlying transduction in *Drosophila* photoreceptors: implications for phosphoinositide-mediated Ca^{2+} mobilization. Trends Neurosci *16*, 371-6.

Harnick, D. J., Jayaraman, T., Ma, Y., Mulieri, P., Go, L. O., and Marks, A. R. (1995). The human type 1 inositol 1,4,5-trisphosphate receptor from T lymphocytes. Structure, localization, and tyrosine phosphorylation. J Biol Chem *270*, 2833-40.

Hasselbach, W., and Migala, A. (1987). Activation and inhibition of the calcium gate of sarcoplasmic reticulum by high-affinity ryanodine binding. FEBS Lett *221*, 119-23.

Hirota, J., Furuichi, T., and Mikoshiba, K. (1999). Inositol 1,4,5-Trisphosphate Receptor Type 1 Is a Substrate for Caspase-3 and Is Cleaved during Apoptosis in a Caspase-3-dependent Manner. J Biol Chem *274*, 34433-34437.

Hirota, J., Michikawa, T., Miyawaki, A., Furuichi, T., Okura, I., and Mikoshiba, K. (1995). Kinetics of calcium release by immunoaffinity-purified inositol 1,4,5-trisphosphate receptor in reconstituted lipid vesicles. J Biol Chem *270*, 19046-51.

Hollmann, M., and Heinemann, S. (1994). Cloned glutamate receptors. Annu Rev Neurosci *17*, 31-108.

Hosey, M. M., Barhanin, J., Schmid, A., Vandaele, S., Ptasienski, J., C, O. C., Cooper, C., and Lazdunski, M. (1987). Photoaffinity labelling and phosphorylation of a 165 kDa peptide associated with dihydropyridine and phenylalkylamine-sensitive calcium channels. Biochem Biophys Res Commun *147*, 1137-45.

Humerickhouse, R. A., Besch, H. R., Jr., Gerzon, K., Ruest, L., Sutko, J. L., and Emmick, J. T. (1993). Differential activating and deactivating effects of natural ryanodine congeners on the calcium release channel of sarcoplasmic reticulum: evidence for separation of effects at functionally distinct sites. Mol Pharmacol *44*, 412-21.

Hussy, N., Lukas, W., and Jones, K. A. (1994). Functional properties of a cloned 5-hydroxytryptamine ionotropic receptor subunit: comparison with native mouse receptors. J Physiol (Lond) *481*, 311-23.

Iida, N., and Bourguignon, L. Y. (1994). A new splice variant of the inositol-1,4,5-triphosphate (IP_3) receptor. Cell Signal *6*, 449-55.

Iino, M. (1990). Biphasic Ca^{2+} dependence of inositol 1,4,5-trisphosphate-induced Ca^{2+} release in smooth muscle cells of the guinea pig *taenia caeci*. J Gen Physiol *95*, 1103-22.

Iino, M. (1991). Effects of adenine nucleotides on inositol 1,4,5-trisphosphate-induced calcium release in vascular smooth muscle cells. J Gen Physiol *98*, 681-98.

Irvine, R. F. (1990). 'Quantal' Ca^{2+} release and the control of Ca^{2+} entry by inositol phosphates--a possible mechanism. FEBS Lett *263*, 5-9.

Irvine, R. F., and Moor, R. M. (1986). Micro-injection of inositol 1,3,4,5-tetrakisphosphate activates sea urchin eggs by a mechanism dependent on external Ca^{2+}. Biochem J *240*, 917-20.

Jay, S. D., Ellis, S. B., McCue, A. F., Williams, M. E., Vedvick, T. S., Harpold, M. M., and Campbell, K. P. (1990). Primary structure of the gamma subunit of the DHP-sensitive calcium channel from skeletal muscle. Science *248*, 490-2.

Jay, S. D., Sharp, A. H., Kahl, S. D., Vedvick, T. S., Harpold, M. M., and Campbell, K. P. (1991). Structural characterization of the dihydropyridine-sensitive calcium channel alpha 2-subunit and the associated delta peptides. J Biol Chem *266*, 3287-93.

Jayaraman, T., and Marks, A. R. (1997). T cells deficient in inositol 1,4,5-trisphosphate receptor are resistant to apoptosis. Mol Cell Biol *17*, 3005-12.

Jayaraman, T., Ondrias, K., Ondriasova, E., and Marks, A. R. (1996). Regulation of the inositol 1,4,5-trisphosphate receptor by tyrosine phosphorylation. Science *272*, 1492-4.

Jonas, P., and Burnashev, N. (1995). Molecular mechanisms controlling calcium entry through AMPA-type glutamate receptor channels. Neuron *15*, 987-90.

Joseph, S. K., Lin, C., Pierson, S., Thomas, A. P., and Maranto, A. R. (1995). Heteroligomers of type-I and type-III inositol trisphosphate receptors in WB rat liver epithelial cells [published erratum appears in J Biol Chem 1996 Mar 29;271(13):7874]. J Biol Chem *270*, 23310-6.

Kaminski, A., Howell, M. T., and Jackson, R. J. (1990). Initiation of encephalomyocarditis virus RNA translation: the authentic initiation site is not selected by a scanning mechanism. EMBO J *9*, 3753-9.

Kawasaki, T., and Kasai, M. (1994). Regulation of calcium channel in sarcoplasmic reticulum by calsequestrin. Biochem Biophys Res Commun *199*, 1120-7.

Keeton, T. P., Burk, S. E., and Shull, G. E. (1993). Alternative splicing of exons encoding the calmodulin-binding domains and C termini of plasma membrane Ca^{2+}-ATPase isoforms 1, 2, 3, and 4. J Biol Chem *268*, 2740-8.

Kerr, L. M., and Yoshikami, D. (1984). A venom peptide with a novel presynaptic blocking action. Nature *308*, 282-4.

Khan, A. A., Soloski, M. J., Sharp, A. H., Schilling, G., Sabatini, D. M., Li, S. H., Ross, C. A., and Snyder, S. H. (1996). Lymphocyte apoptosis: mediation by increased type 3 inositol 1,4,5- trisphosphate receptor. Science *273*, 503-7.

Khan, A. A., Steiner, J. P., and Snyder, S. H. (1992). Plasma membrane inositol 1,4,5-trisphosphate receptor of lymphocytes: selective enrichment in sialic acid and unique binding specificity. Proc Natl Acad Sci U S A *89*, 2849-53.

Kim, D. H., Ohnishi, S. T., and Ikemoto, N. (1983). Kinetic studies of calcium release from sarcoplasmic reticulum *in vitro*. J Biol Chem *258*, 9662-8.

Kirkwood, K. L., Homick, K., Dragon, M. B., and Bradford, P. G. (1997). Cloning and characterisation of the type I inositol 1,4,5-trisphosphate receptor gene promoter. Regulation by 17beta-estradiol in osteoblasts. J Biol Chem *272*, 22425-31.

Kiselyov, K., Mignery, G. A., Zhu, M. X., and Muallem, S. (1999). The N-terminal domain of the IP_3 receptor gates store-operated hTrp3 channels. Mol Cell *4*, 423-9.

Kiselyov, K., Xu, X., Mozhayeva, G., Kuo, T., Pessah, I., Mignery, G., Zhu, X., Birnbaumer, L., and Muallem, S. (1998). Functional interaction between $InsP_3$ receptors and store-operated Htrp3 channels. Nature *396*, 478-82.

Kiselyov, K. I., Mamin, A. G., Semyonova, S. B., and Mozhayeva, G. N. (1997). Low-conductance high selective inositol (1,4,5)-trisphosphate activated Ca^{2+} channels in plasma membrane of A431 carcinoma cells. FEBS Lett *407*, 309-12.

Kitts, P. A., and Possee, R. D. (1993). A method for producing recombinant baculovirus expression vectors at high frequency. Biotechniques *14*, 810-7.

Klein, M. G., Cheng, H., Santana, L. F., Jiang, Y. H., Lederer, W. J., and Schneider, M. F. (1996). Two mechanisms of quantized calcium release in skeletal muscle. Nature *379*, 455-8.

Kohler, M., Burnashev, N., Sakmann, B., and Seeburg, P. H. (1993). Determinants of Ca^{2+} permeability in both TM1 and TM2 of high affinity kainate receptor channels: diversity by RNA editing. Neuron *10*, 491-500.

Komalavilas, P., and Lincoln, T. M. (1994). Phosphorylation of the inositol 1,4,5-trisphosphate receptor by cyclic GMP-dependent protein kinase. J Biol Chem *269*, 8701-7.

Kozak, M. (1987a). An analysis of 5'-noncoding sequences from 699 vertebrate messenger RNAs. Nucleic Acids Res *15*, 8125-48.

Kozak, M. (1987b). At least six nucleotides preceding the AUG initiator codon enhance translation in mammalian cells. J Mol Biol *196*, 947-50.

Krause, E., Pfeiffer, F., Schmid, A., and Schulz, I. (1996). Depletion of intracellular calcium stores activates a calcium conducting nonselective cation current in mouse pancreatic acinar cells. J Biol Chem *271*, 32523-8.

Kroemer, G., Dallaporta, B., and Resche-Rigon, M. (1998). The mitochondrial death/life regulator in apoptosis and necrosis. Annu Rev Physiol *60*, 619-42.

Kume, S., Muto, A., Aruga, J., Nakagawa, T., Michikawa, T., Furuichi, T., Nakade, S., Okano, H., and Mikoshiba, K. (1993). The *Xenopus* IP_3 receptor: structure, function, and localisation in oocytes and eggs. Cell *73*, 555-70.

Kunkel, T. A. (1990). Misalignment-mediated DNA synthesis errors. Biochemistry *29*, 8003-11.

Kyrozis, A., Goldstein, P. A., Heath, M. J., and MacDermott, A. B. (1995). Calcium entry through a subpopulation of AMPA receptors desensitized neighbouring NMDA receptors in rat dorsal horn neurons. J Physiol (Lond) *485*, 373-81.

Laemmli, U. K. (1970). Cleavage of structural proteins during the assembly of the head of bacteriophage T4. Nature *227*, 680-5.

Lee, H. C., Aarhus, R., and Walseth, T. F. (1993). Calcium mobilization by dual receptors during fertilization of sea urchin eggs. Science *261*, 352-5.

Leist, M., and Nicotera, P. (1997). The shape of cell death. Biochem Biophys Res Commun *236*, 1-9.

Leung, A. T., Imagawa, T., and Campbell, K. P. (1987). Structural characterization of the 1,4-dihydropyridine receptor of the voltage-dependent Ca^{2+} channel from rabbit skeletal muscle. Evidence for two distinct high molecular weight subunits. J Biol Chem *262*, 7943-6.

Liu, X., Kim, C. N., Yang, J., Jemmerson, R., and Wang, X. (1996). Induction of apoptotic program in cell-free extracts: requirement for dATP and cytochrome c. Cell *86*, 147-57.

Llinas, R., Sugimori, M., and Silver, R. B. (1992). Presynaptic calcium concentration microdomains and transmitter release. J Physiol Paris *86*, 135-8.

Llinas, R., Yarom, Y., and Sugimori, M. (1981). Isolated mammalian brain *in vitro*: new technique for analysis of electrical activity of neuronal circuit function. Fed Proc *40*, 2240-5.

Llinas, R. R., Sugimori, M., and Cherksey, B. (1989). Voltage-dependent calcium conductances in mammalian neurons. The P channel. Ann N Y Acad Sci *560*, 103-11.

MacKenzie, A. E., Korneluk, R. G., Zorzato, F., Fujii, J., Phillips, M., Iles, D., Wieringa, B., Leblond, S., Bailly, J., Willard, H. F., Duff, C., Worton, R. G., and MacLennan, D. H. (1990). The human ryanodine receptor gene: its mapping to 19q13.1, placement in a chromosome 19 linkage group, and exclusion as the gene causing myotonic dystrophy. Am J Hum Genet *46*, 1082-9.

MacLennan, D. H., Rice, W. J., and Odermatt, A. (1997). Structure/function analysis of the Ca^{2+} binding and translocation domain of SERCA1 and the role in Brody disease of the *ATP2A1* gene encoding SERCA1. Ann N Y Acad Sci *834*, 175-85.

Maranto, A. R. (1994). Primary structure, ligand binding, and localization of the human type 3 inositol 1,4,5-trisphosphate receptor expressed in intestinal epithelium. J Biol Chem *269*, 1222-30.

Marks, A. R. (1996). Cellular functions of immunophilins. Physiol Rev *76*, 631-49.

Marrion, N. V., and Adams, P. R. (1992). Release of intracellular calcium and modulation of membrane currents by caffeine in bull-frog sympathetic neurones. J Physiol (Lond) *445*, 515-35.

Martin, S. K., Jett, M., and Schneider, I. (1994). Correlation of phosphoinositide hydrolysis with exflagellation in the malaria microgametocyte. J Parasitol *80*, 371-8.

Matter, N., Ritz, M. F., Freyermuth, S., Rogue, P., and Malviya, A. N. (1993). Stimulation of nuclear protein kinase C leads to phosphorylation of nuclear inositol 1,4,5-trisphosphate receptor and accelerated calcium release by inositol 1,4,5-trisphosphate from isolated rat liver nuclei. J Biol Chem *268*, 732-6.

Mayrleitner, M., Chadwick, C. C., Timerman, A. P., Fleischer, S., and Schindler, H. (1991). Purified IP_3 receptor from smooth muscle forms an IP_3 gated and heparin sensitive Ca^{2+} channel in planar bilayers. Cell Calcium *12*, 505-14.

McBain, C. J., and Mayer, M. L. (1994). N-methyl-D-aspartic acid receptor structure and function. Physiol Rev *74*, 723-60.

McCleskey, E. W., Fox, A. P., Feldman, D. H., Cruz, L. J., Olivera, B. M., Tsien, R. W., and Yoshikami, D. (1987). Omega-conotoxin: direct and persistent blockade of specific types of calcium channels in neurons but not muscle. Proc Natl Acad Sci U S A *84*, 4327-31.

McGehee, D. S., and Role, L. W. (1995). Physiological diversity of nicotinic acetylcholine receptors expressed by vertebrate neurons. Annu Rev Physiol *57*, 521-46.

McPhalen, C. A., Strynadka, N. C., and James, M. N. (1991). Calcium-binding sites in proteins: a structural perspective. Adv Protein Chem *42*, 77-144.

McPherson, P. S., and Campbell, K. P. (1993). The ryanodine receptor/Ca^{2+} release channel. J Biol Chem *268*, 13765-8.

Medina, I., Filippova, N., Charton, G., Rougeole, S., Ben-Ari, Y., Khrestchatisky, M., and Bregestovski, P. (1995). Calcium-dependent inactivation of heteromeric NMDA receptor-channels expressed in human embryonic kidney cells. J Physiol (Lond) *482*, 567-73.

Meissner, G. (1984). Adenine nucleotide stimulation of Ca^{2+}-induced Ca^{2+} release in sarcoplasmic reticulum. J Biol Chem *259*, 2365-74.

Meissner, G., and Henderson, J. S. (1987). Rapid calcium release from cardiac sarcoplasmic reticulum vesicles is dependent on Ca^{2+} and is modulated by Mg^{2+}, adenine nucleotide, and calmodulin. J Biol Chem *262*, 3065-73.

Meldolesi, J., Krause, K. H., and Michalak, M. (1996). Calreticulin: how many functions in how many cellular compartments? Como, April 1996. Cell Calcium *20*, 83-6.

Mery, L., Mesaeli, N., Michalak, M., Opas, M., Lew, D. P., and Krause, K. H. (1996). Overexpression of calreticulin increases intracellular Ca^{2+} storage and decreases store-operated Ca^{2+} influx. J Biol Chem *271*, 9332-9.

Mignery, G. A., Johnston, P. A., and Sudhof, T. C. (1992). Mechanism of Ca^{2+} inhibition of inositol 1,4,5-trisphosphate ($InsP_3$) binding to the cerebellar $InsP_3$ receptor. J Biol Chem *267*, 7450-5.

Mignery, G. A., Newton, C. L., Archer, B. T. d., and Sudhof, T. C. (1990). Structure and expression of the rat inositol 1,4,5-trisphosphate receptor. J Biol Chem *265*, 12679-85.

Mignery, G. A., and Sudhof, T. C. (1990). The ligand binding site and transduction mechanism in the inositol- 1,4,5-triphosphate receptor. EMBO J *9*, 3893-8.

Mignotte, B., and Vayssiere, J. L. (1998). Mitochondria and apoptosis. Eur J Biochem *252*, 1-15.

Mikoshiba, K. (1993). Inositol 1,4,5-trisphosphate receptor. Trends Pharmacol Sci *14*, 86-9.

Milani, D., Malgaroli, A., Guidolin, D., Fasolato, C., Skaper, S. D., Meldolesi, J., and Pozzan, T. (1990). Ca^{2+} channels and intracellular Ca^{2+} stores in neuronal and neuroendocrine cells. Cell Calcium *11*, 191-9.

Missiaen, L., De Smedt, H., Droogmans, G., Declerck, I., Plessers, L., and Casteels, R. (1991). Uptake characteristics of the $InsP_3$-sensitive and -insensitive Ca^{2+} pools in porcine aortic smooth-muscle cells: different Ca^{2+} sensitivity of the Ca^{2+}-uptake mechanism. Biochem Biophys Res Commun *174*, 1183-8.

Miyawaki, A., Furuichi, T., Ryou, Y., Yoshikawa, S., Nakagawa, T., Saitoh, T., and Mikoshiba, K. (1991). Structure-function relationships of the mouse inositol 1,4,5- trisphosphate receptor. Proc Natl Acad Sci U S A *88*, 4911-5.

Monkawa, T., Miyawaki, A., Sugiyama, T., Yoneshima, H., Yamamoto-Hino, M., Furuichi, T., Saruta, T., Hasegawa, M., and Mikoshiba, K. (1995). Heterotetrameric complex formation of inositol 1,4,5-trisphosphate receptor subunits. J Biol Chem *270*, 14700-4.

Montell, C. (1997). New light on TRP and TRPL. Mol Pharmacol *52*, 755-63.

Morikawa, K., Ohbayashi, T., Nakagawa, M., Konishi, Y., Makino, Y., Yamada, M., Miyawaki, A., Furuichi, T., Mikoshiba, K., and Tamura, T. (1997). Transcription initiation sites and promoter structure of the mouse type 2 inositol 1,4,5-trisphosphate receptor gene. Gene *196*, 181-5.

Morrissette, J., Heisermann, G., Cleary, J., Ruoho, A., and Coronado, R. (1993). Cyclic ADP-ribose induced Ca^{2+} release in rabbit skeletal muscle sarcoplasmic reticulum. FEBS Lett *330*, 270-4.

Mourey, R. J., Estevez, V. A., Marecek, J. F., Barrow, R. K., Prestwich, G. D., and Snyder, S. H. (1993). Inositol 1,4,5-trisphosphate receptors: labeling the inositol 1,4,5- trisphosphate binding site with photoaffinity ligands. Biochemistry *32*, 1719-26.

Mourey, R. J., Verma, A., Supattapone, S., and Snyder, S. H. (1990). Purification and characterization of the inositol 1,4,5- trisphosphate receptor protein from rat vas deferens. Biochem J *272*, 383-9.

Moutin, M. J., and Dupont, Y. (1988). Rapid filtration studies of Ca^{2+}-induced Ca^{2+} release from skeletal sarcoplasmic reticulum. Role of monovalent ions. J Biol Chem *263*, 4228-35.

Murphy, A. N., Bredesen, D. E., Cortopassi, G., Wang, E., and Fiskum, G. (1996). Bcl-2 potentiates the maximal calcium uptake capacity of neural cell mitochondria. Proc Natl Acad Sci U S A *93*, 9893-8.

Murphy, T. H., Worley, P. F., Nakabeppu, Y., Christy, B., Gastel, J., and Baraban, J. M. (1991). Synaptic regulation of immediate early gene expression in primary cultures of cortical neurons. J Neurochem *57*, 1862-72.

Myers, J. N., LeVea, C. M., Smith, J. E., Kallen, R. G., Tung, L., and Greene, M. I. (1992). Expression, purification, and characterization of Bacneu. A soluble protein tyrosine kinase domain encoded by the neu-oncogene. Receptor *2*, 1-16.

Nagasaki, K., and Kasai, M. (1983). Fast release of calcium from sarcoplasmic reticulum vesicles monitored by chlortetracycline fluorescence. J Biochem (Tokyo) *94*, 1101-9.

Nakagawa, T., Shiota, C., Okano, H., and Mikoshiba, K. (1991). Differential localization of alternative spliced transcripts encoding inositol 1,4,5-trisphosphate receptors in mouse cerebellum and hippocampus: in situ hybridization study. J Neurochem *57*, 1807-10.

Nakai, J., Dirksen, R. T., Nguyen, H. T., Pessah, I. N., Beam, K. G., and Allen, P. D. (1996). Enhanced dihydropyridine receptor channel activity in the presence of ryanodine receptor. Nature *380*, 72-5.

Nakai, J., Imagawa, T., Hakamat, Y., Shigekawa, M., Takeshima, H., and Numa, S. (1990). Primary structure and functional expression from cDNA of the cardiac ryanodine receptor/calcium release channel. FEBS Lett *271*, 169-77.

Nakamura, T., and Gold, G. H. (1987). A cyclic nucleotide-gated conductance in olfactory receptor cilia. Nature *325*, 442-4.

Nelson, M. T., Cheng, H., Rubart, M., Santana, L. F., Bonev, A. D., Knot, H. J., and Lederer, W. J. (1995). Relaxation of arterial smooth muscle by calcium sparks. Science *270*, 633-7.

Nelson, T. E. (1987). Ryanodine: antithetical calcium channel effects in skeletal muscle sarcoplasmic reticulum. J Pharmacol Exp Ther *242*, 56-61.

Nielsen, D. A., and Shapiro, D. J. (1986). Preparation of capped RNA transcripts using T7 RNA polymerase. Nucleic Acids Res *14*, 5936.

Niki, I., Yokokura, H., Sudo, T., Kato, M., and Hidaka, H. (1996). Ca^{2+} signaling and intracellular Ca^{2+} binding proteins. J Biochem (Tokyo) *120*, 685-98.

North, R. A. (1996). P2X receptors: a third major class of ligand-gated ion channels. Ciba Found Symp *198*, 91-105; discussion 105-9.

Nowycky, M. C., Fox, A. P., and Tsien, R. W. (1985). Three types of neuronal calcium channel with different calcium agonist sensitivity. Nature *316*, 440-3.

Nucifora, F. C., Jr., Li, S. H., Danoff, S., Ullrich, A., and Ross, C. A. (1995). Molecular cloning of a cDNA for the human inositol 1,4,5-trisphosphate receptor type 1, and the identification of a third alternatively spliced variant. Brain Res Mol Brain Res *32*, 291-6.

Nunn, D. L., and Taylor, C. W. (1990). Liver inositol, 1,4,5-trisphosphate-binding sites are the Ca^{2+}-mobilizing receptors. Biochem J *270*, 227-32.

Nunn, D. L., and Taylor, C. W. (1992). Luminal Ca^{2+} increases the sensitivity of Ca^{2+} stores to inositol 1,4,5- trisphosphate. Mol Pharmacol *41*, 115-9.

Obukhov, A. G., Harteneck, C., Zobel, A., Harhammer, R., Kalkbrenner, F., Leopoldt, D., Luckhoff, A., Nurnberg, B., and Schultz, G. (1996). Direct activation of trpl cation channels by G alpha11 subunits. EMBO J *15*, 5833-8.

Olivera, B. M., Miljanich, G. P., Ramachandran, J., and Adams, M. E. (1994). Calcium channel diversity and neurotransmitter release: the omega- conotoxins and omega-agatoxins. Annu Rev Biochem *63*, 823-67.

O'Reilly, D., Miller, L. K., and Luckow, V. A. (1992). Baculovirus expression vectors: A laboratory manual (New York, NY: W. H. Freeman and Company).

Otsu, K., Willard, H. F., Khanna, V. K., Zorzato, F., Green, N. M., and MacLennan, D. H. (1990). Molecular cloning of cDNA encoding the Ca^{2+} release channel (ryanodine receptor) of rabbit cardiac muscle sarcoplasmic reticulum. J Biol Chem *265*, 13472-83.

Parekh, A. B., and Penner, R. (1997). Store depletion and calcium influx. Physiol Rev *77*, 901-30.

Parks, G. D., Duke, G. M., and Palmenberg, A. C. (1986). Encephalomyocarditis virus 3C protease: efficient cell-free expression from clones which link viral 5' noncoding sequences to the P3 region. J Virol *60*, 376-84.

Parys, J. B., de Smedt, H., Missiaen, L., Bootman, M. D., Sienaert, I., and Casteels, R. (1995). Rat basophilic leukemia cells as model system for inositol 1,4,5-trisphosphate receptor IV, a receptor of the type II family: functional comparison and immunological detection. Cell Calcium *17*, 239-49.

Patel, S., Joseph, S. K., and Thomas, A. P. (1999). Molecular properties of inositol 1,4,5-trisphosphate receptors. Cell Calcium *25*, 247-64.

Pelham, H. R., and Jackson, R. J. (1976). An efficient mRNA-dependent translation system from reticulocyte lysates. Eur J Biochem *67*, 247-56.

Penniston, J. T., and Enyedi, A. (1998). Modulation of the plasma membrane Ca^{2+} pump. J Membr Biol *165*, 101-9.

Peppelenbosch, M. P., Tertoolen, L. G., den Hertog, J., and de Laat, S. W. (1992). Epidermal growth factor activates calcium channels by phospholipase A2/5-lipoxygenase-mediated leukotriene C4 production. Cell *69*, 295-303.

Petersen, O. H. (1996). Can Ca^{2+} be released from secretory granules or synaptic vesicles? Trends Neurosci *19*, 411-3.

Pietri, F., Hilly, M., and Mauger, J. P. (1990). Calcium mediates the interconversion between two states of the liver inositol 1,4,5-trisphosphate receptor. J Biol Chem *265*, 17478-85.

Pinton, P., Pozzan, T., and Rizzuto, R. (1998). The Golgi apparatus is an inositol 1,4,5-trisphosphate-sensitive Ca^{2+} store, with functional properties distinct from those of the endoplasmic reticulum. EMBO J *17*, 5298-308.

Promega. (1996). Protocols and Applications Guide, Third Edition (Madison, WI, USA: Promega Corporation).

Putney, J. W., Jr. (1986). A model for receptor-regulated calcium entry. Cell Calcium *7*, 1-12.

Putney, J. W., Jr. (1997). Type 3 inositol 1,4,5-trisphosphate receptor and capacitative calcium entry. Cell Calcium *21*, 257-61.

Raffray, M., and Cohen, G. M. (1997). Apoptosis and necrosis in toxicology: a continuum or distinct modes of cell death? Pharmacol Ther *75*, 153-77.

Randall, A., and Tsien, R. W. (1995). Pharmacological dissection of multiple types of Ca^{2+} channel currents in rat cerebellar granule neurons. J Neurosci *15*, 2995-3012.

Rapp, P. E., Mees, A. I., and Sparrow, C. T. (1981). Frequency encoded biochemical regulation is more accurate than amplitude dependent control. J Theor Biol *90*, 531-44.

Reuter, H., Cachelin, A. B., De Peyer, J. E., and Kokubun, S. (1983). Modulation of calcium channels in cultured cardiac cells by isoproterenol and 8-bromo-cAMP. Cold Spring Harb Symp Quant Biol *48 Pt 1*, 193-200.

Rios, E., Ma, J. J., and Gonzalez, A. (1991). The mechanical hypothesis of excitation-contraction (EC) coupling in skeletal muscle. J Muscle Res Cell Motil *12*, 127-35.

Robitaille, R., Adler, E. M., and Charlton, M. P. (1990). Strategic location of calcium channels at transmitter release sites of frog neuromuscular synapses. Neuron *5*, 773-9.

Ronde, P., and Nichols, R. A. (1998). High calcium permeability of serotonin 5-HT_3 receptors on presynaptic nerve terminals from rat striatum. J Neurochem *70*, 1094-103.

Rooney, T. A., Joseph, S. K., Queen, C., and Thomas, A. P. (1996). Cyclic GMP induces oscillatory calcium signals in rat hepatocytes. J Biol Chem *271*, 19817-25.

Rosen, L. B., Ginty, D. D., and Greenberg, M. E. (1995). Calcium regulation of gene expression. Adv Second Messenger Phosphoprotein Res *30*, 225-53.

Rosenmund, C., Feltz, A., and Westbrook, G. L. (1995). Calcium-dependent inactivation of synaptic NMDA receptors in hippocampal neurons. J Neurophysiol *73*, 427-30.

Ross, C. A., Danoff, S. K., Schell, M. J., Snyder, S. H., and Ullrich, A. (1992). Three additional inositol 1,4,5-trisphosphate receptors: molecular cloning and differential localization in brain and peripheral tissues. Proc Natl Acad Sci U S A *89*, 4265-9.

Rousseau, E., Smith, J. S., Henderson, J. S., and Meissner, G. (1986). Single channel and $^{45}Ca^{2+}$ flux measurements of the cardiac sarcoplasmic reticulum calcium channel. Biophys J *50*, 1009-14.

Rozov, A., Zilberter, Y., Wollmuth, L. P., and Burnashev, N. (1998). Facilitation of currents through rat Ca^{2+}-permeable AMPA receptor channels by activity-dependent relief from polyamine block. J Physiol (Lond) *511*, 361-77.

Ruth, P., Rohrkasten, A., Biel, M., Bosse, E., Regulla, S., Meyer, H. E., Flockerzi, V., and Hofmann, F. (1989). Primary structure of the beta subunit of the DHP-sensitive calcium channel from skeletal muscle. Science *245*, 1115-8.

Sabbadini, R. A., Betto, R., Teresi, A., Fachechi-Cassano, G., and Salviati, G. (1992). The effects of sphingosine on sarcoplasmic reticulum membrane calcium release. J Biol Chem *267*, 15475-84.

Sambrook, J., Fritsch, E. F., and Maniatis, T. (1989). Molecular Cloning: A Laboratory Manual, Second Edition (Cold Spring Harbor, NY, USA: Cold Spring Harbor Laboratory Press).

Sanger, F., Nicklen, S., and Coulson, A. R. (1977). DNA sequencing with chain-terminating inhibitors. Proc Natl Acad Sci U S A *74*, 5463-7.

Schaaper, R. M. (1993). Base selection, proofreading, and mismatch repair during DNA replication in *Escherichia coli*. J Biol Chem *268*, 23762-5.

Sedlak, T. W., Oltvai, Z. N., Yang, E., Wang, K., Boise, L. H., Thompson, C. B., and Korsmeyer, S. J. (1995). Multiple Bcl-2 family members demonstrate selective dimerizations with Bax. Proc Natl Acad Sci U S A *92*, 7834-8.

Seguela, P., Wadiche, J., Dineley-Miller, K., Dani, J. A., and Patrick, J. W. (1993). Molecular cloning, functional properties, and distribution of rat brain alpha 7: a nicotinic cation channel highly permeable to calcium. J Neurosci *13*, 596-604.

Shou, W., Aghdasi, B., Armstrong, D. L., Guo, Q., Bao, S., Charng, M. J., Mathews, L. M., Schneider, M. D., Hamilton, S. L., and Matzuk, M. M. (1998). Cardiac defects and altered ryanodine receptor function in mice lacking FKBP12. Nature *391*, 489-92.

Shuttleworth, T. J., and Thompson, J. L. (1998). Muscarinic receptor activation of arachidonate-mediated Ca^{2+} entry in HEK293 cells is independent of phospholipase C. J Biol Chem *273*, 32636-43.

Sienaert, I., De Smedt, H., Parys, J. B., Missiaen, L., Vanlingen, S., Sipma, H., and Casteels, R. (1996). Characterization of a cytosolic and a luminal Ca^{2+} binding site in the type 1 inositol 1,4,5-trisphosphate receptor. J Biol Chem *271*, 27005-12.

Sienaert, I., Missiaen, L., De Smedt, H., Parys, J. B., Sipma, H., and Casteels, R. (1997). Molecular and functional evidence for multiple Ca^{2+}-binding domains

in the type 1 inositol 1,4,5-trisphosphate receptor. J Biol Chem *272*, 25899-906.

Singer-Lahat, D., Liu, J., Wess, J., and Felder, C. C. (1996). The third intracellular domain of the M3 muscarinic receptor determines coupling to calcium influx in transfected Chinese hamster ovary cells. FEBS Lett *386*, 51-4.

Singer-Lahat, D., Rojas, E., and Felder, C. C. (1997). A9 fibroblasts transfected with the M3 muscarinic receptor clone express a Ca^{2+} channel activated by carbachol, GTP and GDP. J Membr Biol *159*, 21-8.

Sinha, M., and Hasan, G. (1999). Sequencing and exon mapping of the inositol 1,4,5-trisphosphate receptor cDNA from *Drosophila* embryos suggests the presence of differentially regulated forms of RNA and protein. Gene *233*, 271-6.

Sommer, B., Keinanen, K., Verdoorn, T. A., Wisden, W., Burnashev, N., Herb, A., Kohler, M., Takagi, T., Sakmann, B., and Seeburg, P. H. (1990). Flip and flop: a cell-specific functional switch in glutamate-operated channels of the CNS. Science *249*, 1580-5.

Sommer, B., and Seeburg, P. H. (1992). Glutamate receptor channels: novel properties and new clones. Trends Pharmacol Sci *13*, 291-6.

Sorrentino, V., Giannini, G., Malzac, P., and Mattei, M. G. (1993). Localization of a novel ryanodine receptor gene (RyR3) to human chromosome 15q14-q15 by in situ hybridization. Genomics *18*, 163-5.

Stehno-Bittel, L., Luckhoff, A., and Clapham, D. E. (1995). Calcium release from the nucleus by $InsP_3$ receptor channels. Neuron *14*, 163-7.

Strehler, E. E. (1991). Recent advances in the molecular characterization of plasma membrane Ca^{2+} pumps. J Membr Biol *120*, 1-15.

Sudhof, T. C., Newton, C. L., Archer, B. T. d., Ushkaryov, Y. A., and Mignery, G. A. (1991). Structure of a novel $InsP_3$ receptor. EMBO J *10*, 3199-206.

Sugawara, H., Kurosaki, M., Takata, M., and Kurosaki, T. (1997). Genetic evidence for involvement of type 1, type 2 and type 3 inositol 1,4,5-trisphosphate receptors in signal transduction through the B-cell antigen receptor. EMBO J *16*, 3078-88.

Sugimori, M., Lang, E. J., Silver, R. B., and Llinas, R. (1994). High-resolution measurement of the time course of calcium-concentration microdomains at squid presynaptic terminals. Biol Bull *187*, 300-3.

Sugiura, Y., Woppmann, A., Miljanich, G. P., and Ko, C. P. (1995). A novel omega-conopeptide for the presynaptic localization of calcium channels at the mammalian neuromuscular junction. J Neurocytol *24*, 15-27.

Sumbilla, C., and Inesi, G. (1987). Rapid filtration measurements of Ca^{2+} release from cisternal sarcoplasmic reticulum vesicles. FEBS Lett *210*, 31-6.

Summers, M. D., and Smith, G. E. (1985). Genetic Engineering of the Genome of the *Autographa californica* Nuclear Polyhedrosis Virus, Volume 22, B. Fields, ed. (Cold Spring Harbor, NY, USA: Cold Spring Harbor Laboratory).

Supattapone, S., Danoff, S. K., Theibert, A., Joseph, S. K., Steiner, J., and Snyder, S. H. (1988). Cyclic AMP-dependent phosphorylation of a brain inositol trisphosphate receptor decreases its release of calcium. Proc Natl Acad Sci U S A *85*, 8747-50.

Supattapone, S., Worley, P. F., Baraban, J. M., and Snyder, S. H. (1988). Solubilization, purification, and characterization of an inositol trisphosphate receptor. J Biol Chem *263*, 1530-4.

Susin, S. A., Lorenzo, H. K., Zamzami, N., Marzo, I., Snow, B. E., Brothers, G. M., Mangion, J., Jacotot, E., Costantini, P., Loeffler, M., Larochette, N., Goodlett, D. R., Aebersold, R., Siderovski, D. P., Penninger, J. M., and Kroemer, G. (1999). Molecular characterization of mitochondrial apoptosis-inducing factor. Nature *397*, 441-6.

Swandulla, D., and Armstrong, C. M. (1988). Fast-deactivating calcium channels in chick sensory neurons. J Gen Physiol *92*, 197-218.

Tabor, S., and Richardson, C. C. (1989). Selective inactivation of the exonuclease activity of bacteriophage T7 DNA polymerase by *in vitro* mutagenesis. J Biol Chem *264*, 6447-58.

Takahashi, M., and Catterall, W. A. (1987). Dihydropyridine-sensitive calcium channels in cardiac and skeletal muscle membranes: studies with antibodies against the alpha subunits. Biochemistry *26*, 5518-26.

Takeshima, H., Nishimura, S., Matsumoto, T., Ishida, H., Kangawa, K., Minamino, N., Matsuo, H., Ueda, M., Hanaoka, M., Hirose, T., and Numa, S. (1989). Primary structure and expression from complementary DNA of skeletal muscle ryanodine receptor. Nature *339*, 439-45.

Tanabe, T., Takeshima, H., Mikami, A., Flockerzi, V., Takahashi, H., Kangawa, K., Kojima, M., Matsuo, H., Hirose, T., and Numa, S. (1987). Primary structure of the receptor for calcium channel blockers from skeletal muscle. Nature *328*, 313-8.

Tang, Y. P., Shimizu, E., Dube, G. R., Rampon, C., Kerchner, G. A., Zhuo, M., Liu, G., and Tsien, J. Z. (1999). Genetic enhancement of learning and memory in mice. Nature *401*, 63-9.

Timerman, A. P., Onoue, H., Xin, H. B., Barg, S., Copello, J., Wiederrecht, G., and Fleischer, S. (1996). Selective binding of FKBP12.6 by the cardiac ryanodine receptor. J Biol Chem *271*, 20385-91.

Timerman, A. P., Wiederrecht, G., Marcy, A., and Fleischer, S. (1995). Characterization of an exchange reaction between soluble FKBP12 and the FKBP.ryanodine receptor complex. Modulation by FKBP mutants deficient in peptidyl-prolyl isomerase activity. J Biol Chem *270*, 2451-9.

Tottene, A., Moretti, A., and Pietrobon, D. (1996). Functional diversity of P-type and R-type calcium channels in rat cerebellar neurons. J Neurosci *16*, 6353-63.

Treves, S., De Mattei, M., Landfredi, M., Villa, A., Green, N. M., MacLennan, D. H., Meldolesi, J., and Pozzan, T. (1990). Calreticulin is a candidate for a calsequestrin-like function in Ca^{2+}-storage compartments (calciosomes) of liver and brain. Biochem J *271*, 473-80.

Vannier, B., Peyton, M., Boulay, G., Brown, D., Qin, N., Jiang, M., Zhu, X., and Birnbaumer, L. (1999). Mouse trp2, the homologue of the human trpc2 pseudogene, encodes mTrp2, a store depletion-activated capacitative Ca^{2+} entry channel. Proceedings of the National Academy of Sciences of the United States of America *96*, 2060-4.

Vaughn, J. L., Goodwin, R. H., Tompkins, G. J., and McCawley, P. (1977). The establishment of two cell lines from the insect *Spodoptera frugiperda* (Lepidoptera; Noctuidae). In Vitro *13*, 213-7.

Vernino, S., Amador, M., Luetje, C. W., Patrick, J., and Dani, J. A. (1992). Calcium modulation and high calcium permeability of neuronal nicotinic acetylcholine receptors. Neuron *8*, 127-34.

Vignes, M., Bleakman, D., Lodge, D., and Collingridge, G. L. (1997). The synaptic activation of the GluR5 subtype of kainate receptor in area CA3 of the rat hippocampus. Neuropharmacology *36*, 1477-81.

Virginio, C., North, R. A., and Surprenant, A. (1998). Calcium permeability and block at homomeric and heteromeric $P2X_2$ and $P2X_3$ receptors, and P2X receptors in rat nodose neurones. J Physiol (Lond) *510*, 27-35.

von zur Muhlen, F., Eckstein, F., and Penner, R. (1991). Guanosine 5'-[beta-thio]triphosphate selectively activates calcium signaling in mast cells. Proc Natl Acad Sci U S A *88*, 926-30.

Wagenknecht, T., Radermacher, M., Grassucci, R., Berkowitz, J., Xin, H. B., and Fleischer, S. (1997). Locations of calmodulin and FK506-binding protein on the three-dimensional architecture of the skeletal muscle ryanodine receptor. J Biol Chem *272*, 32463-71.

Walker, J. M. (1998). Protein Protocols on CD-ROM, J. M. Walker, ed. Chapter 4.22 (Totowa, NJ: Humana Press).

Walter, P., Gilmore, R., and Blobel, G. (1984). Protein translocation across the endoplasmic reticulum. Cell *38*, 5-8.

Westenbroek, R. E., Ahlijanian, M. K., and Catterall, W. A. (1990). Clustering of L-type Ca^{2+} channels at the base of major dendrites in hippocampal pyramidal neurons. Nature *347*, 281-4.

Westenbroek, R. E., Hell, J. W., Warner, C., Dubel, S. J., Snutch, T. P., and Catterall, W. A. (1992). Biochemical properties and subcellular distribution of an N-type calcium channel alpha 1 subunit. Neuron *9*, 1099-115.

Westenbroek, R. E., Sakurai, T., Elliott, E. M., Hell, J. W., Starr, T. V., Snutch, T. P., and Catterall, W. A. (1995). Immunochemical identification and subcellular distribution of the alpha 1A subunits of brain calcium channels. J Neurosci *15*, 6403-18.

White, R. J., and Reynolds, I. J. (1996). Mitochondrial depolarization in glutamate-stimulated neurons: an early signal specific to excitotoxin exposure. J Neurosci *16*, 5688-97.

Willcocks, A. L., Cooke, A. M., Potter, B. V., and Nahorski, S. R. (1987). Stereospecific recognition sites for [^{3}H]inositol 1,4,5-triphosphate in particulate preparations of rat cerebellum. Biochem Biophys Res Commun *146*, 1071-8.

Williams, A. J. (1995). Ion Channels, R. H. Ashley, ed. Chapter 2, pp 43-67 (Walton Street, Oxford, UK: Oxford University Press).

Wojcikiewicz, R. J. (1995). Type I, II, and III inositol 1,4,5-trisphosphate receptors are unequally susceptible to down-regulation and are expressed in markedly different proportions in different cell types. J Biol Chem *270*, 11678-83.

Wojcikiewicz, R. J., and He, Y. (1995). Type I, II and III inositol 1,4,5-trisphosphate receptor co-immunoprecipitation as evidence for the existence of

heterotetrameric receptor complexes. Biochem Biophys Res Commun *213*, 334-41.

Wojcikiewicz, R. J. H., and Oberdorf, J. A. (1996). Degradation of inositol 1,4,5-trisphosphate receptors during cell stimulation is a specific process mediated by cysteine protease activity. J Biol Chem *271*, 16652-5.

Wolf, M. J., Wang, J., Turk, J., and Gross, R. W. (1997). Depletion of intracellular calcium stores activates smooth muscle cell calcium-independent phospholipase A2. A novel mechanism underlying arachidonic acid mobilization. J Biol Chem *272*, 1522-6.

Wong, F., Knight, B. W., and Dodge, F. A. (1982). Adapting bump model for ventral photoreceptors of Limulus. J Gen Physiol *79*, 1089-113.

Yamada, M., Miyawaki, A., Saito, K., Nakajima, T., Yamamoto-Hino, M., Ryo, Y., Furuichi, T., and Mikoshiba, K. (1995). The calmodulin-binding domain in the mouse type 1 inositol 1,4,5- trisphosphate receptor. Biochem J *308*, 83-8.

Yamada, N., Makino, Y., Clark, R. A., Pearson, D. W., Mattei, M. G., Guenet, J. L., Ohama, E., Fujino, I., Miyawaki, A., Furuichi, T., and Mikoshiba, K. (1994). Human inositol 1,4,5-trisphosphate type-1 receptor, $InsP_3R1$: structure, function, regulation of expression and chromosomal localization. Biochem J *302*, 781-90.

Yamamoto-Hino, M., Sugiyama, T., Hikichi, K., Mattei, M. G., Hasegawa, K., Sekine, S., Sakurada, K., Miyawaki, A., Furuichi, T., Hasegawa, M., and Mikoshiba, K. (1994). Cloning and characterization of human type 2 and type 3 inositol 1,4,5- trisphosphate receptors. Receptors Channels *2*, 9-22.

Yang, S. N., Tang, Y. G., and Zucker, R. S. (1999). Selective induction of LTP and LTD by postsynaptic $[Ca^{2+}]i$ elevation. J Neurophysiol *81*, 781-7.

Yao, Y., Choi, J., and Parker, I. (1995). Quantal puffs of intracellular Ca^{2+} evoked by inositol trisphosphate in Xenopus oocytes. J Physiol (Lond) *482*, 533-53.

Yao, Y., and Tsien, R. Y. (1997). Calcium current activated by depletion of calcium stores in Xenopus oocytes. J Gen Physiol *109*, 703-15.

Yau, K. W., and Baylor, D. A. (1989). Cyclic GMP-activated conductance of retinal photoreceptor cells. Annu Rev Neurosci *12*, 289-327.

Yoneshima, H., Miyawaki, A., Michikawa, T., Furuichi, T., and Mikoshiba, K. (1997). Ca^{2+} differentially regulates the ligand-affinity states of type 1 and type 3 inositol 1,4,5-trisphosphate receptors. Biochem J *322*, 591-6.

Yoshikawa, F., Iwasaki, H., Michikawa, T., Furuichi, T., and Mikoshiba, K. (1999). Cooperative formation of the ligand-binding site of the inositol 1,4,5-trisphosphate receptor by two separable domains. J Biol Chem *274*, 328-34.

Yoshikawa, F., Morita, M., Monkawa, T., Michikawa, T., Furuichi, T., and Mikoshiba, K. (1996). Mutational analysis of the ligand binding site of the inositol 1,4,5- trisphosphate receptor. J Biol Chem *271*, 18277-84.

Yoshikawa, S., Tanimura, T., Miyawaki, A., Nakamura, M., Yuzaki, M., Furuichi, T., and Mikoshiba, K. (1992). Molecular cloning and characterization of the inositol 1,4,5- trisphosphate receptor in *Drosophila melanogaster*. J Biol Chem *267*, 16613-9.

Yu, X., Carroll, S., Rigaud, J. L., and Inesi, G. (1993). H^+ countertransport and electrogenicity of the sarcoplasmic reticulum Ca^{2+} pump in reconstituted proteoliposomes. Biophys J *64*, 1232-42.

Yule, D. I., Ernst, S. A., Ohnishi, H., and Wojcikiewicz, R. J. (1997). Evidence that zymogen granules are not a physiologically relevant calcium pool. Defining the distribution of inositol 1,4,5-trisphosphate receptors in pancreatic acinar cells. J Biol Chem *272*, 9093-8.

Zhang, L., Kelley, J., Schmeisser, G., Kobayashi, Y. M., and Jones, L. R. (1997). Complex formation between junctin, triadin, calsequestrin, and the ryanodine receptor. Proteins of the cardiac junctional sarcoplasmic reticulum membrane. J Biol Chem *272*, 23389-97.

Zholos, A. V., Komori, S., Ohashi, H., and Bolton, T. B. (1994). Ca^{2+} inhibition of inositol trisphosphate-induced Ca^{2+} release in single smooth muscle cells of guinea-pig small intestine. J Physiol (Lond) *481*, 97-109.

Zorzato, F., Fujii, J., Otsu, K., Phillips, M., Green, N. M., Lai, F. A., Meissner, G., and MacLennan, D. H. (1990). Molecular cloning of cDNA encoding human and rabbit forms of the Ca^{2+} release channel (ryanodine receptor) of skeletal muscle sarcoplasmic reticulum. J Biol Chem *265*, 2244-56.